

UC San Diego

UC San Diego Electronic Theses and Dissertations

Title

Novel Silica Lipid Nano Carriers for Diagnostics and Therapeutics

Permalink

<https://escholarship.org/uc/item/6h13n57q>

Author

Vaidyanathan, Mukanth

Publication Date

2017

Peer reviewed|Thesis/dissertation

UNIVERSITY OF CALIFORNIA, SAN DIEGO

**Novel Silica Coated Lipid Nanocarriers for Diagnostics and
Therapeutics**

A dissertation submitted in partial satisfaction of the
requirements for the degree
Doctor of Philosophy

in

Chemical Engineering

by

Mukanth Vaidyanathan

Committee in charge:

Professor Sadik Esener, Chair
Professor Donald Sirbuly, Co-Chair
Professor Michael Heller
Professor Kuo-Fen Lee
Professor William Trogler

2017

Copyright
Mukanth Vaidyanathan, 2017
All rights reserved.

The dissertation of Mukanth Vaidyanathan is approved, and it is acceptable in quality and form for publication on microfilm and electronically:

Co-Chair

Chair

University of California, San Diego

2017

DEDICATION

To
Amma, Appa and my future dog!

EPIGRAPH

Ever Tried

Ever Failed

No Matter

Try Again

Fail Again

Fail Better.

—Samuel Beckett

TABLE OF CONTENTS

	Signature Page	iii
	Dedication	iv
	Epigraph	v
	Table of Contents	vi
	List of Figures	ix
	Acknowledgements	xi
	Vita	xv
	Abstract	xvi
Chapter 1	Introduction	1
Chapter 2	Silica Coated Enzyme Encapsulated Cationic Liposomes	4
	2.1 Liposome	4
	2.1.1 Silica Coated Liposomes	6
	2.1.2 Active Targeting of the Liposomes	6
	2.2 Materials	9
	2.3 Methods	9
	2.3.1 Synthesis of Enzyme Loaded Cationic Lipid nanoparticles (liposomes) (CeLi)	9
	2.3.2 Synthesis of Silica Coated Enzyme Loaded Liposomes (SiLi)	11
	2.3.3 Synthesis of Calcium Phosphate (CaP) Coated Enzyme Loaded Liposomes (CaL)	12
	2.3.4 Characterization of the CeLi, SiLi and CaL	12
	2.3.5 Nitrocefin Assay for the Measurement of BLA activity	13
	2.3.6 Measurement of <i>in vivo</i> Activity	13
	2.3.7 Measurement of Activation of the CeLi and SiLi using Ultrasound	13
	2.4 Results	14
	2.5 Discussion	17
	2.6 Conclusion	19
	2.7 Acknowledgments	20

Chapter 3	Therapeutic Applications of SiLi	23
	3.1 Glucose Oxidase encapsulated SiLi (Glu-SiLi) for <i>in vivo</i> generation of Hydrogen Peroxide	23
	3.1.1 Enzymes Assisted Oxidative Therapy	26
	3.2 Materials	28
	3.3 Synthesis of Glu-SiLi	28
	3.3.1 Characterization of Glucose Oxidase	29
	3.3.2 Glucose oxidase kinetics and activity study	29
	3.3.3 Toxicity Study of Glu-SiLi with MTT Assay	29
	3.3.4 <i>In vivo</i> Therapeutic Efficacy	30
	3.4 Results	30
	3.5 Discussion	32
	3.6 Conclusion	34
	3.7 Acknowledgments	35
Chapter 4	Diagnostic Application of SiLi	36
	4.1 Acetylcholine (ACh)	36
	4.2 Acetylcholinesterase (AChE)	37
	4.2.1 Importance of ACh Detection	39
	4.2.2 Current Detection Techniques	41
	4.3 Materials	44
	4.4 Preparation of AChE Loaded Liposomes	45
	4.4.1 Synthesis of Silica coated AChE/ChOx/HRP Loaded Liposomes(ACH-SiLi)	46
	4.4.2 Characterization of the ACH-SiLi	46
	4.4.3 Characterization of AChE Activity using Amplex Red Assay kit	47
	4.5 Results	47
	4.6 Discussion	48
	4.7 Conclusion	51
	4.8 Acknowledgments	52
Chapter 5	Synthetic Hollow Enzyme Loaded Silica Nanoparticle for ATP Detection	53
	5.1 Adenosine Tri-Phosphate (ATP)	53
	5.2 Role of ATP	54
	5.2.1 Current Techniques to Detect ATP	55
	5.2.2 ATP Release in cells	56
	5.3 LuciSHELs	58
	5.4 Materials	58
	5.5 Method	58
	5.5.1 Synthesis of LuciSHELs	58
	5.5.2 Characterization of the LuciSHELs	60
	5.5.3 Enzyme Encapsulation Efficiency Determination	60

	5.5.4	Luciferin ATP assay for the Measurement of Luciferase Activity	60
	5.5.5	Luminescence Detection <i>in vitro</i>	60
	5.6	Results	61
	5.7	Discussion	62
	5.8	Conclusion	63
	5.9	Acknowledgments	64
Chapter 6		Conclusion and Final Notes	69
Bibliography		71

LIST OF FIGURES

Figure 2.1:	Schematic representation of a small monodispersed liposome elucidating the versatility of liposomes by incorporating various compounds either by encapsulation or by surface attachment of the lipid membrane [7]	5
Figure 2.2:	Effect of ultrasound on the lipid nanoparticles	8
Figure 2.3:	Step wise enzyme loaded cationic liposome (CeLi) synthesis . .	11
Figure 2.4:	A silica formation process using PBS and TMOS	12
Figure 2.5:	A schematic representation of the formation of silica on CeLi .	12
Figure 2.6:	The size of the non dialyzed CeLi (Blue), Dialyzed CeLi (Orange) and SiLi (Grey) were all measured at the same dilution in 1X PBS with 12 runs for each measurement using disposable clear size cuvettes	14
Figure 2.7:	The change in the surface charge between non dialyzed CeLi (Blue), dialyzed CeLi (Orange) and SiLi (Grey) were all measured at the same dilution in DI water with 12 runs for each measurement using disposable clear zeta cuvettes	15
Figure 2.8:	Activity plots of BLA in SiLi and unencapsulated	16
Figure 2.9:	Activity plots of BLA with different surface coatings on CeLi .	17
Figure 2.10:	Activity plots of BLA-CeLi and BLA-SiLi on application of ultrasound	18
Figure 2.11:	Demonstration of BSA-AlexaFLuor688 fluorescence in free and BSA-CeLi upon intra muscular injection	21
Figure 2.12:	Demonstration of BSA-AlexaFLuor688 fluorescence in BSA-SiLi upon intra muscular injection at different time points. Inset is Dye-IR fluorescence image to label the lipids to form the liposomes	22
Figure 3.1:	Schematic representation illustrating homeostasis of ROS in the body and the drawbacks due to excess generation of ROS and suppression of defense mechanisms	24
Figure 3.2:	Schematic representation of XO reaction: Hypoxanthine is converted to xanthine in the XO while Xanthine is catalyzed to uric acid also in presence of XO while both the catalysis steps generate ROS	26
Figure 3.3:	Schematic representation of DAO reaction: D amino acids is catalysed to α amino acid to generate ammonia and ROS . . .	27
Figure 3.4:	Percentage viability of cells upon incubation of free GluOX, Glu-CeLi and Glu-SiLi for 24 hours and 3 hours respectively . .	31
Figure 3.5:	Percent change in the tumor volume measured between the mice treated IT with Glu-SiLi (blue) and untreated-PBS (red) .	32

Figure 3.6:	Histology slide of the tumors of GluOx treated and control (untreated). The circle represents the area of necrosis in the region of section	33
Figure 3.7:	Histology slide of the tumors of GluOx treated and control (untreated). TUNNEL staining was performed to stain the area of apoptosis on the slide section	34
Figure 4.1:	Schematic illustration of ACh synthesis in a cholinergic presynaptic nerve terminal and synapse	38
Figure 4.2:	Illustration of AChE structure derived from the <i>Torpedo californica</i>	39
Figure 4.3:	Comparison of structural MRIs of Hippocampus between alzheimers patient (a) and normal adult(b)	42
Figure 4.4:	AmyloidPET scans of Alzheimers patient and Healthy patient	43
Figure 4.5:	Flow chart of the cascading reactions using AChE, ChOx and HRP to detect ACh optically from commercially available kits .	44
Figure 4.6:	AChE activity in three different particles before and after PK treatment and with and without sonication	48
Figure 4.7:	Kinetics of Free, three enzyme (AChE, ChOx and HRP) in one SiLi particle and 3 SiLi particles each containing a different enzyme of the cascade at $1\mu\text{M}$ of ACh and $1\mu\text{M}$ of Ch	49
Figure 5.1:	The electron transport chain in cells	54
Figure 5.2:	Schematic representation of the synthesis of LuciSHELs	65
Figure 5.3:	Luciferase luminescence at different ATP concentration with different surface coating. Si: Just Silicic Acid. APTMS: Silicic acid and APTMS. PEG: Silicic acid and PEG-2000	66
Figure 5.4:	Luminescence of SHELs coated with and without PEG and loaded with different enzyme concentration, 1mg/ml and 30mg/ml at 1nM of ATP and 0.1mg/ml of D-luciferin	66
Figure 5.5:	Comparison of enzyme kinetic study between the luciferase and LuciSHELs performed at different concentrations of ATP at 0.1mg/ml of D-Luciferin	67
Figure 5.6:	Luminescence measured at a single location after 1 second and 10 seconds after the addition of 1nM ATP	67
Figure 5.7:	Luminescence measured at a multiple location at 10 seconds after the addition of 1nM ATP, L1: Location before the addition of ATP. L1-a: Area closer to ATP addition. L2: Location Further away laterally to L1-a.	68

ACKNOWLEDGEMENTS

First and foremost, I would like to thank Professor Sadik Esener for giving me the opportunity to pursue a PhD in his group. It was his confidence in me that made me believe in myself on the projects i undertook. He has always been there for me during the tough times even when he is travelling. The freedom he provided encouraged me to come up with unique ideas which has resulted into many projects which led to great collaborations and taught me to be an independent researcher. Professor Esener never discouraged my involvement in many campus groups and organizations which added to an exciting graduate school experience.

I would like to thank the members of my excellent committee, which included Professors Sadik Esener, Michael Heller, Kuo-Fen Lee, Donald Sirbuly, and William Trogler.

I would like to thank Prof Kuo-Fen Lee for helping me understand various concepts about the brain and the nervous system. He couldnt been more helpful in answering all my questions as soon as possible and always being open minded and encouraging on various projects i would bring in front of him.

Prof David Miller supported me by letting me TA his class every fall and winter from 2011 to 2014. All his advise on how to teach made me a better TA. It was undoubtedly the hardest class i have taught but it was an experience i always went back for every fall.

Ya-san Yeh has truly been the lab "mama" for me. Her support and encouragement has helped me through tough times both personally and professionally. Her patience and knowledge has truly come handy to me for almost all my projects. The collaboration with her on two projects has helped me develop my critical thinking capabilities and multitasking. Her personality, her love for food and dogs has truly made me better researcher and a better human being. Thank you so much for this experience.

Negin Mokhtari has been truly a great labmate and friend. Her persistence and determination is very contagious and has provided me with inspiration during tough times. Negin's support during thesis writing and presentation and *in vivo* experiment has been truly motivating. Its without a doubt that those late night

experiments and long gruelling meetings have etched a fine memory that i would cherish forever. She has helped me to over come my stage fright and provided confidence to speak in front of an audience.

Jared Fisher has helped me a lot in animal experiments upon moving to Portland. He has never hesitated in helping me in conducting different *in vivo* experiments even during weekends. His suggestion and expertise in animal experiments taught me a great deal which kept motivated even when certain experimental results were inconclusive .

Mike Benchimol taught me to synthesize HiFU liposomes and PFN emulsions. He has been a great mentor and provided strong mentorship when i needed. Mike has also been a huge influence during the initial conception of my PhD thesis

Inanc Ortac has also been a great mentor to me. He taught me how to make the SHELS particles and how to conduct ELISA assay. Without his support, the LuciSHELS wouldn't have been this successful.

Zeynep Sayar, Brice Turner and Anna Young helped me in making the liposomes as well with LuciSHELS experiments. Anna especially has been extremely meticulous while characterizing liposomes.

I would like to thank the whole OHSU team (Dr Bree Mitchel, Dr Paul Howard and Faith Buckley) for being extremely understanding to my needs during the initial move to Portland, OR. Their support in conducting the experiments to graduate have been paramount in Portland, OR.

Special thanks to Dana Jiminez and Ji Song for looking out for me and making the transition from Portland to San Diego extremely easy. I wouldn't be graduating debt free from grad school if it weren't for Dana's suggestions to apply for various teaching opportunities. Hands down, Dana and Ji have been the best and easiest administrative people to work with in UCSD.

The whole GSA 2014-15 team (Lindsay, Jon and Dan) for being the best crew to work with on GSA. My GSA experience truly shaped my graduate experience at UCSD. I learn't a great deal about student politics and management.

Rumpa Sarkar and i have been friends since my undergraduate. Without a doubt, she has the perfect vacation and "ranting" buddy. Her "planned" vacations always surpasses any expectations and its always been a topic of our friendly

banter. Her support and encouragement has gotten us more closer than anyone else. Thank you Rumpa Ben !!

Tennis has been a huge part of my graduate career and has been my avenue to blow off some steam. I would like to thank my coach Anthony for being very strict with my tennis workout and keeping me in check on court. His motivation and stubbornness has taught me not to give up without the fight. Corey and Mary for being cool headed tennis partners. Roger Federer, Thank you for being my inspiration and role model #TeamFED.

I would like to thank my uncle, Vijay for being my guardian in this foreign land. Without his advise and support, my initial days in graduate school would have been really hard.

I also would like to thank my cousin, Arvind and his wife, Nitya for continuous support and being an great big brother to me. Your support and help are always something i can rely on.

I express my deepest regards to my best friends for 27 years and my pillar of support, Amma and Appa. Their support both financially and emotionally has been a tremendous influence throughout my graduate career. I thank them for putting up with me during tough times. This thesis couldn't have happened without them and hence the dedication.

Lastly to this fluffy ball, Kova who has graced my life for just 7 days. His absence is still a void that cannot be filled. Hopefully he is happy in doggy heaven.

Methods described in chapters 2 is patented (Nanoscale delivery device and uses thereof,15/449,830). The collaborator for the patent: Negin Mokhtari, Yasan Yeh, Mukanth Vaidyanathan, Ajay Sapre, Bartu Ahiska, Sadik Esener.

Chapter 2, in part is currently being prepared for submission for publication of the material. Mukanth Vaidyanathan, Zeynep Sayar, Jared Fischer, Ya-san Yeh, Negin Mokhtari and Sadik Esener. The dissertation/thesis author was the primary investigator and author of this material.

Chapter 3, in part is currently being prepared for submission for publication of the material. Mukanth Vaidyanathan, Jared Fisher and Sadik Esener. The dissertation/thesis author was the primary investigator and author of this material.

Chapter 4, in part is currently being prepared for submission for publication

of the material. Mukanth Vaidyanathan, Zeynep Sayar, Negin Mokhtari and Sadik Esener. The dissertation/thesis author was the primary investigator and author of this material.

Chapter 5, in part is currently being prepared for submission for publication of the material. Mukanth Vaidyanathan, Yaoguang Ma, Ya-san Yeh and Sadik Esener. The dissertation/thesis author was the primary investigator and author of this material.

VITA

2011	B.Tech in Chemical Engineering , National Institute of Technology Surat, India
2011-2014	Graduate Teaching Assistant, University of California, San Diego
2013	M.S. in Chemical Engineering , University of California, San Diego
2014-2016	Graduate Teaching Assistant, University of California, San Diego
2017	Ph. D in Chemical Engineering , University of California San Diego

PUBLICATIONS

M Vaidyanathan, N Mokhtari, Y Yeh , S Esener “Nanoparticle mediated enzyme delivery for application in cancer therapy”, *Drug Target review* , 1, 2017.

F. Soto, A. Martin, S. Ibsen, M. Vaidyanathan, S. Esener, J. Wang “Acoustic Microcannons: Towards advanced microballistics”, *ACS nano* , 10(1), 1522-1528, 2016

M Hod, C Dobbrow, M Vaidyanathan, D Guin, L Belkhoura, R Strey, M Gottlieb, A M Schmidt “Controlling self assembly of magnetic nanoparticles by competing dipolar and isotropic particle interactions”, *Journal of Colloid and Interface Science* , 83, 436 , 2014.

C. Dobbrow, M. Vaidyanathan, L Belkoura, D Guin, A M Schmidt “ Cobalt Nanoparticles with tuned interaction potential: Towards worm and chain-like aggregates”, *Magnetohydrodynamics*, 47(2), 183 , 2011

P D Vaidya, P Konduru, M Vaidyanathan, E Y Kenig “Kinetics of carbon dioxide removal by aqueous alkaline amino acid salts”, *Industrial and Engineering Chemistry Research*, 49 (21), 11067, 2010.

PATENTS

Sadik Esener, Negin Mokhtari, Mukanth Vaidyanathan, Yasan Yeh, Bartu Ahiska, Ajay Sapre “Nano-Scale delivery device and applications thereof“, provisional patent 15/449,83

Sadik Esener, Mukanth Vaidyanathan, Negin Mokhtari, Yasan Yeh “Multiple enzyme cascading nanoparticle system“, disclosure accepted, provisional review

Abstract of the Dissertation

**Novel Silica Coated Lipid Nanocarriers for Diagnostics and
Therapeutics**

by

Mukanth Vaidyanathan

Doctor of Philosophy in Chemical Engineering

University of California San Diego, 2017

Professor Sadik Esener, Chair

While enzymes of non-human origin are attractive for therapeutic and diagnostic applications like in cancer, viral infection and brain diseases, their clinical use has been limited due to the immune response against foreign proteins. These enzyme can be hidden and incorporated in particles that are capable of harnessing ultrasound energy such that focused ultrasound can expose the enzyme to its substrate. However, the immune evasion and delivery specificity are key challenges needing to be addressed.

We propose a silica coated enzyme encapsulated lipid nanoparticle (SiLi) that protects the enzymes encapsulated within its hollow core of the liposome from immune attack whilst allowing access to their substrates through its porous secondary silica layer. The accessibility of the substrate to the enzyme is controlled

through ultrasound.

In this dissertation, The unique fabrication process of the liposome is discussed whose integrity can be exploited by the application of ultrasound. The ability of the secondary coating prevents the proteases to neutralize the enzymes in SiLi particles whilst maintaining structural integrity. The residence time of the liposomes and SiLi are also evaluated through intramuscular injections at the hind limbs *in vivo*. Additionally different methods to fabricate silica on top of the liposomes are also discussed.

Finally the application of SiLi with different enzymes for therapy and diagnosis are also explored. Enzyme based oxidative therapy were investigated to generate ROS at the site of injection. Glucose oxidase was used to test the therapeutic efficacy in cells as well as tumor xenografts. SiLi loaded with cocktail of enzymes are fabricated to optically detect small molecules like ACh. ACh is an important neurotransmitter which play a key role in the manifesting Alzheimer's and Parkinson's pathology. Thereby a nanoparticle optical probe to detect ACh plays a pivotal role in brain mapping which could provide insights to disease progression and possible therapeutic targets.

Chapter 1

Introduction

Enzymes are protein reactors that conduct chemical reaction in the body. Enzymes are globular proteins that catalyze alone or through the formation of several complexes. Several enzymes are found in a living body which catalyze different reactions which are necessary to facilitate, sustain and thrive life on earth. There are several enzymes which are devoid in humans but present in several other organisms that we have harvested for our benefits like the zymase which are still being used to generated alcohol from sugar. However this has led to the discovery of several enzymes which have been found to have a therapeutic and diagnostic aspect in human.

Non human enzymes have been employed for the treatment of several diseases especially cancer. Almost all the therapies in the clinic used so far includes small molecules and radiation. Unfortunately, they lack the tumor specificity and accompanies with severe side effects which undermines any therapeutic treatments. Hence there is a need for the treatment techniques with improved specificity and prolonged sustenance in the body. Enzymes offer this specificity by interfering with innate immune mechanisms and regulated processes in the body like angiogenesis, apoptosis. However, most of these promising enzymes are not suitable for clinical use, since they fail to remain active inside the body without aggravating the immune response which results in poor bio availability. Thus foreign enzyme based therapies and diagnostics require an effective delivery platform that can allow stealth operation whilst preventing any access of antibody or serum proteases

to the enzyme encapsulated. The delivery method must be performed at low cost and complexity without compromising the enzyme activity.

The most commonly used delivery platform without compromising the enzyme activity is with the use of nanoparticles. Several nanoparticles organic and inorganic have been employed to release the drug or proteins at site of interest. However, certain enzymes when exposed to the substrate which are ubiquitous in the body might undermine the therapeutic efficacy of enzyme based therapies like in oxidation therapy (The addition of enzyme to generate ROS in the presence of substrate leads to systemic toxicity). In order to prevent systemic toxicity by localizing the effect of these therapies to the site of interest and to achieve target-specific release, the next inevitable step is for remote-triggered activated release. Instead of depending on the biological local environment of the target tissue, release would be reliant on an independent external trigger. One of the strategies used effectively in the clinic is the use of ultrasound. Ultrasound is desirable trigger because there is no risk of exposure to ionizing radiation present and offers area-specific penetration without being invasive in the body.

This dissertation elucidates a novel nanoparticle platform, Silica coated enzyme loaded Cationic Liposomes (SiLi). The enzyme encapsulated through the emulsion process remain suspended in the hollow core remain active whilst being protected through the secondary silica layer. Chapter 2 explains the synthesis and fabrication of these Silica coated enzyme loaded Cationic Liposomes (SiLi), efficient protection from antibody access and neutralization, protection from proteolysis, stability with and without the application of ultrasound *in vivo* and "activation" of the enzyme activity upon application of the ultrasound.

Chapter 3 discusses potential applications of SiLi with therapeutic enzymes, including Glucose Oxidase (GluOx) and Choline Oxidase (ChOx) for various types of cancer through oxidation therapy. These enzymes have proven efficacy *in vitro* but fail to make it to clinic because of systemic generation of toxicity. However this chapter explains the possible use of GluSiLi.

Chapter 4 discusses potential diagnostic application using multiple enzymes with different size for detecting neurotransmitters. These enzymes are successful in optical detection of neurotransmitter *in vitro* but suffer the same fate as other

enzymes because of the innate immunity generated against these foreign enzymes.

Chapter 5 explains the ATP detection nanoparticle mechanism using luciferase. The luciferase was loaded in Synthetic Hollow Enzyme loaded silica nano spheres (SHELS). These were designed to detect ATP in tumor sites and in pericellular cavity of the neurons. The synthesis and fabrication of SHELS are explained along with the activity retention of the enzyme upon exposure to proteases. The effect of different surface coating was explored for effective ATP detection. Lastly the luminescence was captured in SHELS through high speed camera.

The dissertation concludes by examining the future potential applications of SiLi for macromolecule delivery.

Chapter 2

Silica Coated Enzyme

Encapsulated Cationic Liposomes

2.1 Liposome

The name liposome is derived from greek works: "Lipos" meaning fat and "soma" meaning body. It is a tiny vesicle made out of the same material as a cell membrane, phospholipids [1]. Under normal conditions, the vesicles are spherical and contain more than one lamellae that are composed of amphiphiles[2][3]. In nature, liposomes are formed by phospholipids which form stable bi-layer membranes in which the hydrophobic part of the amphiphiles forms the interior of the bilayer and the hydrophilic part (head group) is in contact with the aqueous phase. There are several other components to a stable liposome, phospho lipids like phosphatidylcholines provide the backbone and structure to lipids, Cholesterol alters the mechanical properties of the lipid bilayers [4] and the anionic dicetylphosphate (3 dihexadecylphosphate) or the cationic stearylamine or DOTAP (1,2-dioleoyl-3-trimethylammonium-propane) with the aim of preventing vesicular fusion[5]. To prevent rapid clearance from the blood, the lipid-polymer derivative of polyethylene glycol (PEG) are used to synthesize liposomes[6]. The interior of the vesicle is an aqueous core which is of the same chemical composition of the protein or drug being encapsulated. In fact, they can contain a wide variety of hydrophobic diagnostic and therapeutic payloads (See figure 2.1). Thus providing a larger

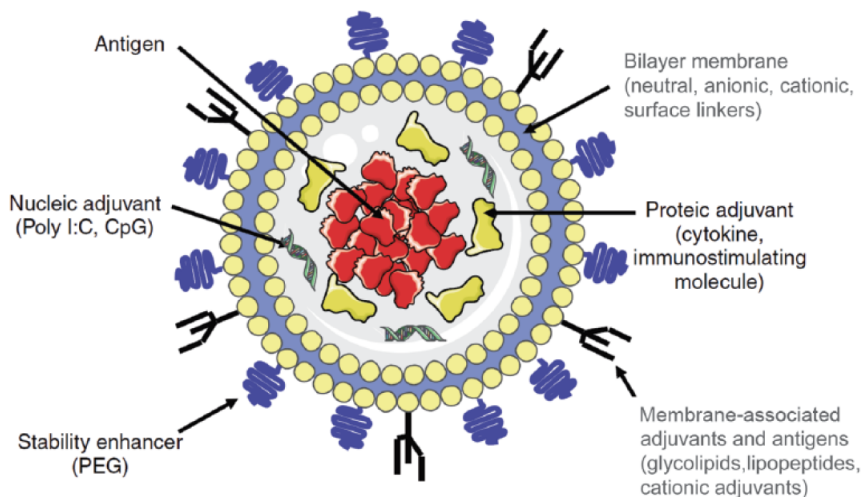


Figure 2.1: Schematic representation of a small monodispersed liposome elucidating the versatility of liposomes by incorporating various compounds either by encapsulation or by surface attachment of the lipid membrane [7]

encapsulation efficiency per particle and also protecting the encapsulated payload from metabolic process and immune clearance[8] [9]. Liposomes are available in many different sizes and shapes. In case of a bilayer structure encapsulating a payload, is called a liposome, a monolayer structure is called a miCeLle while a multiple concentric bi-layers is called a large lamellar vesicles [10]. The size of liposomes vary from 50-1000 nm in diameter which serves as a convenient delivery tool.

Because of their biocompatibility, biodegradability, low toxicity and multifunctionality to encapsulate both hydrophilic and hydrophobic payloads and ease in manufacturing has led to its use in vaccines like Inflexal V for influenza [11], chemotherapy and synthesis of anti-cancer drugs like Doxil [12], anti bacterial[13] and anti fungal treatments (Abelcet, Amphotec [14]), protein delivery like insulin [15]. The critical factors for successful formulation of liposomes are their colloidal and chemical stability of the lipid bilayer. Unfortunately, Vesicular aggregation, fusion and creaming are the major concerns for the stability of the liposomes which could lead to the increase in size and change in charge which could limit the application of liposomes. It also suffers from physical instability during manufacturing and

storage. Phospholipids are sensitive to acidic or basic hydrolysis and unsaturated phospholipids are susceptible to oxidative degradation which makes it unsuitable for oral delivery[16]. Apart from oxidative degradation, chemical degradation and hydrolysis of the ester bonds linking the fatty acids (Cholesterol) to the glycerol backbone could lead to performance failure and peroxidation of unsaturated acyl chains [17][18][19].

2.1.1 Silica Coated Liposomes

Extensive research have been conducted to improve the stability of liposomes either by addition of lipid-PEG conjugate [20], polymers [21], polyelectrolyte layer-layer assembly[22] and colloidosomes[23]. However, the chemically assembling Silica layer onto the external surface of the liposomes have been very successful because it retains the fundamental properties of the free liposomes [24]. Silica coated liposomes act as nonporous spheres for larger molecules like protein but extremely permeable for smaller molecules like glucose, ATP, vitamins. Silica nanoparticles can be prepared from various process: noncovalently bound organic substrates (surfactants, lipids, polymers), cavitation, electrodeposition, spray drying, super critical fluid technology, self assembly and sol-gel polymerization [25][26] [27] [28]. Due to the inert nature of Silica, it has been used for enhanced oral absorption of hydrophobic drugs like CeLecoxib and indomethacin [29].

2.1.2 Active Targeting of the Liposomes

The stability of the liposomes to retain their payload on circulation have been exploited to deliver drugs to disease tissues. Apart from passive targeting through EPR, triggering the release of the payload upon reaching the target site would vastly improve the therapeutic efficacy with minimal side effects. Two main kinds of triggers have been studied, one is remote trigger through external source like the heat, ultrasound, light and magnetism and second, endogenous triggers that are mainly prevalent in the target site like through enzyme and pH.

To release the loaded payloads in the liposomes, one could change the temperature to below the glass transition temperature of the lipids which leads to

aberrations in the lipid bi-layer packing, thereby creating transient pores [30], the use of pulses of strong electric field to break the membrane apart [31], the use of magnetic field to induced 2-4°C change in temperature leading to the phase transition temperature of the lipids used [32], visible light which could lead to photo degradation of lipids or a photo sensitive molecule attached to the cholesterol [33], pH [34] and use of ultrasound (US) to acoustically disrupt the bi-layer through cavitation [35][36][37].

Ultrasound is widely used in medicine for many years mostly as a diagnostic tool in gynaecology, obstetrics and cardiology[38]. Ultrasound can be categorized as either low- or high-intensity. The High Intensity Ultrasound (HiFU) (1MHz) are usually focused at a point of interest to increase the temperature to 60°C which causes ablation[39] while Low Frequency Ultra Sound (LFUS) (20kHz to 1MHz) are used to imaging and improve the permeability of biological barriers like the skin[40][41]. Ultrasounds contrast agent like air, gas and low diffusive gases like perfluoro carbons was developed to enhanced the reflected signal from the site of interest. These contrast agents were called as echo enhancers. Due to low toxicity of the liposomes and the tendency of the lipids to expand under low frequency ultrasound let to the usage of the liposome as carriers of the echo enhancers. Thereby, Exposing the liposomes to low-frequency ultrasound causes the formation of transient pores on the packing arrangement of the lipid bi-layer within the membrane resulting in an increase in the permeability of the liposome and thereby releasing the drug.[42][43].

Recently there has been growing interest in combining ultrasound and liposome for triggered release of anti cancer drugs that have low release kinetics like the cisplatin[41][44][45]. The advantages foreseen to encapsulating this drug within a liposome was to achieve reduced toxicity and drug resistance. Since cisplatin and doxorubicin in doxil are highly small neoplastic compounds, The liposome should maintain enough structural integrity to retain the drugs and remain in circulation so that it accumulates in the cancer tumors and release the payload upon ultrasound exposure. Hence the lipid formulation plays a very vital role in this combined treatment [46][47]. However with larger payloads like enzymes, the released enzymes upon application of ultrasound would be counter productive as the

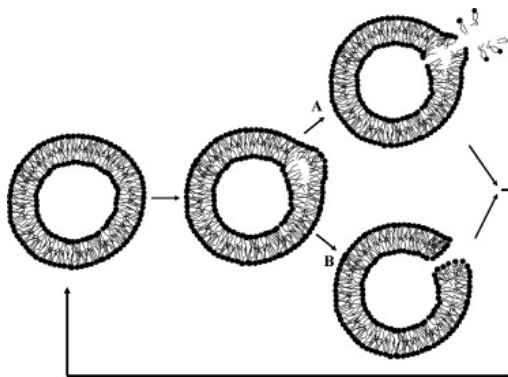


Figure 2.2: A schematic representation of the formation of transient pores in the liposome membrane by ultrasound. The transient pores may occur due to formation of small gas nuclei in the hydrophobic region of the lipid bilayer under the effect of an ultrasonic field. The pores may be either hydrophobic (A) or hydrophilic (B) in nature, and tend to reseal after short periods of time. The formation of transient pores may free membrane fragments from the liposomes, which will then form into smaller lipid aggregates. [41]

released enzyme would generate heightened immune response as the enzymes are of foreign source. Hence liposomes loaded with enzymes require access to the substrate in the serum but remain protected from antibody neutralization and hence require additional secondary coating like Silica, whose structure and function remains unaffected by the ultrasound[48].

This chapter would elucidate the combination therapy of liposomes coated with secondary layer of hydrolyzed Silica and Ultrasound. The application of ultrasound triggers the breakage of the lipids and hence making the particle porous to substrate. The enzyme remain active upon ultrasound with little to no immune response. We specifically show the activation of the enzyme and its sustained activity upon treatment with the serine proteases. Subsequently section also compares the bio availability of the Silica coated liposomes to the cationic liposomes through the encapsulation of BSA conjugated fluorophore. We have also demonstrated that upon subsequent exposure of the ultrasound doesn't affect the bio availability of the Silica coated liposomes *in vivo*.

2.2 Materials

L-Alpha-Phosphatidylcholine derived from egg yolk (Egg-PC) of 25 mg/ml stock solution in chloroform, Cholesterol powder, 1,2-Distearoyl-sn-glycero-3-phospho ethanol amine Poly-ethylene Glycol MW5000 (DPSE-PEG) powder and 1,2-Dioleoyl-3-trimethyl ammonium-propanol (DOTAP) of 10mg/ml stock solution in chloroform were purchased from Avanti polar lipids, USA. Diethyl ether and Tetramethyl orthoSilicate (TMOS) were purchased from Sigma Aldrich, MO, USA. Phosphate buffer saline was purchased from Life Technologies, USA. Nucleopore Track-Etch Whatman filters 13mm (800 nm, 400nm and 200 nm) used in the extrusion process and 19mm Nucleopore Track-Etch Whatman 30 nm pore size filter were purchased from EMD Millipore, Darmstadt, DE. The magnetic dialyzing cartridge: fast SpinDialyzer was purchased from Harvard Apparatus, Holliston, MA. Lyophilized betalactamase (BLA) from *Enterobacter cloacae* was purchased from Sigma Aldrich, St Louis, MO, USA. Bovine serum albumin conjugated with alexafluor 680 (BSA-AF) was purchased from Thermo Fisher Scientific, Waltham, MA. Nitrocefin was purchased from Millipore MD, Darmstadt, DE and used to test the enzyme kinetic of BLA. Phosphate Buffer Saline (PBS) was purchased from Hyclone Laboratories Inc, Logan, UT. All the chemicals were used as received.

2.3 Methods

2.3.1 Synthesis of Enzyme Loaded Cationic Lipid nanoparticles (liposomes) (CeLi)

The cholesterol stock solution was prepared with 38.7 mg of lyophilized powder of cholesterol in 1 ml of Chloroform. The DSPE-PEG stock solution was prepared by mixing 50mg of DSPE -PEG in 1 ml of chloroform. All the lipid stock solutions were prepared in chloroform and stored in -20°C freezer. Egg-PC and DOTAP was used as received. Liposomes were synthesized through a modified version of the reverse phase evaporation technique developed by Papahadjopoulos [49]. It consists of three step process.

Solution A: 295 ul of 25mg/ml of Egg-PC, 40 ul of 38.7 mg/ml of Cholesterol, 50ul of 10mg/ml of DOTAP were mixed in a glass vial and the chloroform was evaporated using Buchi Rotavapor R-300 at 100 rpm at 25° C for 20 minutes to form a thin lipid film. Then 1ml of diethyl ether was added to re-suspend the lipids in ether.

Solution B: 40 ul of 38.7mg/ml of cholesterol, 50 ul of 25mg/ml of DOTAP and 60 ul of DSPE-PEG stock solutions were mixed in 0.5 ml eppendorf tube. The chloroform was evaporated under a gentle stream of nitrogen while vortexing the open tube. 100ul of the PBS was added while making empty liposomes or 100 ul of 100mg/ml of BLA was added to make enzyme loaded liposomes. All the enzymes were hydrolyzed individually using PBS. The lipid-payload solution was vortexed thoroughly for 30 secs until all the lipids are constituted in the solution.

Solution C: 60 ul of DSPE-PEG stock solution was evaporated under gentle nitrogen stream while vortexing in a 1 ml eppendorf tube. Then 1 ml of PBS was mixed until all the lipids are evenly mixed in the solution.

Solution B was added dropwise in the glass vial containing solution A under vortex. Then solution was allowed to vortex in high speed for 1 minute. This emulsion is homogenized to ensure proper mixing using the Power Gen 125 homogenizer from Fisher Scientific for 2 minutes. The ether in the stabilized emulsion is evaporated under vacuum using Buchi Rotavapor at 100rpm at 30°C for 25 minutes. This produces a sol-gel like precipitate. The sol-gel mixture is then hydrated by addition solution C dropwise under gentle vortex. Gentle stream of nitrogen was used to create vortex to break apart large chunks and then vortexed for 30 seconds. This solution was placed in vacuum for 45 minutes under a water bath at 30°C. The liposomes are then extruded three times using a syringe extruder with 800nm, 400nm and 200nm filters respectively. The extrusion process was slow and steady to ensure homogeneous solutions of liposomes are formed. To remove excess enzyme and lipids, the solution was dialyzed at 160 rpm at room temperature overnight using the fast SpinDialyzer with 19mm whatman filters with pore size of 30nm. Schematic representation on the synthesis of CeLi is shown in the figure2.3.

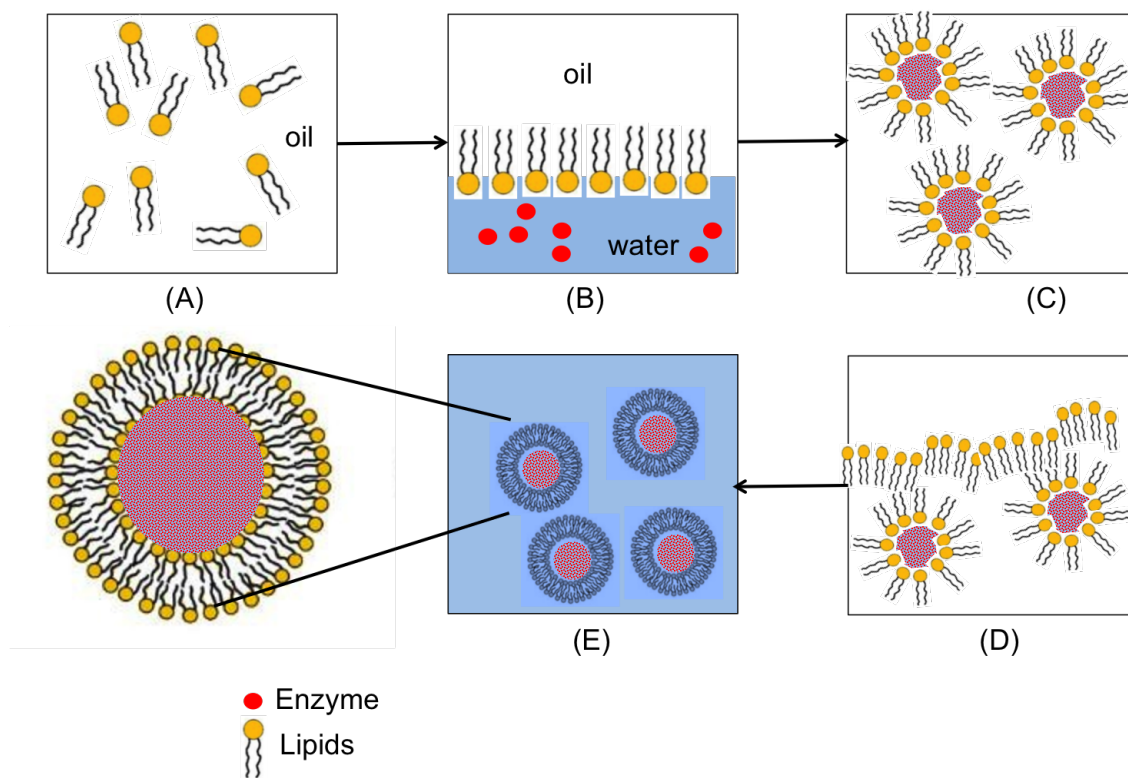


Figure 2.3: A schematic representation of the formation of liposomes through reverse phase evaporation. (A) Solution A (B) Addition of solution B to Solution A (C) Water in oil emulsion is formed to form stable micelles (D) Gel formation upon solvent evaporation (E) Dissolution of the gel with solution C

2.3.2 Synthesis of Silica Coated Enzyme Loaded Liposomes (SiLi)

The CeLi are used as a template to precipitate Silica using sol-gel method as shown below in figure 2.4. 50 μl of the liposomes is diluted with 1 ml of PBS. 2 μl of TMOS is added drop wise over vortex to this solution and mixed for 4 hours at 3200 rpm in a shaker at room temperature to form Silica coated Liposomes (SiLi). To terminate the hydrolysis of TMOS, the SiLi solution was washed three times in PBS using a centrifuge at 3000 rpm for 15 minutes at 25°C.

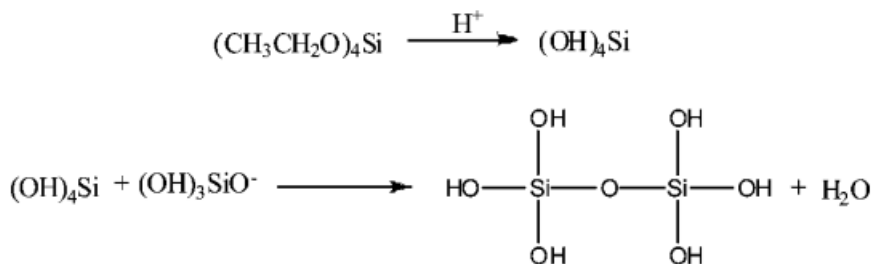


Figure 2.4: A silica formation process using PBS and TMOS

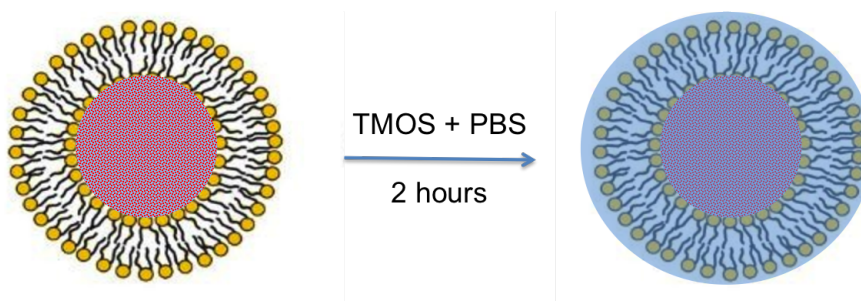


Figure 2.5: A schematic representation of the formation of silica on CeLi

2.3.3 Synthesis of Calcium Phosphate (CaP) Coated Enzyme Loaded Liposomes (CaL)

50 μ l of CeLi is diluted with 1ml of 0.1X PBS. 100ul of 1mM of calcium chloride (CaCl_2) is added dropwise under vortex to diluted CeLi mixture. The mixture was mixed for 30 mins to 1 hour at 3200 rpm at room temperature. To terminate the deposition, the solution was washed three times in PBS using a centrifuge at 3000rpm for 15 minutes at 4°C.

2.3.4 Characterization of the CeLi, SiLi and CaL

The size and surface charge of the liposomes were characterized using Zetasizer Nano from Malvern Instruments, Malvern, UK. The size was also characterized using electron microscope images using the Helios NanoLab DualBeam from FEI. The particle count was analyzed using ViewSizer 3000 from Manta, San Diego, CA. The activity of the enzyme was optically detected using Spark M20 from Tecan, Mannerdorf, SUI.

2.3.5 Nitrocefin Assay for the Measurement of BLA activity

For the colorimetric determination of penicillinase activity, 100 μ l enzyme solutions were transferred onto a 96-well microtiter plate. 25 μ l nitrocefin working solution was added to each well. 5 milligram nitrocefin was dissolved in 500 μ l DMSO, and 9.5 mL 1X PBS was added to obtain the working solution. Absorbance at 486 nm was measured at 37°C using Infinite 200 PRO Plate reader and Spark M20 Tecan (Switzerland) .

2.3.6 Measurement of *in vivo* Activity

Athymic, nude mice were purchased from the Jackson Laboratories (Stock number: 002019). Mice were housed in high-efficiency particulate air (HEPA) cages in a specific-pathogen free (SPF) facility at OHSU. Mice were fed a diet of PicoLab Mouse Diet 20 (LabDiet, 5058) ad libitum and started one week prior to imaging. 10 week old male nude mice were given a single 100uL intramuscular injection of either SiLi, CeLi and Free BSA-AlexaFlur in the both high leg muscle. Mice were imaged for fluorescence (excitation wavelength = 680nm, emission wavelength = 710nm, exposure = 0.2sec) after correcting for background fluorescence using the IVIS Lumina XRMS Series III (PerkinElmer). All experiments performed were approved by the Institutional Animal Care and Use Committee (IACUC) at OHSU.

2.3.7 Measurement of Activation of the CeLi and SiLi using Ultrasound

For *in vitro* ultrasound activation, The BLA encapsulated in the liposomes and SiLi were treated with 50KHz bench top sonicator. The samples were treated with pulsed ultrasound at 2 second on and 1 second off intervals for 2 minutes at 40% amplitude under ice bath to prevent overheating of the sample and therefore leading to enzyme denaturation.

For *in vivo* ultrasound activation, SiLi, CeLi and unencapsulated BSA-Alexa

Flur were injected on the left and right hind leg muscle. The left hind leg was exposed to ultrasound at 25-55MHz for 30 seconds and the region of injection was scanned at 100frames/second using (write this equipment down). The fluorescence was measured using IVIS Lumina XRMS Series III (PerkinElmer) as described above.

2.4 Results

The proteins (BLA and BSA-AF) are encapsulated during the formation of water-oil emulsion during the formation of the liposome nanoparticles. The size of the nanoparticles are of utmost importance to ensure higher circulation or retention time in the body. The size of the nanoparticles synthesized was measured before and after dialysis as well after coating it with Silica. The figure2.6 shows the size distribution of CeLi (before and after dialysis) and SiLi particle to around 215 nm irrespective of the coating.

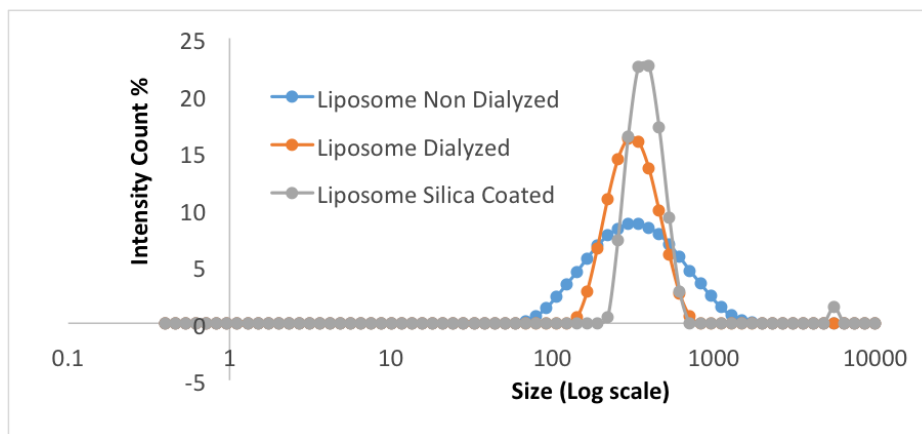


Figure 2.6: The size of the non dialyzed CeLi (Blue), Dialyzed CeLi (Orange) and SiLi (Grey) were all measured at the same dilution in 1X PBS with 12 runs for each measurement using disposable clear size cuvettes

The CeLi particles are cationic and with an average charge of around +15mV. This cationic charge is due to the presence of DOTAP in on the lipid bilayer. Since Silica (from TMOS) is anionic, it would preferentially deposit on the cationic CeLi particles thereby changing the charge of the particles to shift from +15mV to -36mV as shown in 2.7.

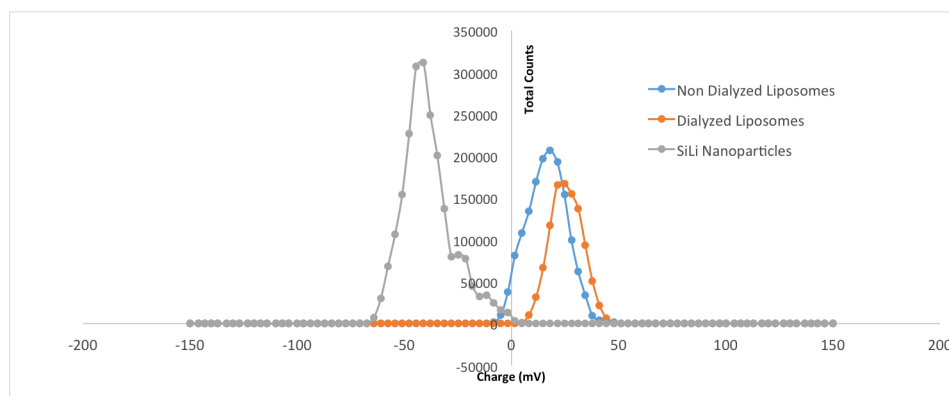


Figure 2.7: The change in the surface charge between non dialyzed CeLi (Blue), dialyzed CeLi (Orange) and SiLi (Grey) were all measured at the same dilution in DI water with 12 runs for each measurement using disposable clear zeta cuvettes

For characterization of the nanoparticles, BLA was encapsulated in the CeLi and SiLi. BLA (43kDa) is a member of the family of beta-lactamases that catalyze the hydrolysis of the beta-lactum ring [50][51]. BLA was selected for the characterization of Silica coated liposome (SiLi) because sensitive chromogenic and fluorogenic assays were available[52]. The encapsulation efficiency of the nanoparticles was determined by incubating all the samples with 0.1mg/ml of proteinase K (28.9kDa) overnight at 37°C while mixing. Proteinase K is a broad spectrum serine protease that cleaves at the peptide bond adjacent to the carboxyl group of the aliphatic and aromatic alpha amine groups [53][54][55]. The activity of the enzyme which is encapsulated by the particles can be determined using nitrocefin assay. Nitrocefin being a cephalosporin contain beta-lactum ring which is susceptible to BLA mediated hydrolysis. Once hydrolysed, nitrocefin rapidly changes color from yellow to red which can be measured as an increase in absorbance at 486nm using UV-Vis spectrometer. Figure 2.8 demonstrates the protection of the enzymes which are encapsulated within the SiLi particles upon sustained exposure to proteinase K.

The purpose of DOTAP while forming the emulsion was to provide a cationic charge to the CeLi particles thereby providing an oppositely charged template to drive preferential silica deposition. Hence, Silica, an FDA approved inorganic material could be electrostatically and chemically deposited on the CeLi surface. Silica can be precipitated on any surface especially nanoparticles using many different

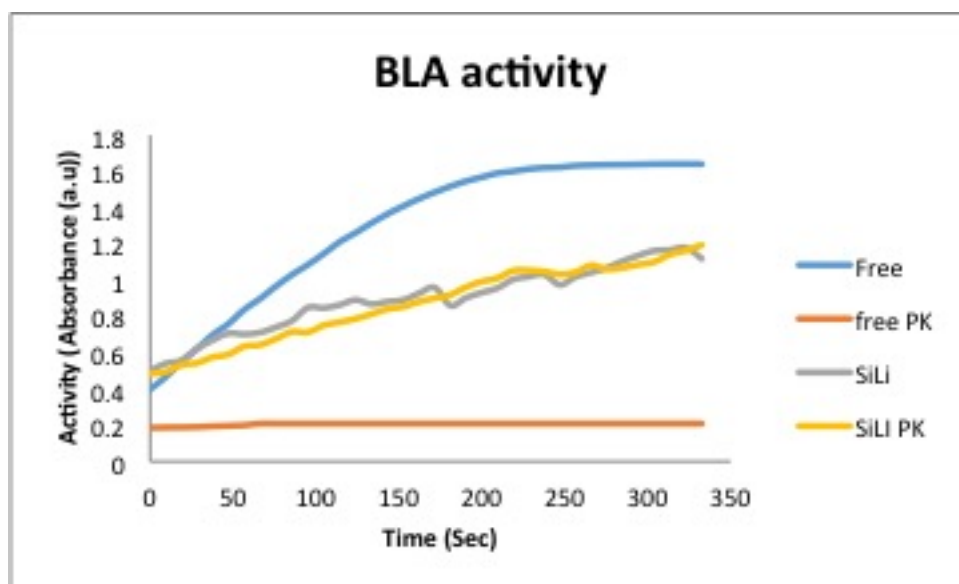


Figure 2.8: Activity plots of unencapsulated and encapsulated BLA in SiLi with and without incubation with proteinase-K for 24 hours at 37°C in 1X PBS in bench top shaker. 0.5 mg/ml of nitrocefin in 1mM phosphate buffer was added to measure the increase in absorbance at 486 nm.

substrates [56]. APTMS, TMOS and Silicic acid (highly reactive and acidified form of TMOS) was the choice of precursor for the formation of synthetic silica shell on the CeLi particles along with CaP. Figure 2.9 shows all the different surface coating techniques were employed on BLA loaded CeLi and tested for BLA activity after encapsulation and also after treatment with proteinase K.

Sonication of the CeLi and SiLi particles were performed for 2 minutes at 40% amplitude at 2 seconds on and 1 seconds off using 500W 20kHz sonicator attached to a cone to prevent sample contamination from the insertion of the probe. As seen from figure 2.10 the sonicated and non sonicated samples were incubated with the PK. The BLA-CeLi particles showed an 700% increase in the activity of the sonication while BLA-SiLi showed an 800% increase in activity. However, upon incubation of the samples with proteases, BLA-CeLi showed 97% loss in activity and upon sustained sonication did not revive the activity of the BLA. Whereas, the BLA-SiLi retained 97% of the enzyme activity and upon sustained exposure for an additional 48 hours with proteases did not lower the enzyme activity.

100 μ l of BLA-SiLi, BLA-CeLi and Free BSA-AF were injected intramuscu-

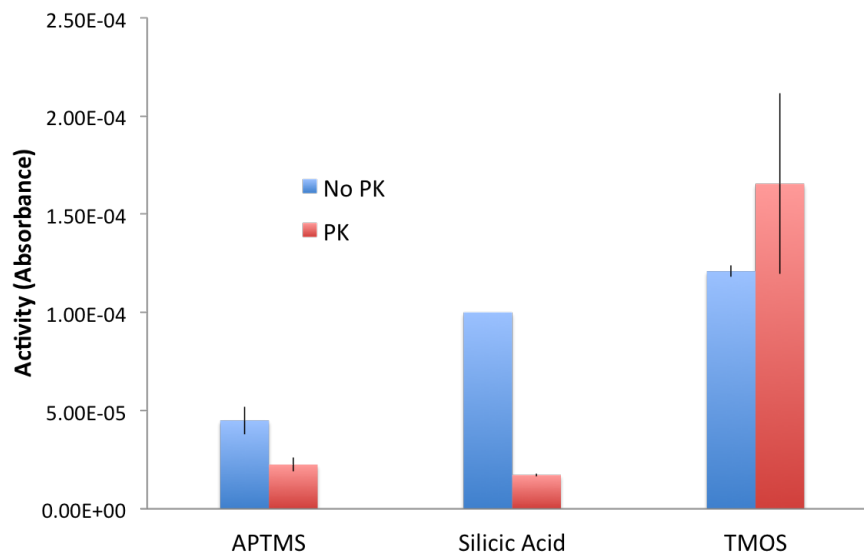


Figure 2.9: Activity plots of BLA with different surface coating with and without the treatment with PK. The PK was treated for 24 hours at 37°C in 1X PBS in benchtop shaker. 0.5 mg/ml of nitrocefin in 1mM phosphate buffer was added to measure the increase in absorbance at 486 nm.

larly on either side of the hind limbs of the mice. 55MHz of US was applied on the left hind limb for 30 seconds and images were captured through IVIS. Figure2.11 and Figure2.12 shows the comparison between different particles with the free. The free BSA and BSA-CeLi lost its fluorescence within 1 day and 4 day respectively while the BSA-SiLi lasted for about 7 days before disappearing. Dye-IR was used to tag the lipids in the liposomes and were found to be at the site of injection even after 9 day post injection.

2.5 Discussion

Strong anionic shift in the surface of the CeLi particles is a clear indication of the addition of silica on the surface of CeLi. As seen in figure2.7 there is a strong shift toward the negative paradigm. This shift is due to the anionic nature of silica. The size of the particles was confirmed with SEM as its nearly impossible to image liposome using the standard SEM as it would collapse under vacuum.

Figure2.8 indicates that secondary silica layer in SiLi provides a physical barrier for against proteases and antibody. Upon sustained exposure to proteases, the

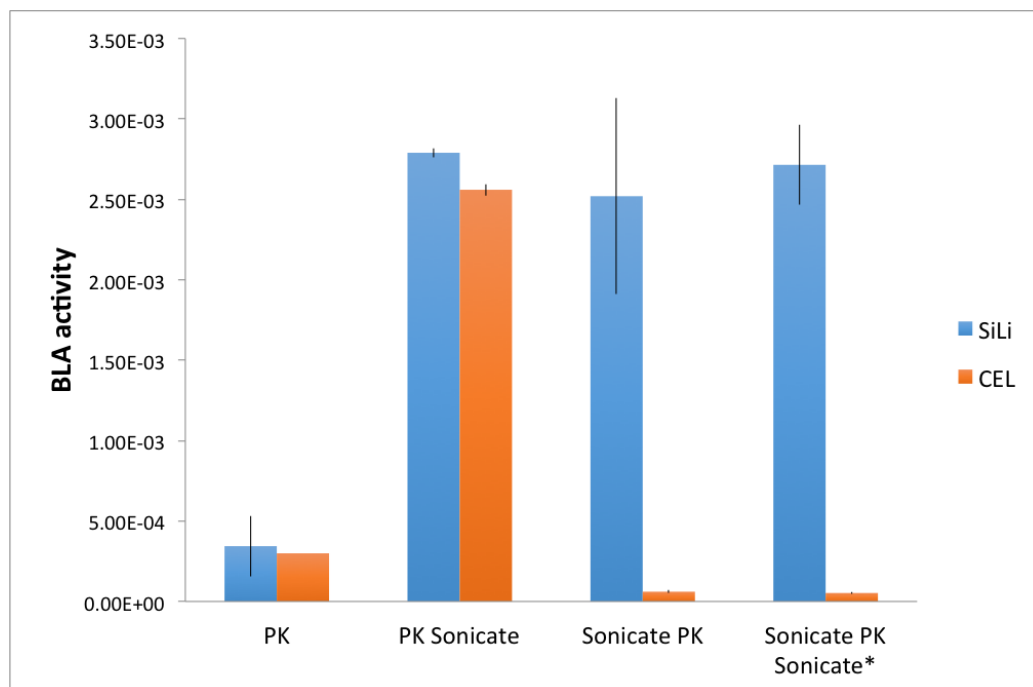


Figure 2.10: Activity plots of the BLA-CeLi and BLA-SiLi particles upon incubation with protease for 24 and 48 hours in 37°C. PK samples: Particles incubated with PK prior to sonication. PK sonicate: Particles that were sonicated 24 hours after the addition of PK. Sonicate PK: Particles were sonicated prior to the addition of PK and incubated for 24 hours. Sonicate PK Sonicate*: Particles were sonicated, incubated with PK for 24 hours. Then sonicated again and incubated with PK for an additional 24 hours

free enzyme would be denatured as there isn't any barrier protecting the enzyme from proteases while the enzyme in SiLi retains its activity indicating complete protection from the proteases whilst having access to the substrate. Silica can be deposited on a template through many precursors while we have tried to use three different precursors. From Figure, TMOS seems to form a much more compact Silica structure while being non-porous to the proteases and hence retaining the most activity after incubation with PK.

CeLi generally tend to form a tight barrier thereby limiting the interaction of the payload with the environment. Hence, it has been proven through many studies that this tight layer can be disrupted through sonication (see figure 2.10). Since the payload in our study is an enzyme, losing the payload upon the application of ultrasound would be counterproductive to our objective. Therefore, the

addition of secondary barrier in SiLi not only protects the enzymes from the environment but also retains the enzymes inside the particles upon sonication. This ability to retain the enzymes after sonication is absolutely necessary *in vivo* to prevent heightened immune response. Figure 2.10 clearly elucidates the retention and protection capabilities of SiLi particles. The addition of PK mimics the proteases present in the body *in vitro*.

To envision the usage of any fabricated nanoparticle, high priority is given to animal experiments. Similarly with CeLi and SiLi, SiLi particles are retained in the muscle for about 7 days post injection. However, the lipids labelled with Dye-IR is clearly visible at the site of injection even after the loss of the BSA-AF fluorescences which is the payload encapsulated inside SiLi. This indicates that SiLi particles clearly can be used for IM injection while the CeLi are really poor choice for IM injection as they tend to behave as free BSA-AF. Due to weak structural integrity of the CeLi particles, the addition of Si improves the retention time of the payload. It also clearly indicates that the addition of US doesn't necessarily affect the retention time of the SiLi.

However, the retention time can be improved further by the usage of additional lipids like sphingolipids, phosphosphingolipids, 1,2-dioleoyl-sn-glycero-3-phospho ethanol amine (DOPE) etc. These lipids are much more rigid and can prevent collapse of liposomes which triggers the release of payload. The secondary layer of silica is however too thin as addition of more TMOS just leads to formation of free silica particles rather coating a thicker layer on the particles.

2.6 Conclusion

Here we have demonstrated a process for consistent production of SiLi containing stabilized cationic liposomes. Though the overall structure is new, the outer Silica layer is amenable to standard functionalization and modifications well documented in the literature. These particles can be selectively insonified with ultrasound. This allows for both spatial and temporal control over activation of the enzymes by triggering perturbations within the lipid bi layer making these particles promising for *in vivo* studies.

The addition of ultrasound improves the enzymatic activity by providing lower diffusive resistance of the substrate into the particles. Certain application may require intravenous injection which may require additional fabrication of the Silica layer to prevent uptake in liver and spleen.

Inspite of the tight binding of the lipids in the liposomes, there are still leakage of the substrate into the particles. The use of sphingolipids in the CeLi may provide additional resistance thereby making the access of substrate to the enzyme even more harder.

2.7 Acknowledgments

This chapter and its methods are patented (Nanoscale delivery device and uses thereof,15/449,830) and the work is ready to be submitted for publication. Collaborator for the patent: Mukanth Vaidyanathan, Negin Mokhtari, Yasan Yeh, Ajay Sapre, Bartu Ahiska, Sadik Esener.

This chapter, in part is currently being prepared for submission for publication of the material. Mukanth Vaidyanathan, Zeynep Sayar, Jared Fischer, Ya-san Yeh, Negin Mokhtari and Sadik Esener. The dissertation/thesis author was the primary investigator and author of this material.

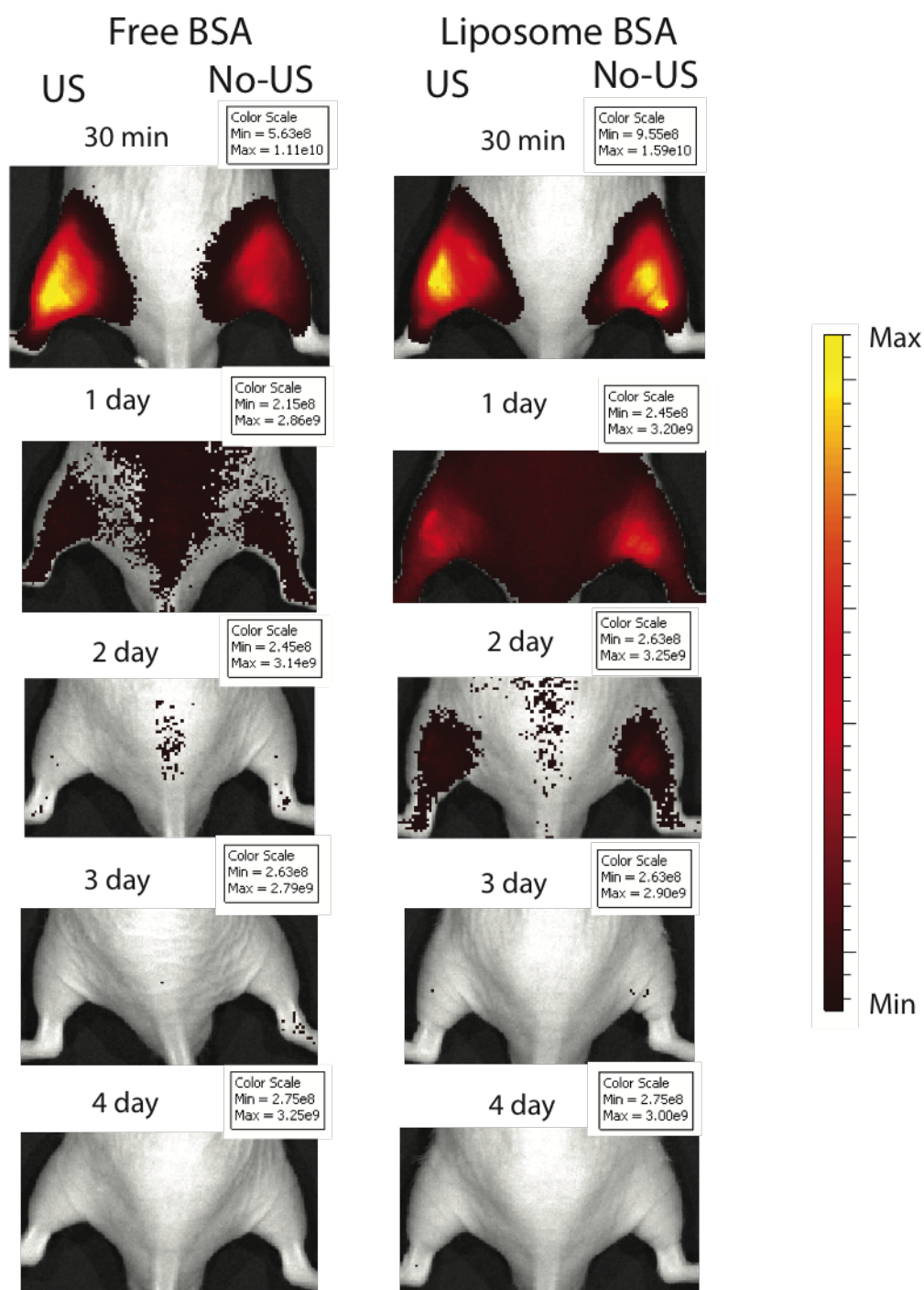


Figure 2.11: Demonstration of BSA-AlexaFLuor688 fluorescence in free and BSA-CeLi upon intra muscular injection

Liposome Silica BSA

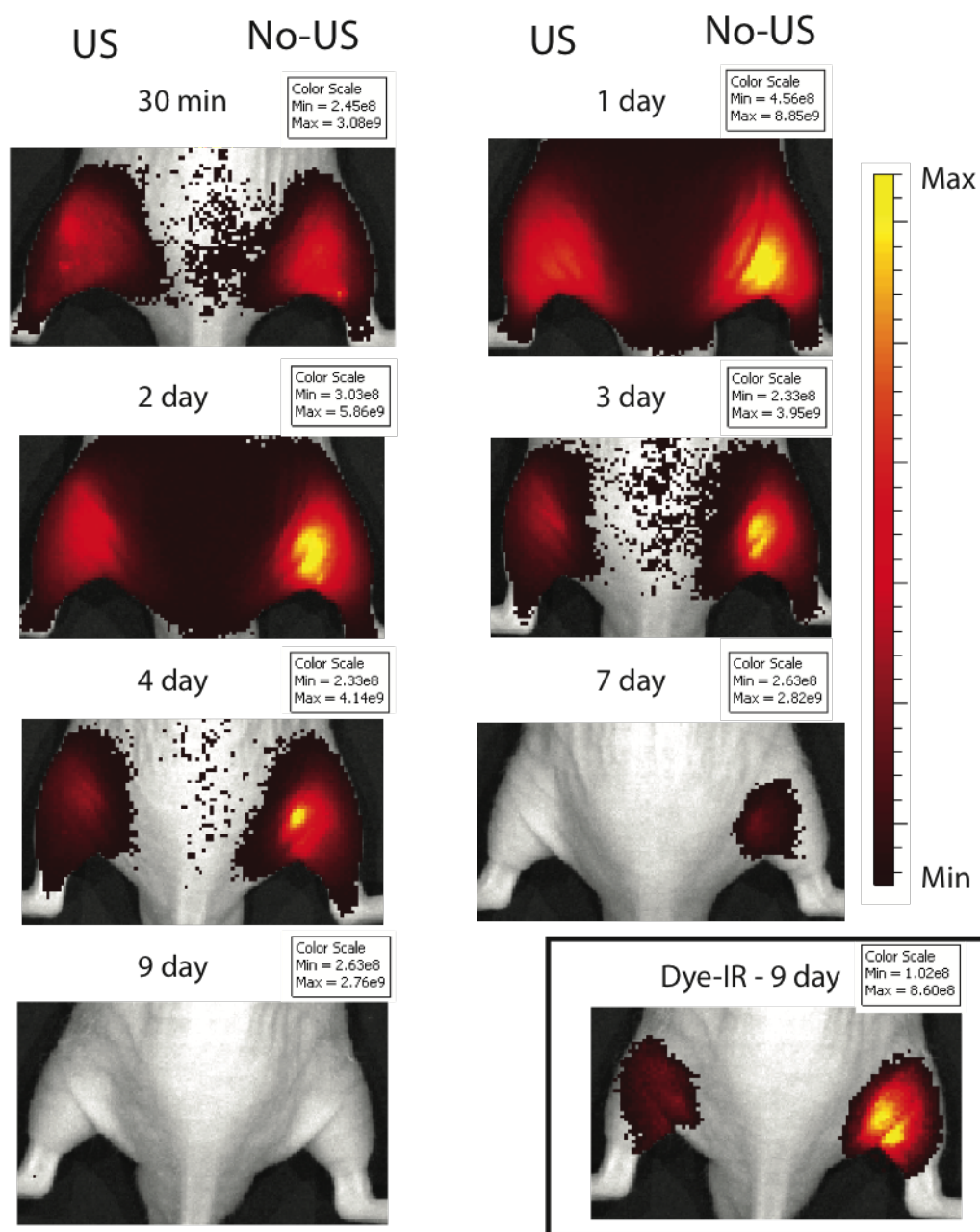


Figure 2.12: Demonstration of BSA-AlexaFLuor688 fluorescence in BSA-SiLi upon intra muscular injection at different time points. Inset is Dye-IR fluorescence image to label the lipids to form the liposomes

Chapter 3

Therapeutic Applications of SiLi

3.1 Glucose Oxidase encapsulated SiLi (Glu-SiLi) for *in vivo* generation of Hydrogen Peroxide

Reactive oxygen species (ROS) are small molecules of oxygen derived species, including both oxygen radicals (anions like O_2^- , OH^- etc) and non oxygen radicals (H_2O_2), that are highly reactive due to the presence of unpaired electrons. In aerobic life forms, molecular oxygen is ubiquitous and hence acts a perfect electron acceptor of the free radicals to form oxygen free radicals. ROS plays an important role in many cellular developments, growth, apoptosis, mutagenesis, drug metabolism, immunogenicity against foreign bodies and development of cancer[57][58]. ROS are predominantly generated during metabolism through various enzymes. However, in a mammalian cell, the ROS is involved in ATP synthesis by aerobic metabolism in mitochondria. However, electrons that escape the mitochondria react with oxygen to form of O_2^- which can be converted to H_2O_2 by superoxide dismutatase[59]. The H_2O_2 can readily cross the cell membrane through lipid peroxidation and lead to DNA damage [57]causing apoptosis. Additionally the free radical oxygens may also react with nitrogen to form reactive nitrogen species (NO ; NO_2). Under pathological conditions, excessive generation of these ROS (also known as oxidative stress) can initiate lethal reactions that initiates and progresses lethal diseases like the cardiovascular diseases, cancer, inflam-

mation, ischemia-reperfusion injury, viral pathogenesis, hypertension, formation of drug or microbe resistance etc. These lethal reactions involve the oxidation of the proteins involved cellular integrity and survival [60][61]. To overcome ROS, normal healthy cells have evolved and maintained a series of anti-oxidative defense mechanisms to minimize the exposure of these dangerous byproducts occurring naturally during cell metabolism[62]. The defense mechanism includes a cocktail of enzymes like super oxide dismutase, catalase and glutathione peroxidase and free radical scavenging compounds like heme oxygenase-1, glutathione, tocopherol, ascorbate. Hence the balance of ROS and anti-oxidative defense level is critical for cellular growth, survival and sustenance as shown in the figure 3.1.

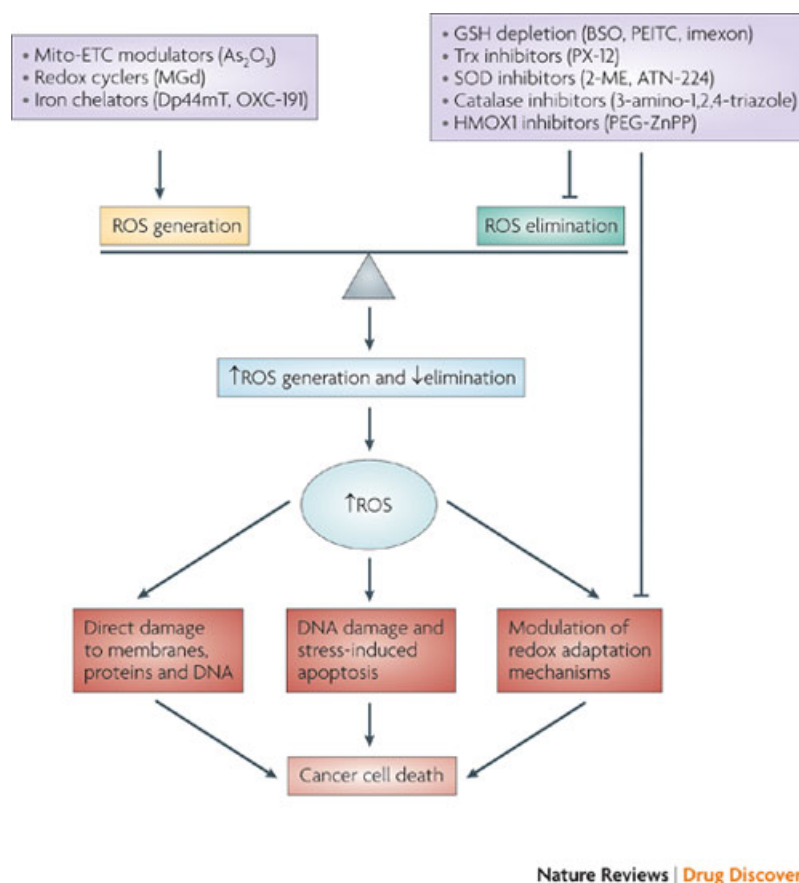


Figure 3.1: Schematic representation illustrating homeostasis of ROS in the body and the drawbacks due to excess generation of ROS and suppression of defense mechanisms

However in cancer it has been proven that the enzymes responsible for anti-oxidative defense are none to minimal[63][64][65][66]. This means that ROS is not

only responsible for promotion and progression of cancer mutagenesis[67] through the activation of redox-responsive signalling like epidermal growth factor, tyrosine phosphorylation and protein kinase C[68] but also increases its vulnerability thus providing a unique anti tumor functionality. This unique antitumor effect via generation of ROS[69] selectively only in tumors is known as oxidative therapy [70][71]. Hence this non linear dependence of cancer on ROS provides an unique opportunity for the treatment of tumors. Surprisingly, many chemotherapy agents like doxorubicin, vinblastine, cisplatin and inostamycin exhibit anti tumor therapeutic effect by generation of ROS[72]. However, ROS like H_2O_2 are highly unstable and extremely hydrophilic so the desired therapeutic effect of H_2O_2 cannot be manifested until it is generated continuously. As H_2O_2 used alone is ineffective in causing the desired level of necrosis in tumors[73][74]. This could be perhaps due to catalase and other anti-oxidative defense systems which could clear the ROS from the region. Thus sustained production of H_2O_2 is an effective approach to achieve antitumor effect. There are several mechanisms through which oxidative therapy can be used as an antitumor therapy. The use of enzymes which generate ROS by metabolizing common substrate available in the system to H_2O_2 like glucose oxidase (GluOx), ChOx, xanthine oxidase (XO) etc. In direct method to generate ROS in a specific location would be through enzyme-prodrug therapy, where HRP can be localized the tumors and a prodrug, in this instance Indole-3-Acetic Acid (IAA) can be supplied systemically. The prodrug is diffused through blood to the site of HRP localization, where HRP converts IAA to H_2O_2 thereby generating an oxidative environment. Hence only a controlled generation of H_2O_2 is achieved through this method, thereby reducing the possible systemic side effects[75]. Most of the enzymes used in oxidative therapy are from non human source. This would lead to generation high immune response and rapid clearance from the blood. In order to prevent the neutralization and maintain the foreign enzyme activity, covalent conjugation with PEG to synthesize enzyme PEG conjugates. PEG by itself improves the solubility in both organic and aqueous solvents, improved circulation half life *in vivo*, none to minimal toxicity and immunogenicity and easy excretion. PEG-protein/enzyme and PEG- drug conjugates have been employed clinically for the treatment of various forms of cancers which high efficacy. PEG provides a rich

pharmacokinetic advantages to any particle, proteins or enzymes. However there are a few downside to this approach, the addition of peg could lead to altering the enzyme activity due to non specific covalent binding of the PEG to the protein. Recent studies have also suggested the generation of immune resistance against PEG which could compromise the therapeutic efficacy of bio molecules conjugated with PEG.

3.1.1 Enzymes Assisted Oxidative Therapy

As mentioned before several enzymes have been used as a source to generate H_2O_2 in situ in the body. Most of the studies has been performed through intra tumor injection to the tumor of the enzyme and PEG-enzymes. Almost all of the enzymes used in oxidative therapy are flavo proteins[76] [77][78]. Earlier experiments were conducted with XO, DAO and GluOx. XO is a iron containing enzyme that oxidizes hypoxathine to generate ROS through a two step process3.2. Even though, XO is an excellent candidate for ROS generation but native XO have known to have a high affinity to endothelial cells lining the blood vessels. This high affinity could be detrimental to the treatment in sight.

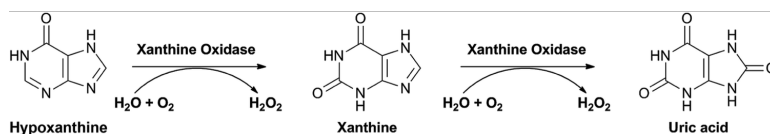


Figure 3.2: Schematic representation of XO reaction: Hypoxanthine is converted to xanthine in the XO while Xanthine is catalyzed to uric acid also in presence of XO while both the catalysis steps generate ROS

H_2O_2 generated from XO could cause oxidative damage to the blood vessels and endogenous nitric oxide (NO) could rapidly react with H_2O_2 thereby resulting in increasing the possibility of elevating the blood pressure. NO is known for its vascular dilation properties and hence lowering NO would lead necrosis or tissue degeneration through insufficient circulation[79][80].

DAO is another flavo-protein that have been studied for its anti-tumor properties by ROS generation3.3. DAO catalyses stereo selective amino acids with the

exception of D-aspartic acid and D-glutamic acid to H_2O_2 and its corresponding -keto acids[70][81].

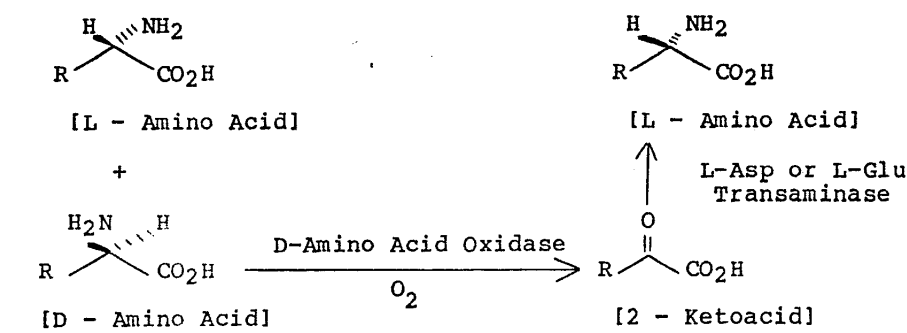


Figure 3.3: Schematic representation of DAO reaction: D amino acids is catalysed to α amino acid to generate ammonia and ROS

Addition of exogenous d-amino acids is necessary because of the insufficient of amino acids levels in the system. DAO when injected *in vivo* has lower circulation time as they can be excreted through urine. This is because the molecular size of DAO is 39KDa while the threshold for renal purification and excretion is 50KDa. To overcome this drawback people have used PEG conjugation on DAO to not only improve the circulation time but also provide protection against the immune system[59][82].

Glucose Oxidase (GluOx) is flavo protein belonging to the oxido reductase class of enzymes. GluOx catalysis the conversion of D-glucose utilizing oxygen to gluconic acid and simulatenous generating toxic H_2O_2 [83][76]. This dimeric enzyme has been used commercially as glucose sensors in diabetes. GluOx have also been used in toothpaste, skin care products and in food and deverage industries as well. However, the use of GluOx as an effective therapeutic agent isnt as heavily studied as compared to other applications. Due to the generation of H_2O_2 by utilizing oxygen and glucose, which are ubiquitous in the body makes GluOx a excellent candidate for oxidative therapy in tumors. The by product, D-gluconolactone which is generated by GluOx is also metabolically inert and on the contrary provides therapeutic relief especially on skin[84][85].

Abundance of glucose and oxygen in the body aids in generation of ROS by GluOX but it would also generate systemic toxicity when GluOx are administered

intravenously due to the generation of H_2O_2 instantly and it would also cause a rapid immune clearance thereby reducing the available enzyme[86]. The latter can be prevented by the conjugating GluOx with PEG while its the former that poses a serious problem. One way to partially localize the generation of cytotoxic H_2O_2 is to inject intratumorally the PEG-GluOx conjugates. PEG-GluOx is highly soluble in aqueous solutions due to PEG, have high probability to leak out of the tumor vasculature and causing systemic toxicity. Hence there is to activate the GluOx only at the site of interest and retain the activitiy at the site of injection.

GluOx primarily generates H_2O_2 (and importantly no other ROS). Since GluOx substrates (glucose and oxygen) are abundant in all biological compartments and since its product (d-gluconolactone) is metabolically inert, the GOX-system can be considered an ideal model for physiological H_2O_2 release.

The main drawback for this kind of therapy is the site specific generation of ROS, tumors in the case of cancer. This can be achieved through multitude of techniques.

3.2 Materials

Lyophilized powder of Glucose Oxidase (GluOx) from *Aspergillus niger* was purchased from Sigma Aldrich, St Louis, MO. Amplex Red Glucose/Glucose Oxidase assay kit was purchased from Invitrogen, Carlsbad, CA. Vybrant MTT Cell Proliferation Assay kit was purchased from ThermoFisher Scientific, Waltham, MA. 5 mg of MTT was aliquotted into 10 ml of DMEM and stored in $4^\circ C$.

3.3 Synthesis of Glu-SiLi

Glucose oxidase (GluOx) loaded CeLi (Glu-CeLi) was synthesized with the method described in chapter 3 using 100mg/ml of glucose oxidase in PBS as the stock solution. Silica coated liposome encapsulating GluOX (Glu-SiLi) was synthesized by adding 1:5 ratio of APTMS: TMOS per $50\mu l$ of Glu-CeLi. The reaction was conducted under vortex for 2 hours and then centrifuged and re suspended three times in PBS at 3200 rcf at room temperature.

3.3.1 Characterization of Glucose Oxidase

0.5 μ l of the sample were mixed in 1ml of PBS to estimate the size range for both the particles while the charge was measured in DI water instead of PBS. The size of the SiLi particles was further confirmed using SEM.

3.3.2 Glucose oxidase kinetics and activity study

GluOx activity was characterized using colorimetric amplex red assay. The assay was conducted for 30 minutes at 37°C with 100 μ M of amplex red reagent, 0.2U/ml of HRP and 100mM of glucose. The fluorescence of resorufin was measured at 545nm and emission at 590nm. The absorbance was also measured at 560nm. The standard curve for GluOX was conducted using the standard enzyme issued in the assay kit and serial diluted to 10mU to 0.1mU. Kinetic cycle was conducted to measure the absorbance and fluorescence. The standard curve was plotted with the absolute values measured after 30 mins of incubation with the enzyme concentration.

3.3.3 Toxicity Study of Glu-SiLi with MTT Assay

Glu-CeLi and Glu-SiLi enzyme encapsulation was determined using the standard curve of the free GluOx. The activity of the enzymes were matched before the addition to the cells. HeLa (ATCC CCL-2) cells was used to test GluOX toxicity and these cells were sub cultured at least 4 times prior to the study. 5000 cells/well were plated and incubated 24 hours prior to any treatment. The treatments were only studied upon 60-70% con fluency each well. All the samples including the free gluOX was serial diluted and incubated with cells for 3 hours and 24 hours. Before the addition of the MTT reagent, the media was removed and replaced with the media containing 0.2mM MTT. The cells were incubated at 37°C incubator for 3 hours before the addition of 50 μ l of DMSO to determine the absorbance at 540nm. The lethal concentration was determined at 50% cell viability for each particles (free, Glu-CEI and Glu-SiLi).

3.3.4 *In vivo* Therapeutic Efficacy

Male athymic (Ncr nu/nu) nude mice, approximately 4-6 weeks old on arrival, were obtained from Jax Laboratory Animal CO. Animals were housed in laminar air-flow cabinets under special pathogen-free conditions and fed with autoclaved standard chow and water at 26-28°C and humidity at 40%-60%. xenografts were initiated by subcutaneous injection of 5×10^{10} A549 cells into the right and left flanks of the nude mice.

Experimental treatments were started when tumors had grown to an average of 60mm^3 in volume. Mice were randomly divided into three groups: group 1 (control, n=2) was injected with just PBS, group 2 (n=2) unencapsulated GluOx while group 3(n=2) was injected with GluOX particle. Prior to the injection all the samples were match with the activity of Glu-SiLi particles. The tumor size was measure for 15 days and upon sustained injections with 200U of Glu-SiLi at day 5 and day 12. The mice was sacrificed after the duration of the experiment and sections were stained for hemotoxylin and eosin to determine necrosis.

3.4 Results

The size of Glu-CeLi and Glu-SiLi are 250 nm and 300 nm respectively however the surface charge of the Glu-CeLi was measured to be around -12mV compared to the BLA-CeLi of +15mV. The addition of silica coating on the Glu-CeLi using APTMS and TMOS was measured to be -26mV.

Standard curve of the GluOx was performed and used to calculate the activity of the GluOx encapsulated in the CeLi and SiLi particles. This was always performed prior to the treatment with cells to determine the lethal concentration for 24 hours and 3 hours. Figure 3.4 shows the percentage viability of 5000 HeLa cells per well. Figure 3.4b shows almost a linear trend in the cell viability with increase enzyme activity. Lethal concentration at 50% cell viability for 3 hours was found to be around 1.5-2 U/ml for all the samples however the lethal concentration at 50% cell viability could be verified for cells incubated with GluOX samples for 24 hours as shown in figure3.4a. Loading efficiency in both Glu-CeLi and Glu-SiLi

was found to be same and there was not much loss in the activity due to the silica coating.

100 μ l of 14U of GluOX was injected in intratumorally (IT) at day 0 followed by

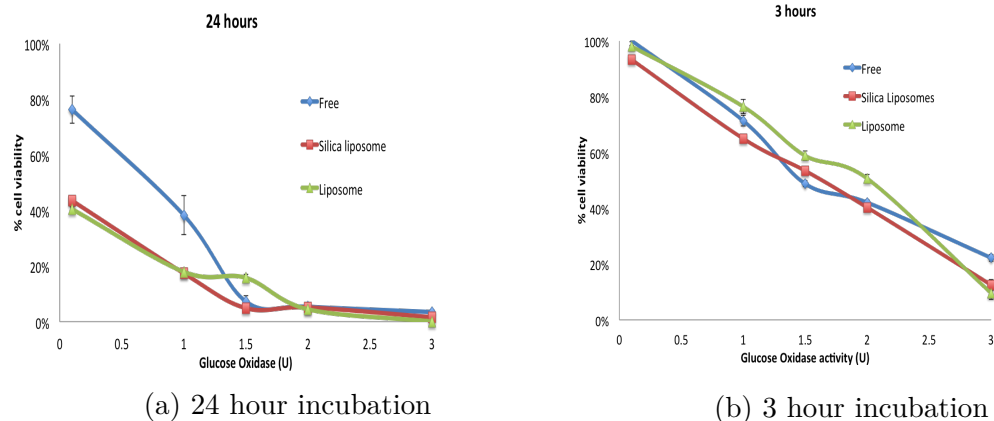


Figure 3.4: Percentage viability of cells upon incubation of free GluOX, Glu-CeLi and Glu-SiLi for 24 hours and 3 hours respectively

100 μ l injection of 220U of Glu-SiLi particles at day 5 and day 11 for the period of experiment of 14 days after which the mice were sacrificed. As from the figure the tumor size didnt not show any change between the tumors injected with Glu-SiLi particles and PBS. The tumors size was to found to be growing regardless of the treatment.

However to test the efficacy of the hydrogen peroxide generation *in vivo* 20U and 200U of free GluOx was injected subcutaneously. the mouse injected with 200U of GluOx subcutaneously died in less than 24 hours while the mouse injected with 20U subcutaneous appear to be losing about 2g of weight in less than 5 days post injection. However, the mouse injected with 20U of GluOX intravenously also died in less than 24 hours. Heat inactivated GluOx was also injected intravenously and subcutaneously to determine that cause of death of mice was due to the generation in hydrodgen peroxide generation due to the GluOx and not due to the endo toxins found in commercially available enzymes. The mouse injected with heat inactivated GluOx appear to be normal even after 14 days. The tumors were harvested and histology slides were prepared to check for apoptosis (see figure3.6) or necrosis markers (see figure3.7). The tumors treated

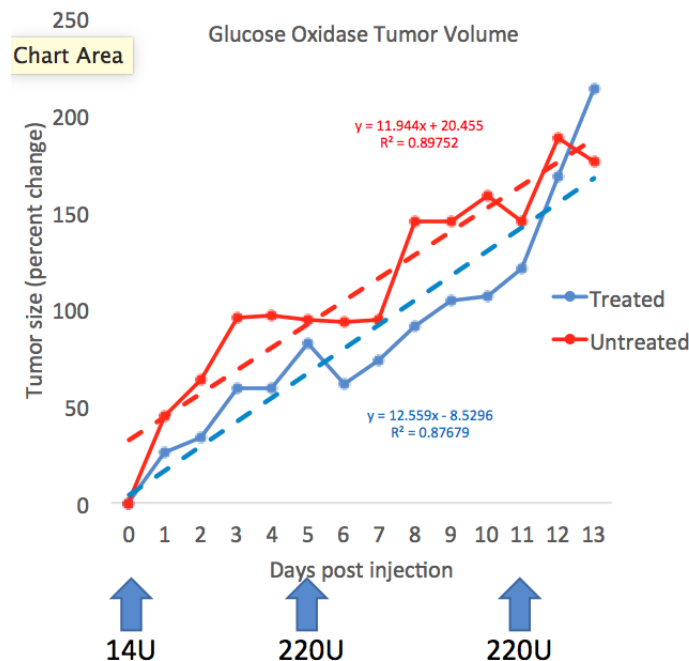


Figure 3.5: Percent change in the tumor volume measured between the mice treated IT with Glu-SiLi (blue) and untreated-PBS (red)

with Glu-SiLi was found to be showing signs of necrosis compared to untreated tumors.

TUNNEL stain was performed to check for apoptosis markers but there wasn't any significant difference between the treated and untreated tumors as seen in the figure3.7.

3.5 Discussion

The size of Glu-CeLi compared very much to the other CeLi formulations loaded with BSA and BLA, thereby the size of the GluOx had little to no effect on the size of the CeLi formed. However, The surface charge is highly influences by the charge of the protein being encapsulated. BSA and BLA CeLi were cationic with +12mV because the charge of BSA and BLA was found to be less than -5mV but the GluOX measured to be -18mV which might have led for the anionic surface charge in spite of the addition of DOTAP. It is highly likely that the most of the inner lipid bilayer must be lined with DOTAP due to preferential electrostatic

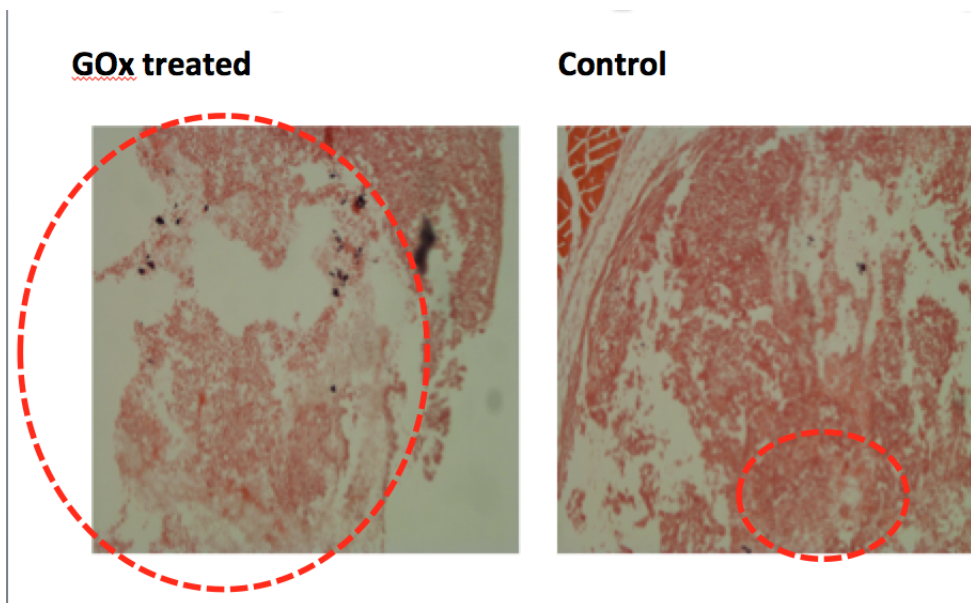


Figure 3.6: Histology slide of the tumors of GluOx treated and control (untreated). The circle represents the area of necrosis in the region of section

attraction to GluOX.

GluOX forces the cells to apoptosis by generating excessive ROS consistently. Figure3.4 shows MTT assay incubated with cells in plate for 24 hours and 3 hours at different GluOX concentrations. It is apparent that even at lower GluOX concentration more than 50% of the cells undergo apoptosis. This could be due to consistent ROS generation while consuming glucose. Since its a static system as no extra glucose supplement were provided to the cells due the treatment. This cell death could be due to ROS and glucose but the *in vivo* the level of glucose is maintained thereby the only cause of cell death would be due to ROS production. However the cells incubated only 3 hours with Glu-SiLi, there appears to be linear trend in cell death with the concentration of GluOx loaded as there isnt sufficient time to generate ROS hence only the maximum doseage generated 50% cell viability.

Figure3.4a and figure3.6 shows that *in vivo* the tumors undergo necrosis due to ROS generation and not just due to glucose depletion. As seen in figure3.6, the xenografts undergo necrosis but the size of the tumor doesnt under any change. The tumor volume doesnt undergo much change even after treatment because the

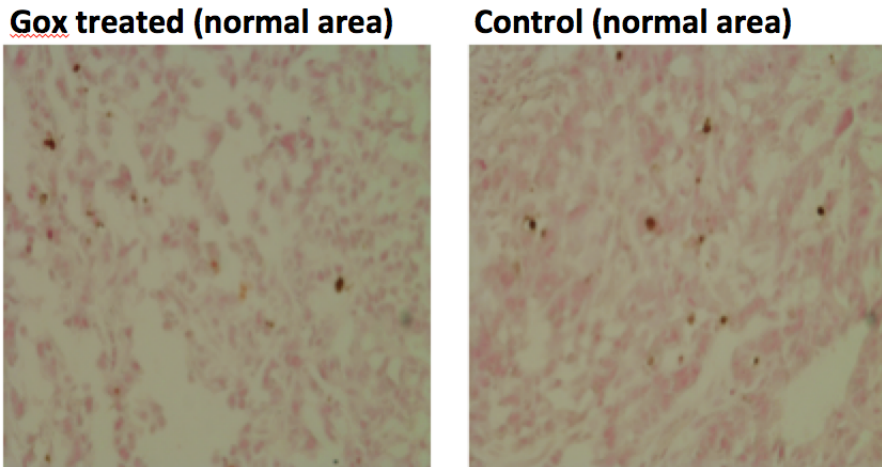


Figure 3.7: Histology slide of the tumors of GluOx treated and control (untreated). TUNNEL staining was performed to stain the area of apoptosis on the slide section

tumor volume is too huge and the since the injection is mostly at the center of the tumor, the ROS has been able to dissipate deep into the tumor periphery. Figure3.7 shows that there is no apoptosis marker in tumor sections as the apoptosis occurs only 24 hours after injection with the ROS. This is consistent that ROS causes the tumor to undergo necrosis through apoptosis.

3.6 Conclusion

We have demonstrated the use of Glu-SiLi to generate ROS for the treatment of tumor. The efficacy is of H_2O_2 generation to trigger cell death is prominent at the site of injection but fails to interact with cells in the periphery. The amount of cell death corresponds to the amount of GluOx loaded in SiLi but even at lower GluOx loading there is visible cell damage.

The ability of Glu-SiLi to kill cells is only through the generation of H_2O_2 and not through depletion of glucose as the un-encapsulated enzyme through IV generated systemic shock through high ROS production leading to mice's death in less than 2 hours.

3.7 Acknowledgments

This chapter, in part is currently being prepared for submission for publication of the material. Mukanth Vaidyanathan, Jared Fisher and Sadik Esener. The dissertation/thesis author was the primary investigator and author of this material.

Chapter 4

Diagnostic Application of SiLi

4.1 Acetylcholine (ACh)

Acetylcholine (ACh) is an organic chemical that is found in brain and body of humans and animals. Its structure is composed of acetyl ester and choline. Predominantly ACh is found in the human body as a neurotransmitter and also acts as a neuromodulator. The parts of the body that is affected by the release of this neurotransmitter are referred to as cholinergic. In central nervous system (CNS), cholinergic projections from the basal forebrain to the cerebral cortex and hippocampus aid in cognitive functions[87]. In addition to cognitive functions, ACh also aids in arousal, increasing attention, memory and motivation. Primarily in the Peripheral nervous system (PNS)[88], this chemical is released by motor neurons in order to activate the muscles. ACh is also the major neurotransmitter in the autonomic nervous system (ANS)[89], as an internal neurotransmitter for the sympathetic nervous system and as the final product released by the parasympathetic nervous system. However, the specific functions of each ACh-releasing neuronal population are largely unknown.

In the cerebral cortex, ACh is released from long axons projecting from the neurons in the basal forebrain with contributions from many cholinergic interneurons [90]. Like the cerebral cortex, hippocampus and its neighboring regions are innervated with extrinsic cholinergic inputs from medial septal nuclei, which is responsible for the theta waves in an EEG and also by intrinsic cholinergic interneu-

rons[91][92]. ACh can activate both excitatory nicotine acetylcholine receptors (nAChRs) and muscarinic acetylcholine receptors (mAChRs) in these systems. These receptors are responsible for regulating the post synaptic release of neurotransmitters from the presynaptic cell which alters synaptic plasticity and post synaptic cellular excitability[93][94].

ACh is synthesized in the presynaptic terminals in cholinergic neurons using choline (Ch) and Acetyl CoEnzyme A (ACoE-A)(see figure4.1). This reaction is catalyzed by Choline Acetyl transferase (ChAT)[95]. The ChAT derived from the brain has a K_D of 1mM for Ch while $1\mu\text{M}$ for ACoE-A. Inhibitors of ChAT do not lower ACh synthesis *in vivo*; this could be because of lack of sufficient local concentration of the inhibitor but it also suggests that this step is not the rate-limiting in the synthesis of ACh. Ch is present in the blood and the concentration is about $10\mu\text{M}$. There are preferentially two choline uptake transporters(ChT): One is the "low affinity" ChUT with a k_M of $10\text{-}100\mu\text{M}$ which are found in all the cells and tissues in the body while the second uptake system is the "high affinity" sodium ChT which are present only in the cholinergic neurons with a K_M of $1\text{-}5\mu\text{M}$ [96]. Since the plasma concentration is enough to saturate the high affinity ChTs, ACh synthesis would be sustained even under high demand neuronal activity. However the Ch concentration inside the presynaptic terminals is not expected to change by increasing the Ch concentration in plasma. Studies have been conducted to specifically block the high affinity ChT at nerve endings using inhibitors like 3-Hemicholinium, to study the effect of ACh synthesis. It has been proven that ACh synthesis has been altered or lowered by the use of ChUT inhibitors. Hence, the rate of ACh synthesis is dependent on the rate of Ch transport into the presynaptic terminals[97][98][99].

4.2 Acetylcholinesterase (AChE)

AChE is a serine hydrolase. The active site of AChE (figure4.2a contains a triad of amino acids: serine, histidine and glutamate (an acid residue), a structure similar to that of trypsin[101]. AChEs are found in the synapse between nerve cells and muscle cells. It catalyzes the hydrolysis of ACh to Ch and acetate.

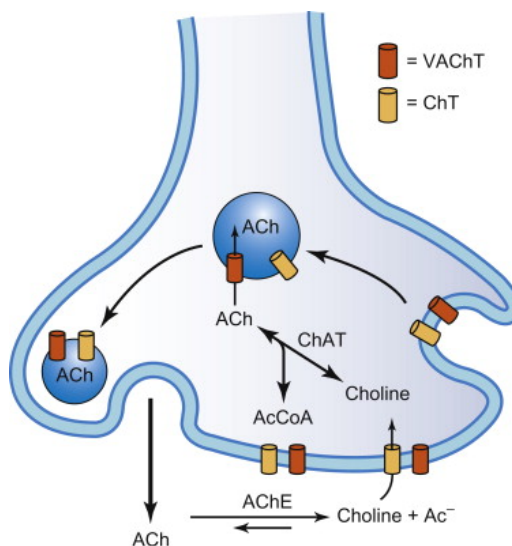


Figure 4.1: Schematic illustration of ACh synthesis in a cholinergic presynaptic nerve terminal and synapse. The choline uptake transporter (ChT) at the membrane of nerve ending transports Ch into the cell, where it is catalyzed by ChAT to generate ACh using AcCoA in the vicinity of the synaptic vesicle. The vesicular acetylcholine transporter (VACht) concentrates ACh in the vesicle. ChT is also found on the vesicle but in a functionally inactive state. Upon nerve stimulation, ACh-containing vesicles fuse with the membrane and release their contents. The fusion of the membrane results in more ChT being exposed to the synaptic gap, where it becomes active. ACh is hydrolyzed to Ch and acetate in the presence of acetylcholinesterase (AChE). The Ch is then bound to ChT which is then transported back to the nerve ending[100]

The breakdown of ACh at the synapses allows the Ch to be re-uptaken by the synaptic terminal for further processing Ch to ACh[102]. This is important in terminating the nerve transmission at the synaptic junctions. AChE is one of the fastest enzymes but the exact mechanism is still unclear. Interestingly, the ACh released in the synaptic junctions are enough to saturate all the cholinergic receptors and AChEs present in the synapses. 80% of ACh binds to the receptors in the receiving cell while only 20% binds to the AChEs[103]. This is because of two reasons: First, the rate at which the ACh binds to the receptors is higher than that rate at which the AChE can hydrolyze the ACh. Second, the rate at which ACh is released from the receptor is slower than the hydrolysis by AChE and hence, there is always a low ACh concentration at the synaptic cleft at any time after the transmission and this also excludes any non specific binding of

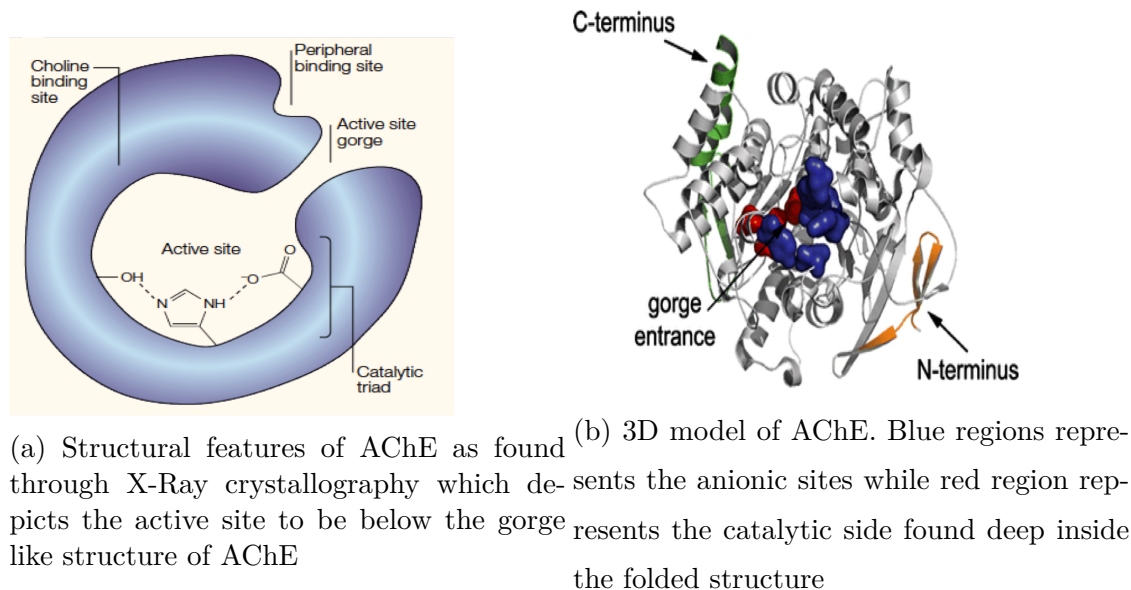


Figure 4.2: Illustration of AChE structure derived from the *Torpedo californica*

ACh to any other cells or receptors[104][105]

AChE has a multitude of roles which are not readily accepted. Studies have suggested that regulated expression of AChE has been found during early embryogenesis[106], synpatogenesis [107]and neuritogenesis [108] but the role of AChE during these early stages of embryogenesis is still being studied. AChE have also been found in regions of the brain with little to no inputs from cholinergic neurons like cerebellum, globus pallidus, hypothalamus and non nervous tissues like the testis[109], haematopoetic [110] , osteogenic and various neoplastic cells and in erythrocytes[111][112]. AChE is extensively prominent in tissues that are innervated with cholinergic neurons like the CNS, ANS and PNS primarily at the neuromuscular junctions[113].

4.2.1 Importance of ACh Detection

Alzheimer's disease (AD) is a neurodegenerative disease characterized by the deposition of β -amyloid ($A\beta$) plaque in the extracellular space, formation of neurofibrillary tangles in neurons, and extensive neuronal loss[114]. The neurodegeneration results in loss of memory, mood and behavior changes and difficulty in speaking, swallowing and walking in severe cases [115][116]. Although the precise

cause of AD remains unclear and is in fact most likely of multiple etiologies, aggregated $A\beta$ -peptides constitute a prime neurotoxic component of senile plaques in the brains of AD patients. In addition to genetic influences, environmental factors appear to play a role in AD pathogenesis, with evidence that environmental factors such as stress and exercise can influence the formation of plaques and tangles [117]. Although other neurotransmitters were known to be involved in learning and memory performance, the functions of cholinergic system in learning and memory were of predominant interest in this aspect[118]. Cholinergic loss is the most severe and consistent biochemical change in AD patients[119]. ACh which acts as the neurotransmitter in cholinergic systems were found to be significantly decreased in AD patients which is a result of decrease in concentration of the ChAT compared to age normalized patients [120]. Several research have concluded that there is a selective loss in a specific globular form of enzymatically active membrane bound AChE in cortical and subcortical regions in AD patients [121][122]. The regional distribution of these deficits is significantly correlated with histopathological features of the disease as the membrane bound form of AChE is predominately found in cholinergic neurons[123]. AD is not the only disease of the brain that is affected by the loss in cholinergic systems. The cholinergic neurons of the cerebral cortex and hippocampus have been described to undergo moderate degenerative changes during aging, thereby resulting in cholinergic hypofunction that is related to the gradual memory loss with aging. Cholinergic atrophy and cell loss in normal brain due to aging is not complemented by reductions in the neural growth factors (NGF) levels as studies have shown that NGF provides tropic support to cholinergic neurons which promote neuronal survival, increases sprouting of cholinergic neurons both *in vitro* and *in vivo*[124] [125][126][127]. Although Parkinson disease (PD) is a progressive disorder of neurons that affect movements due to denervation of dopaminergic neurons, recent studies have shown the effects of this progressive disease in non motor features such as dementia. This elucidates the multi-system neuron denervation which extends beyond dopaminergic systems[128]. Cognitive impairment in PD is manifested in patients mainly by attention and executive dysfunctions which can be attributed to the significant loss in cholinergic neurons in the forebrain. In fact the loss in cholinergic functions have been found to be greater in forebrain in PD

than in AD[129][130]. Hence with the necessity for the detection of various neurotransmitters and outlining the map of the brain plays a very crucial role in drug discovery and targets for treating several diseases which manifest due to not just one neurological pathway mutation but multi-system mutation. We chose ACh because of its role in not just in cognitive and motor development and regulation but also the source for many debilitating conditions like paralysis[131], dementia, AD, PD, schizophrenia [132] and addiction[133].

4.2.2 Current Detection Techniques

Imaging has played a variety of roles in the study of AD, PD, mild cognitive impairment, Schizophrenia and dementia over the past couple of decades. Initially, computed tomography (CT) and then magnetic resonance imaging (MRI) were used to diagnose dementia and several other brain anomalies. Recently different varieties of imaging modalities like Structural Magnetic Resonance Imaging (MRI), Functional magnetic resonance imaging (fMRI) and Positron emission tomography (PET) have been employed in the clinic to study and characterize the neuronal metabolic fluctuations using chemical compounds known as tracers. The signals obtained with PET and fMRI are based on changes in blood flow, oxygen consumption and glucose utilization that correspond to a precise way to the cellular activity of the brain, including astrocytes and neurons. Structural MRI with different field strengths (1-3T) has been used to achieve better resolution and improving the signal to noise ratio to clearly differentiate between vascular structures, white and gray matter. However with higher power(7-9T), resolution can be improved of several 100's of microns[134][135]. This has enabled quantification of cortical volume with high precision and hence aids in the monitoring of disease progression (refer figure4.3). MRI includes several other imaging techniques like the Diffusive tensor imaging MRI(DTI-MRI), resting state MRI, Real time MRI, Diffusion MRI, Magnetic resonance angiography, T1rho MRI, Neuromelanin imaging, Fluid attenuated inversion recovery (FLAIR) etc.

Studies have shown that with novel rapid data acquisition programs and the confinement of contrast agents within the vascular compartments has led to mea-

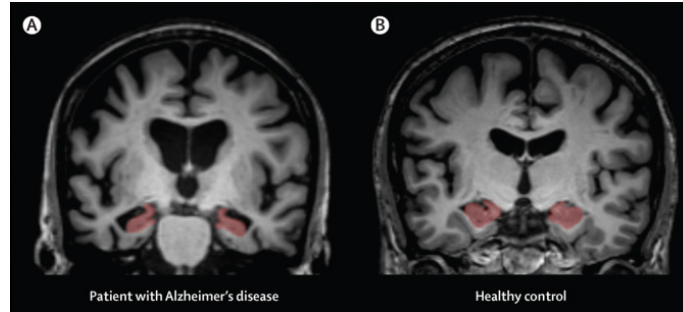


Figure 4.3: Comparison of structural MRIs of Hippocampus between alzheimer's patient (a) and normal adult(b)

measurements of changes in blood brain volume using MRI technique. This led to the demonstration of functional mapping of the brain along with its precise anatomical features using MRI. This type of MRI is called functional MRI (fMRI)[136]. fMRI was also used to evaluate the magnetic susceptibility of oxygenated and deoxygenated blood due to change in the oxygen and glucose concentrations in brain. This led to the development of Blood-oxygen-level dependent fMRI (BOLD-fMRI) which is the most widely used imaging tool in brain[137]. Apart from BOLD, there are several other fMRI techniques like arterial spin labelling (ASL), cerebral blood flow, cerebral blood volume.

PET derives its name and its fundamental properties from a group of radionuclides which measure the metabolic activities in the body. The radionuclides emit positrons which generate gamma rays which are then captured by the detectors. Currently, 3-dimensional images are generated with PET along with CT scan. PET scans are currently employed to image cancer tumors, pharmacokinetics, cardiovascular system and neuronal activities. Most widely used imaging modalities for brain activity, especially in characterizing the progression of AD, is amyloid PET. In short, ^{18}F -labelled amyloid PET binds specifically to amyloid aggregates but not to tau proteins or α -synuclein, which are usually the underlying causes for the progression of neural disorders.

This strong affinity of the tracers provides positive or negative amyloid load in the brain but cannot provide an accurate quantification of amyloid aggregates. Hence, it has to be used in conjunction with fMRI and DTI-MRI to provide precise information on both functional and metabolic anomalies. In spite of the

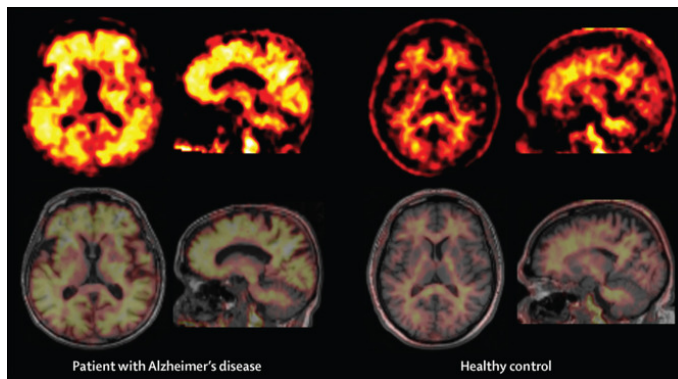


Figure 4.4: AmyloidPET scans of Alzheimers patient and Healthy patient

drawbacks of amyloid PET, it still can be classify patients who are at a higher risk of progressing to AD from MCI[138].

Since brain is highly heterogenous with both complex structural and functional regions at various sites in the brain, the ability for an imaging technique to fully resolve these complexities is in part dependent on its spatial and temporal resolution. There isn't one imaging modality that can serve all purposes as each one have their own unique strengths and weaknesses[139]. The challenge for the future will be to correlate the imaging biomarkers efficiently to facilitate diagnosis, disease staging, and, development of effective disease-modifying therapies. Therefore, it is desirable to develop nanoscale devices that can (i) probe the concentration of ACh with high resolution to understand and characterize in space and time of ACh production and/or depletion in response to a stimulus, and (ii) modulate non invasively at desired locations and time the ACh in the brain to carry on behavioral longitudinal tests. Unfortunately, presently, there are no techniques available to track and sense the rapidly changing concentration of neurotransmitters in response to specific stimulus and to modulate the concentrations with high spatiotemporal specificity. In addition, very few methods exist to non-invasively and spatiotemporally modulate neurotransmitter concentrations[140][141][142].

However, In this chapter, we explain the use of enzyme for optical detection of ACh. There are several commercially available kits that can be used *in vitro* to detect ACh but cannot function with similar capabilities in vivo without causing adverse immune reaction. The use of three different enzymes (AChE, ChOx and

HRP) in SiLi is elucidated in detail below (see figure4.5).

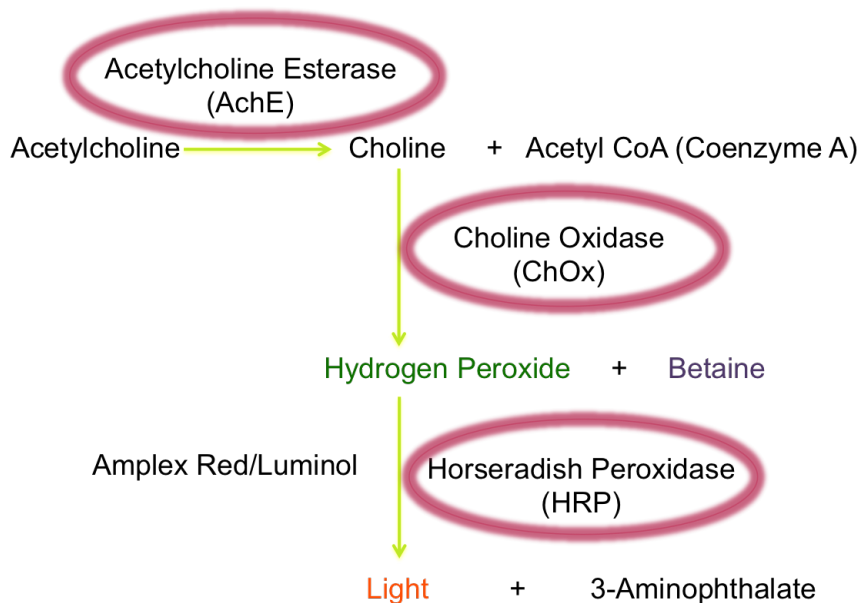


Figure 4.5: Flow chart of the cascading reactions using AChE, ChOx and HRP to detect ACh optically from commercially available kits

4.3 Materials

L- α -Phosphatidylcholine derived from egg yolk (Egg-PC) of 25mg/ml stock solution in chloroform, Cholesterol powder, 1,2-Distearoyl-sn-glycero-3- phospho ethanol amine Poly-ethylene Glycol MW5000 (DPSE - PEG) powder and 1,2-Dioleoyl -3- trimethyl ammonium-propanol (DOTAP) of 10mg/ml stock solution in chloroform were purchased from Avanti polar lipids, USA. Diethyl ether and Tetramethyl orthosilicate (TMOS) were purchased from Sigma Aldrich, MO, USA. Phosphate buffer saline was purchased from Life Technologues, USA. Nucleopore Track-Etch Whatman filters 13mm (800 nm, 400nm and 200 nm) used in the extrusion process and 19mm Nucleopore Track-Etch Whatman 30 nm pore size filter were purchased from EMD Millipore, Darmstadt, DE. The magnetic dialyzing cartridge, fast SpinDialyzer was purchased from Harvard Apparatus, Holliston, MA. Lyophilized Acetylcholinesterase (AChE) from *Electrophorus electricus* (electric eel), Choline Oxidase (ChOx) from *Alcaligenes sp.*, Peroxidase from Horseradish

(HRP) were purchased from Sigma Aldrich, St Louis, MO, USA. Fluorometric Amplex Red assay kit to detect acetylcholine /acetylcholinesterase was purchased from ThermoFisher Scientific, USA. Phosphate Buffer Saline (PBS) was purchased from Hyclone Laboratories Inc, Logan, UT.

4.4 Preparation of AChE Loaded Liposomes

The cholesterol stock solution was prepared with 38.7 mg of lyophilized powder of cholesterol in 1 ml of Chloroform. The DSPE-PEG stock solution was prepared by mixing 50mg of DSPE -PEG in 1 ml of chloroform. All the lipid stock solutions were prepared in chloroform and stored in -20°C freezer. Egg-PC and DOTAP was used as received. Liposomes were synthesized through a modified version of the reverse phase evaporation technique developed by Papahadjopoulos [49]. It consists of three step process.

Solution A: 295 ul of 25 mg/ml of Egg-PC, 50 ul of 38.7 mg/ml of Cholesterol, 50ul of 10mg/ml of DOTAP were mixed in a glass vial and the chloroform was evaporated using Buchi Rotavapor R-300 at 100 rpm at 25°C for 20 minutes to form a thin lipid film. Then 1ml of diethyl ether was added to re-suspend the lipids in ether.

Solution B: 40 ul of 38.7mg/ml of cholesterol, 50 ul of 25mg/ml of DOTAP and 60 ul of DSPE-PEG stock solutions were mixed in 0.5 ml eppendorf tube. The chloroform was evaporated under a gentle stream of nitrogen while vortexing the open tube. 100ul of the PBS was added while making empty liposomes or 100 ul of enzyme cocktail was added to make enzyme loaded liposomes. The enzyme cocktail consisted of 33.3 ul of 50mg/ml of AChE, 33.3 ul of 50mg/ml of ChOx and 33.3 ul of HRP. All the enzymes were hydrolyzed individually using PBS. The lipid-payload solution was vortexed thoroughly for 30 secs until all the lipids are constituted in the solution.

Solution C: 60 ul of DSPE-PEG stock solution was evaporated under gentle nitrogen stream while vortexing in a 1 ml eppendorf tube. Then 1 ml of PBS was mixed until all the lipids are evenly mixed in the solution.

Solution B was added dropwise in the glass vial containing solution A un-

der vortex. Then solution was allowed to vortex in high speed for 1 minute. This emulsion is homogenized to ensure proper mixing using the Power Gen 125 homogenizer from Fisher Scientific for 2 minutes. The ether in the stabilized emulsion is evaporated under vacuum using Buchi Rotavapor at 100rpm at 30°C for 25 minutes.

This produces a sol-gel like precipitate. The sol-gel mixture is then hydrated by addition solution C dropwise under gentle vortex. If needed, Gentle stream of nitrogen was used to create vortex to break apart large chunks and then vortexed for 30 seconds. This solution was placed in vacuum for 45 minutes under a water bath at 30°C. The liposomes are then extruded three times using a syringe extruder with 800nm, 400nm and 200nm filters respectively. The extrusion process was slow and steady to ensure homogeneous solutions of liposomes are formed. To remove excess enzyme and lipids, the solution was dialyzed at 160 rpm at room temperature overnight using the fast SpinDialyzer with 19mm whatman filters with pore size of 30nm.

4.4.1 Synthesis of Silica coated AChE/ChOx/HRP Loaded Liposomes(ACH-SiLi)

These cationic liposomes are used as a template to precipitate silica. 500 μ l of the liposomes is diluted with 1.5 ml of PBS. 20 ul of TMOS is added dropwise over vortex to this solution and mixed for 4 hours at 3200 rpm in a shaker at room temperature to form Silica coated Liposomes (SiLi). To terminate the hydrolysis of TMOS, the SiLi solution was washed three times in PBS using a centrifuge at 3200 ref for 15 minutes at 25°C.

4.4.2 Characterization of the ACH-SiLi

The size and surface charge of the liposomes were characterized using Zeta-sizer Nano from Malvern Instruments, Malvern, UK. The size was also characterized using electron microscope images using the Helios NanoLab DualBeam from FEI. The particle count was analyzed using ViewSizer 3000 from Manta, San Diego, CA.

The activity of the enzyme was optically detected using Spark M20 from Tecan, Mannerdorf, SUI.

4.4.3 Characterization of AChE Activity using Amplex Red Assay kit

AChE activity was characterized using colorimetric amplex red assay. The assay was conducted for 60 minutes at 37°C with 400 μ M of amplex red reagent, 2U/ml of HRP, 0.2 U/mL choline oxidase and 100 μ M acetylcholine. The fluorescence of resorufin was measured at 545nm and emission at 590nm. The absorbance was also measured at 560nm.

The standard curve for AChE was conducted using the standard enzyme issued in the assay kit and serial diluted to 100U to 0.1U. Kinetic cycle was conducted to measure the change in absorbance and fluorescence. The standard curve was plotted with the absolute values measured after 60 mins of incubation with the enzyme concentration and also with the slope of enzyme activity with time.

4.5 Results

The size of AChE-CeLi and AChE-SiLi were found to be similar to BLA-CeLi and SiLi. In spite of the higher size of the enzyme, AChE loading did not compromise the surface charge of the CeLi particles unlike the glucose oxidase loaded CeLi. As to simulate the breaking of lipids in the liposomes to allow access of the substrate to the AChE, Two different surface coating was employed on AChE-CeLi. From the figure 4.6, calcium phosphate coated CeLi (CaPLi) and SiLi particles loaded with AChE did increase the AChE activity by almost 150% compared to the CeLi particles. However, Sustained exposure to PK did lower neutralize the AChE encapsulated in the CeLi particles but retained most of the activity in CaPLi and SiLi particles.

For the detection of the ACh *in vivo* there requires a cascade of enzymes for this process as mentioned before. To mildly simulate *in vivo* condition, SiLi particles

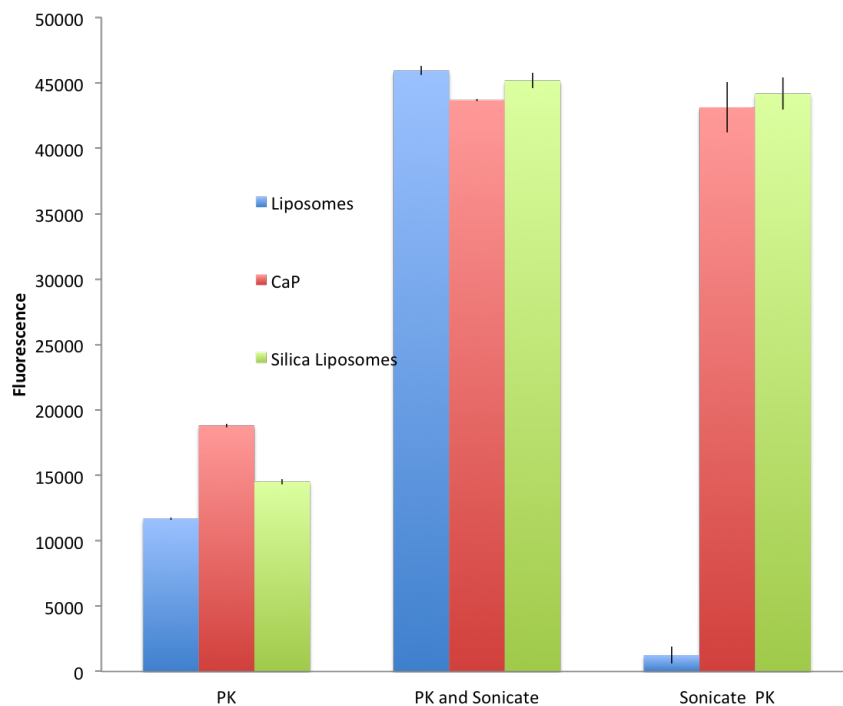


Figure 4.6: AChE activity in three different particles before and after PK treatment and with and without sonication

were synthesized containing all the 3 enzymes (AChE, ChOx and HRP) and SiLi containing individual enzymes separately. All the SiLi particles were tested with only ACh and also with ACh and Ch. Experimental results as seen in figure 4.7 showed that free enzymes (AChE, ChOx and HRP) provided the quickest and fastest detection of ACh in the solution. However, the particles containing all the 3 enzymes (AChE, ChOx and HRP) in one SiLi particle showed faster and better detection compared to 1 enzyme encapsulated in individual SiLi particles. The addition of Ch to solution however improved the detectability of 1 enzyme SiLi particles but it did not provide the detection signal as compared to other 3 enzymes in one single SiLi particles.

4.6 Discussion

AChE is a large molecule enzyme which could hinder the surface charge or the size of the CeLi and SiLi particles. However the size and charge remains the

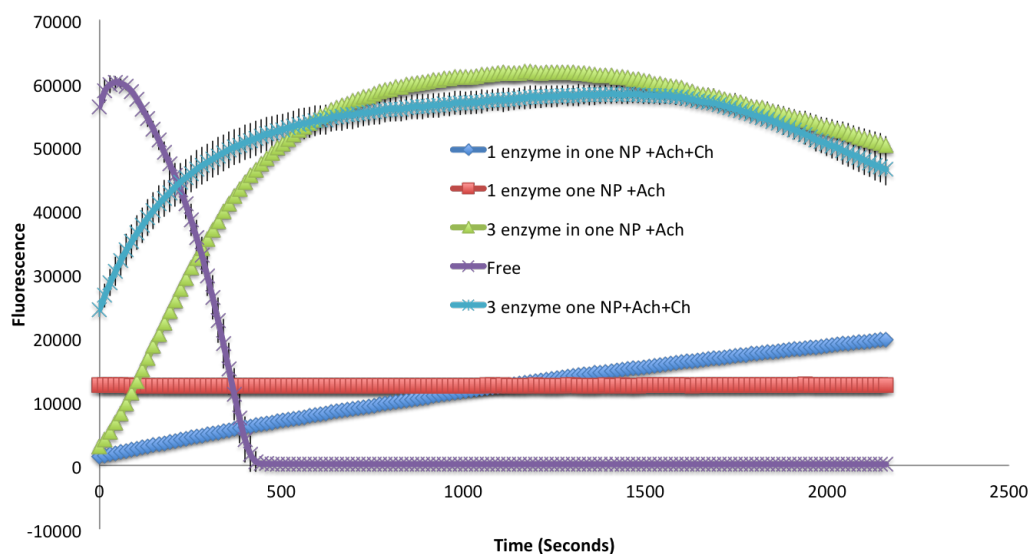


Figure 4.7: Kinetics of Free, three enzyme (AChE, ChOx and HRP) in one SiLi particle and 3 SiLi particles each containing a different enzyme of the cascade at $1\mu\text{M}$ of ACh and $1\mu\text{M}$ of Ch

same as of the BLA-CeLi and SiLi particles which shows that the enzyme shows little to no affect on the encapsulating nanoparticle. Proteases are found to be effective on AChE and hence was used a surrogate for the immune system in vitro. Different coating was conducted on the CeLi particles in order to show the versatility on surface conjugation and modification of CeLi particles without affecting the payload activity. The coatings not only maintained the enzyme activity, it also provides a physical barrier to AChE from the proteases to prevent degradation and neutralization. As seen from the figure 4.6, two FDA approved inorganic compounds were used and both were effective in maintain the enzyme activity even after sonication. Due to the application of these particles in detecting neurotransmitters, CaP coating was employed to mimic hydroxyapatite present in our body to trigger least immune reaction in the brain. This would be extremely important as the end product from this cascading enzyme leads to the production of hydrogen peroxide which is highly toxic in any part of the body mainly the neurons. The addition of silica and CaP coating also provides the an avenue for

external activation of these particles through ultrasound. However, Silica proved to be a better coating material compared to CaP because of its ability to minimize enzyme-substrate reaction before the application of the ultrasound.

Since majority of the reactions in nanoparticles requires the substrates to diffuse through the particles. Any addition surface coating would provide diffusion resistance to ACh and Ch to diffuse into the particle. These nanoscale barrier does cause a significant delay in detection the ACh. Also our body is a concoction of various proteins, amino acids and vitamins. Since our process involves the conversion of ACh to hydrogen peroxide which reacts with HRP and amplex red or luminol to generate an optical readout, there are many situations that can interfere with the fluorescence. The second enzyme in the cascading process is ChOx whose substrate is Ch which is formed by the degradation of ACh through AChE. Ch is also consumed through diet and is used in many different processes in a human body. The presence of Ch in the brain especially drastically increases the chances of cross talk. In order to determine the effect of choline to the optical detection, we purged some Ch along with ACh to observe any change or shift in the peak.

As seen from the figure 4.7, 4 different combination of SiLi particles were synthesized. One SiLi particle containing all the 3 enzymes of the cascading process and three other SiLi containing individual enzymes of the cascading in each SiLi particle respectively. According to the hypothesis, more diffusion barrier the more time it takes to detect ACh and Ch while less physical barrier, the quicker it takes to detect the particles. As seen in the figure 4.7, free which represents unencapsulated enzymes of the cascade (AChE, ChOx and HRP) provide the quickest detection because of the ease inaccessibility of the substrates for each enzyme. 3 enzymes in SiLi particles provides the second quickest detection time, as the only barrier between the ACh and the three enzymes in the nanoparticles is just the silica coating of one single SiLi particle as all the three enzymes are present in one SiLi particle. The addition of Ch to ACh doesn't change the detection time and remains the same which could be attributed to the fact that the time required for ACh to diffuse into the particle and Ch particles are the same since both these

particles are small molecules. However, when there are 3 different SiLi particles each containing one of the enzymes of the cascade i.e one SiLi loaded with AChE, one SiLi loaded with ChOx and one SiLi loaded with HRP only, the amount of physical barriers for the substrate to diffuse through already triples thereby further increasing the detection time of the ACh. The addition of Ch to ACh tremendously improved the detection time as ChOx can metabolize Ch simultaneously as AChE is degrading ACh to Ch. However this detection time isnt as quick as 3 enzymes encapsulated in one SiLi particle.

4.7 Conclusion

This low cost method can be used to deliver at the sight of interest to detect the rapidly degraded neurotransmitter. It will not only provide insights to the neural connection but also bridge the small incidence to large scale pathological symptom picked up in larger scanners. As we have demonstrated the ability to encapsulate several enzymes with different size and charge to detect ACh. However the rapidity in detection is lower compared to the free enzymes. However, the ability to shield and activate the enzymes through ultrasound provides multitude of advantages: The ability of the particles to be retained in the system till 7-8 days post injection suggests that the enzymes can be used for repeated detection of ACh under different stimuli thereby providing insights to neural networks.

Three enzymes encapsulated in one particle performs better than 3 particles each encapsulated with one enzyme, thereby hinting the diffusivity resistance of the substrate/product through the silica. This method is analogous to kits that are available commercially to detect ACh however, it can be scaled up to load multiple independent enzymes detecting multiple neurotransmitters. This research echos the sentiments of the brain mapping initiative and provides a powerful tool to aid in optical detection of neuron activity.

4.8 Acknowledgments

This chapter, in part is currently being prepared for submission for publication of the material. Mukanth Vaidyanathan, Zeynep Sayar, Negin Mokhtari and Sadik Esener. The dissertation/thesis author was the primary investigator and author of this material.

Chapter 5

Synthetic Hollow Enzyme Loaded Silica Nanoparticle for ATP Detection

5.1 Adenosine Tri-Phosphate (ATP)

Adenosine 5 Triphosphate, is a compound that captures the energy released from catabolic processes and is able to transfer it to energy intensive reactions, serving as a universal energy currency in the cells and therefore is available in all living entities [143]. ATP molecule consists of three different functionally distinct parts, The purine base ring- Adenine, Ribose sugar moiety and Triphosphate tail. In Neurons, ATP levels are predominantly maintained through oxidative phosphorylation in the mitochondria which generates ATP from ADP (Adenosine Diphosphate) [144]. Newly synthesized ATP is produced and transported out of the mitochondria via the oxidative phosphorylation with a steady state cytosolic concentration of 3-10mM.

All living organisms use different mechanisms to monitor its functions internally and also with the environment to adapt, sustain and thrive in various physiological conditions. These afferent mechanisms share a common mechanism which involves the release of ATP

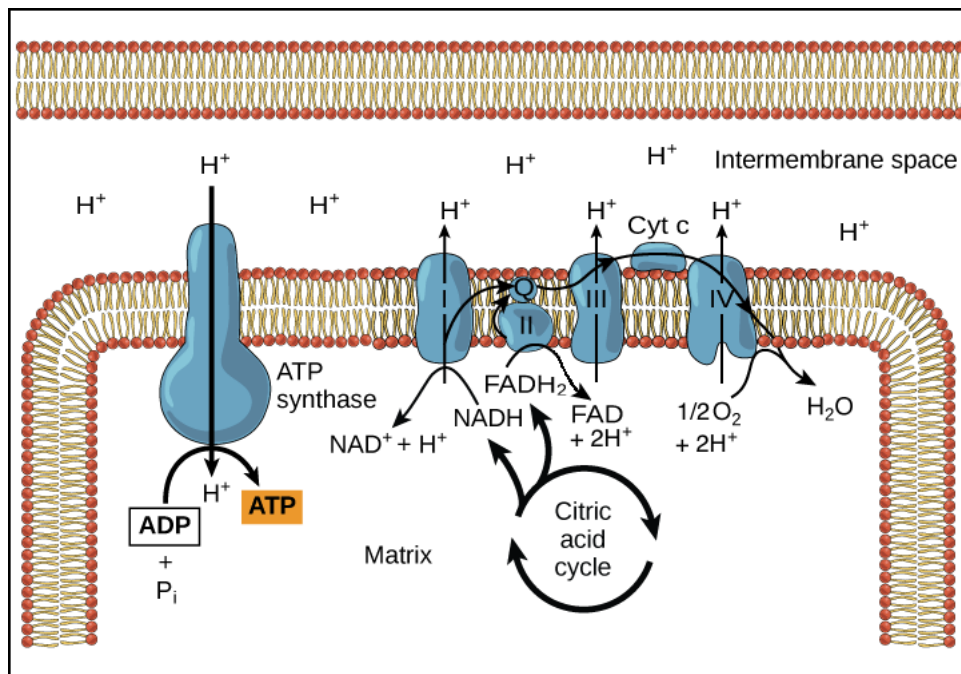


Figure 5.1: The electron transport chain in the cell is the site of oxidative phosphorylation. The NADH and succinate generated in the citric acid cycle are oxidized, releasing energy to power the ATP synthase for generating ATP from ADP

5.2 Role of ATP

Unlike in many organs, Glucose is not the main source of energy in the brain. Under certain circumstances, blood-derived energy substrates, like ketone bodies and lactates also serve as energy sources at times of starvation and during periods of intensive physical activity [145]. The brain has high energy requirements. About 20% of the oxygen and 25% of the glucose consumed by the human body are dedicated to cerebral functions, yet the brain represents only 2% of the total body mass. Maintenance and restoration of ion gradients dissipated by signaling processes such as postsynaptic and action potentials, as well as uptake and recycling of neurotransmitters, are the main processes contributing to the high brain energy needs [146]. Among them, synaptic potentials, appear to represent the main energetic cost related to maintenance of excitability especially in the glutamatergic neurons [147]. Under normal metabolic condition, The cytoplasmic concentration of ATP is 10mmol/l [148]. This acts as the source for ATP for various reactions like:

- GTP and G protein activity
- Exocytosis
- Resting potential of the membrane maintained by Na^+/K^+ ATPase the which consumes 60% of the ATP [146]
- Signal transduction and various protein kinases

Apart from the use in brain, many peripheral sensory excite different nerve fibre through a common mechanism that involves the activation of ionotropic cell receptors (P2X) and metabotropic cell receptors (P2Y).

5.2.1 Current Techniques to Detect ATP

There are currently three methods for detecting exogenous ATP:

- Luciferase-Luciferin Assay[149]
- High Performance Liquid Chromotography (HPLC) (HPLC)[150]
- Radioactive labelling of the Purines [151]
- Patch-sniffing

However, The first two methods have a great sensitivity to the levels of exogeneous ATP. The introduction of a foreign gene to produce luciferase by the cells would limit the use of this assay based system to animal models. HPLC also has the same sensitivity as the luciferase-luciferin assay system and it can also be used to detect various other nucleotides and nucleosides in a single run. However the main pitfall of this method of detection is that the detection isnt real time and would require frequent and repeated injections to collect samples.

However studies have been conducted to study the ATP generation and release in the pericellular spaces using electrodes. These electrodes are conjugated with synthetic glycerol kinase and glycerol-3-phosphate oxidase. These methods require complex signal processing techniques and have not been applied to physiological measurements. Furthermore, this technique can also measure ambient change in glucose concentration and hence cannot be applied on biological tissue[152].

5.2.2 ATP Release in cells

There are four general mechanisms by which intracellular ATP can be released into extracellular spaces[153][154]. [155].

- The intracellular concentration of ATP in cytoplasm can range from 3-5mM, non specific lysis of healthy cells by trauma (physical and chemical) can be contribute to release in extracellular ATP.
- Release through compartmentalized vesicles formed during regulated and unregulated exocytosis where ATP is packaged along with the package present the vesicles like in neurons, endocrine etc.
- Efflux of ATP in cytoplasm via membrane transport proteins
- Release through cell membrane rupture caused due to hypoxia, inflammation, drug metabolism and apoptosis.

ATP is released from several tissues and organs. In 1929, Albert Szent-Gyorgyi and Alan Drury concluded that adenylic acid is the molecule in muscle extract that caused contraction of the smooth muscles. Boyd and Forrester studied several substances that were released by muscle, which when applied to frog heart would increase their heart rate which was later found to contain ATP [156]. Exercise [157][158], hypoxia [159], fluid shear [160] and various ligands [161] lead to release in ATP in the bloodstream in humans but the specific mechanism of release is still unclear. As we know, any biological function in the human cell requires energy including neurons. The activation of Na^+/K^+ channels is mediated by the hydrolysis of ATP to ADP (Adenosine Diphosphate). Because ATP is a very essential substrate for metabolism, the release of ATP is met with some consequences inside the cells. However, If one assumes that the steady-state extracellular ATP is approximately 10 nM under basal conditions and intracellular ATP is 10 mM, the gradient for ATP secretion is approximately 10^6 -fold. This gradient is 100-fold greater, yet opposite to, the gradient for calcium entry into cells. Thus only 1% of the intracellular ATP is released to activate almost all the receptors. Hence, the release of ATP is accomplished without any affect in the cellular metabolism [162].

Administration of ATP to various regions of the brain produced biochemical or electro-physiological changes like an injection of ATP into the lateral ventricle in cats resulted in muscular weakness, ataxia and put the animal to sleep[163]. ATP is also a neurotransmitter as they were released during antidromic stimulation of sensory neurons supplying the artery of rabbit ears and eyes [164][165]. The half life of ATP once released into the extra cellular matrix is very low. This is because ATP is degraded by ectoenzymes localized in surrounding tissues. Thus the extracellular level of ATP measured in the outside the tissue reflects not only the rate of release of ATP, but also the rate of breakdown of released ATP, which is dependent on the activity of the surface located ectoATPases in a given tissue. Chemical drugs and treatment which affect the release of ATP may also affect inactivation of ATP so that measurements on the release and degradation of extracellular ATP provides a better quantification for the release process [166]. Apart from ATP being released by cells that are dying [167], recent research suggests that ATP can also act as a chemical messenger between the glial cells and neurons [168]. ATP can also be released in the neuromuscular junctions and is considered as a Neurotransmitter. Nerve terminal ATP is generated from ADP during glycolysis , citric acid cycle and mostly by oxidative phosphorylation. Storage of synthesized ATP is in different types of synaptic vesicles and also in cytoplasm. They are sometimes co-packages with many other neurotransmitters like the ACh and noradrenaline in purinergic neurons [143].

Several factors complicates the detection and measurement of physiological availability of extracellular ATP that are released. The ubiquitous nature of ATP makes it even more difficult to determine the source of ATP being released. Furthermore the ecto-nucleotidases rapidly hydrolyse ATP thereby making it harder to detect the ATP released[169][170]. In spite of the hydrolysis, the rapid motion of blood and fluid diffuses the ATP thereby diluting the concentration of the ATP. Due to this dynamic nature, most measurement techniques employed to detect ATP in the bulk fluid would vastly underestimate the amount of ATP released, this may be particularly true in cells that do not have direct contact with flowing fluids and blood like the neurons. Hence, the ATP released is enough to activate cells locally but not in the bulk solutions[171][172].

Since firefly luciferase can be used to detect pico molar and nano molar concentration of ATP through luminescence, it is the most widely used technique to detect ATP[173][174][175]. However majority of the measurement of ATP has been through the analysis of the bulk solutions after the release of ATP, the results derived have results in disagreement among many researchers with contradicting results[174]. In principle, the sensitivity of luciferase as a sensor of ATP release into localized or restricted extracellular spaces can be improved dramatically without causing any immune reaction against luciferase in live animals by the use of nanoparticles.

5.3 LuciSHELs

5.4 Materials

200 nm diameter NIST (National Institute of Standards and Technology) polystyrene (PS) beads were purchased from Polysciences Inc, Warminster, PA. 60nm PS beads functionalized with carboxyl group were purchased from Bangs Laboratories inc, Fishers, In. Luciferase from from Photinus *pyralis*, D-Luciferin, (3-Aminopropyl) trimethoxysilane (APTMS), Tetramethyl orthosilicate (TMOS) were purchased from Sigma Aldrich, St Louis, MO. 190 proof ethyl alcohol was purchased from FisherScientific, Waltham, MA. Phosphate Buffer Saline (PBS) was purchased from Hyclone Laboratories Inc, Logan, UT. Poly-l-lysine (PLL) ,

5.5 Method

5.5.1 Synthesis of LuciSHELs

The hollow silica particle was synthesized using the modified version as described by Ortac [28]. In brief, 60 ul of larger PS bead (200nm)-template, was mixed with 40ul of smaller PS beads (60nm)- mask for 15 mins at high speed. This results with the PS masks electrostatically bonded to the template thereby resulting in a spike ball like structure. 1ml of 190 proof ethanol was added drop

wise to the template-mask mixture. 1ul of APTMS and 2ul of TMOS was added sequentially to the ethanol mixture and mixed for 4 hours in room temperature. The spike ball like nanostructure forms the base over which the silica is templated. The 200nm PS beads serves as a template over which the silica begins to grow. The rate of the silica precipitation on the template can be controlled by the amount of water and APTMS added. The silica precipitation reaction was stopped by washing the sample in centrifuge at 14 g for 10 mins. The pellet was resuspended in 1ml of ethanol and this process is repeated for 3 times. After the final wash, the pellet was re-suspended to 60 ul of ethanol. The solution is calcined in a ceramic crucible at 475°C overnight in a laboratory grade convection oven.

The calcined product was redispersed in ethanol from the crucible and washed into DI water. Until the last centrifuge process, where the pellet is not dispersed in water but in 60ul of 50mg/ml of luciferase solution in PBS. The said mixture is mixed under vortex overnight in 4°C. This ensures that the enzyme has enough time to diffuse into the hollow silica nanoparticles. The enzyme-nanoparticle solution can be sonicated in an ice bath for 60 seconds with 1 sec on and 1 sec off pulse under 20 % amplitude. (Refer figure5.2B)

After overnight mixing, the enzyme-nanoparticle complex is mixed with 5ul of 10% w/v PLL for 10 minutes. This produces a uniform coating of the long chain polymer- PLL to cover the mesoporous holes through electrostatic attraction (PLL is positively charged and silica is negatively charged). This prevents the enzymes to leak out temporarily from the nanoparticle (Refer figure5.2C). To ensure that the enzyme is completely sealed in the nanoparticle, the enzyme-nanoparticle mixture is diluted with 1 ml of PBS and mixed with 25 ul of silicic acid overnight at 4°C . Silicic acid is produced by mixing 100ul of 1mM of HCl with 14.8 ul of TMOS. Silicic acid is highly reactive and generates silicon hydroxide hydrogel layer on the nanoparticle which is preferentially grown on the PLL, which covers the surface of the nanoparticle (Refer figure5.2D). Due to the high reactivity of the silicic acid, this solution has to be prepared right before the addition to the particles.

5.5.2 Characterization of the LuciSHELs

The size and surface charge of the liposomes were characterized using Zeta-sizer Nano from Malvern Instruments, Malvern, UK. The size was also characterized using electron microscope images using the Helios NanoLab DualBeam from FEI. The luminescence activity of the enzyme was optically detected using Infinite 200 PRO series from Tecan, Mannerdorf, SUI.

5.5.3 Enzyme Encapsulation Efficiency Determination

The enzyme encapsulation efficiency was conducted with Luciferase-luciferin luminescence assay. A standard curve was conducted with different concentration of luciferase along with 0.01mg/ml of D-luciferin and 1 μ M ATP dissolved in deionized water (DI water).

5.5.4 Luciferin ATP assay for the Measurement of Luciferase Activity

The LuciSHELs and unencapsulated luciferase activity was measured using luminescence assay at 512 nm. The sample was incubated with 0.01mg/ml of D-luciferin at 37°C while mixing for 5 mins prior to the addition of 50 μ l of ATP (concentrations ranging from 1mM to 1pM).

5.5.5 Luminescence Detection *in vitro*

Far-field optical signals were collected using an upright optical microscope equipped with a 50x (Nikon, NA 0.55) objective and an EMCCD camera (Ixon, Andor Technology). The particles were injected in certain pre-determined locations on the PDMS mould. 100 μ l of 0.1mg/ml of luciferin was added prior to addition of ATP. 100 μ l of ATP with different concentrations were prepared and added dropwise at the end of the PDMS mould away from the predetermined locations of LuciSHELs.

5.6 Results

The size of SHELS through DLS was determined to be around 240 nm and the surface charge to be -26mV before encapsulation with luciferase. The size of SHELS was found to be 215nm using scanning electron microscopy (SEM) before sealing with luciferase. However there is a huge change in the charge of the SHELS once it has been sealed using a sol-gel layer from the bare SHELS. The charge of the the sealed particles was determined to be -18mV.

Different methods to coat the surface have been studied to influence the activity of the enzyme inside the LuciSHES. Several other surface coatings were also tested in addition to silicic acid. APTMS was added to provide another uniform layer of Si-amines on the surface thereby making the surface more cationic compared to just the anionic silicic acid. However, the addition on PEG to the sol-gel layer makes the surface change of the SHELS more neutral. As seen from the figure5.3, addition of PEG does show a higher detectable signal compared to other coating at the same ATP concentrations. This is very dramatic at lower ATP concentrations. All the LuciSHELs used in this experiment were loaded with 50mg/ml of luciferase. The figure5.3 shows that addition of PEG on the surface is important in improving the signal at lower ATP concentrations. Similar experiments were conducted to tested the luminescence at 1nM of ATP of LuciSHELs with and without the addition of PEG, with two different enzyme concentrations: 30mg/ml and 1mg/ml. As inferred from the figure5.4, the luminescence of all the samples coated with PEG performed better to the ones that did not undergo PEGlation. Especially, PEGlated version of SHELS loaded with 1mg/ml of luciferase did perform better compared to its counterpart (non peglation), which shows almost no detectable signal. LuciSHELs activity was measured along with the unencapsulated luciferase at different concentration of ATP to determine any changes in the enzyme kinetics due to encapsulation in the SHELS. Figure5.5 shows that the enzyme kinetics between free and LuciSHELs were found to follow the similar trend. To detect ATP in a dynamic solution and to capture the flash and glow luminescence. LuciSHELs loaded with 80mg/ml of luciferase was embedded in a clear PDMS mould at different locations across the surface. the whole mould was filled

with 0.1mg/ml of D-luciferin. Figure 5.6 shows the luminescence immediately and after 10 seconds after the addition of 500 μ l of 1nM ATP. The luminescence signal clearly appears to be decaying with time. However, the figure 5.7 shows luminescence measured at 10 seconds after the addition of 500 μ l of 1nM ATP at 2 different locations of SHELS, L1-a refers to the position closer to the site of the addition of ATP while L2 is further away from L1-a while L1 is the same location as of L1-a taken prior to the addition of ATP. This shows the path of ATP diffusion across a flat PDMS mould.

5.7 Discussion

Luciferase encapsulated SHELS provide a platform for detecting ATP in site specific regions like the brain and cardiomyocytes. The charge of the SHELS prior to the coating with PLL forms the a charge based anionic template due to the presence of silica. The attraction of PLL onto the silica is purely electrostatic and the shift in the surface charge of the particles shifts from anionic to cationic domain. PLL is cationic due to the presence of primary amine groups in a long chain polymer [176]. Condensation of silicic acids leads to the formation of long chain polymeric silicic acid in aqueous solutions which preferentially forms over the PLL electrostatically. Sol-gel silica tends to be less anionic compared to calcinated silica which is what is inferred from the zeta measurements of LuciSHELS particles. As seen from the figure??, the surface charge of the SHELS does play an important role in transport of the small molecules across the nanopores formed during the solgel process. D-Luciferin and ATP are both anionic [177] molecules which would be repelled by the anionic silica coating. The APTMS coating would preferentially change the surface charge from negative to positive but has little to no improvement in the luminescence as seen in figure 5.3. This may be because the substrates might be attracted to the particles but retained at the surface rather than being metabolized with luciferase. However, Neutralizing the surface charge with PEG provides little to no hindrance in diffusion of the substrate across the nanoparticles thereby being consumed by luciferase which can be inferred by the increase in luminescence even at lower concentrations of ATP. Figure 5.3 shows the effect of

different surface on the diffusivity of the substrate and interact with 50mg/ml of luciferase loaded in SHELS. Further to see the effect of different enzyme loading concentration with SHELS coated with PEG. Figure5.4 shows a drastic increase in the detection signal at lower concentrations of luciferase encapsulated in SHELS coated with PEG. At physiological ATP concentration of 1nM, PEG coated LuciSHELS loaded with 1mg/ml of enzyme provides roughly 100 folds increase in activity compared to its no PEG counterpart. In Addition to the PEG, activity of free luciferase and LuciSHELS at same ATP concentration provide similar luminescence readout. This shows that the enzyme, even though encapsulated inside a nanoparticle behaves like the free enzyme and it further reaffirms that no chemical or physical modification was performed with the enzyme during encapsulation that lead to any change in the activity kinetics.

Figure5.6 shows the luminescence decay with time. The catalysis of the luciferin and ATP is instantaneous and rapid, hence can be used for detecting nerve impulse and electrical impulses that releases ATP like in cardiomyocytes. However, the diffusion of ATP is uncontrolled in the body and can diffuse randomly, figure5.7 shows the luminescence decay measured at the same time between two locations which are embedded with SHELS. The location L2 which is further away from L1-a shows a lower intensity while the L1-a shows higher intensity due to the close proximity of the location of the injection of 1nM ATP. The incidence captured in the figure5.7 indicates that any ATP that diffuses through the fluid can still be picked up and metabolised. This provides a foundation to conduct further experiments on tracking the nerve impulse along a specific nerve pathway, thereby a strong tool for mapping the brain activity.

5.8 Conclusion

We have demonstrated a hollow silica nanoparticle loaded with luciferase to detect ATP in the presence of luciferin. The synthesis and fabrication indicated that different concentration of luciferase can be loaded in the particle to improve the detection. We have also demonstrated that the surface charge of the nanoparticle plays a very vital role in detecting ATP. Neutrally charged nanoparticles seem

to provide better dynamic range for detection even at lower concentration of ATP. To simulate the ATP diffusion in real system, we have employed the use of a PDMS which indicates that the luciSHELs are able to detect the ATP at different time intervals. The present formulation allows the nanoparticles to localize at the site of injection, this would be desirable in detecting ATP levels both in neurons and in cardiomyocytes.

However, the formulation does have its pitfalls. The enzyme used for the detection of luminescence doesn't perform well at lower concentrations of ATP. This might mandate the research to synthesize synthetic luciferase with higher light units yield per ATP hydrolysed. Secondly, Apart from the high enzyme loading capabilities of SHELs. The fabrication process is extremely sensitive to the composition of the template and the mask. Since this nanoparticle is completely synthesized from silica, there are possibilities to toxicities at higher dosage.

5.9 Acknowledgments

This chapter, in part is currently being prepared for submission for publication of the material. Mukanth Vaidyanathan, Yaoguang Ma, Ya-san Yeh and Sadik Esener. The dissertation/thesis author was the primary investigator and author of this material.

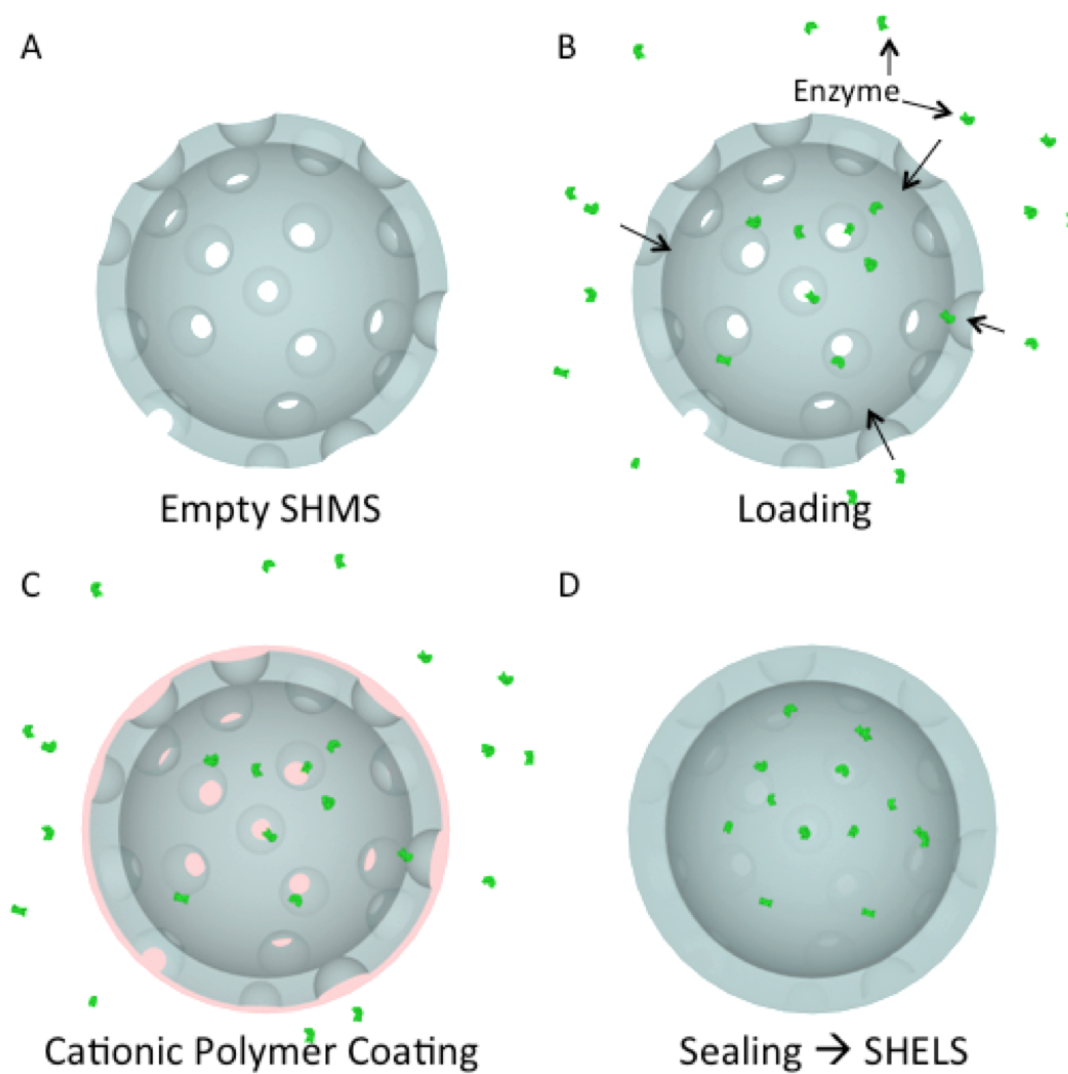


Figure 5.2: Schematic representation of the synthesis of SHELS. (A) Hollow silica nanoparticle (B) High concentration enzyme loading through diffusion. (C) PLL-Cationic polymer coated hollow silica nanoparticles (D) Hollow silica nanoparticles sealed with another sol-gel layer through silicic acid

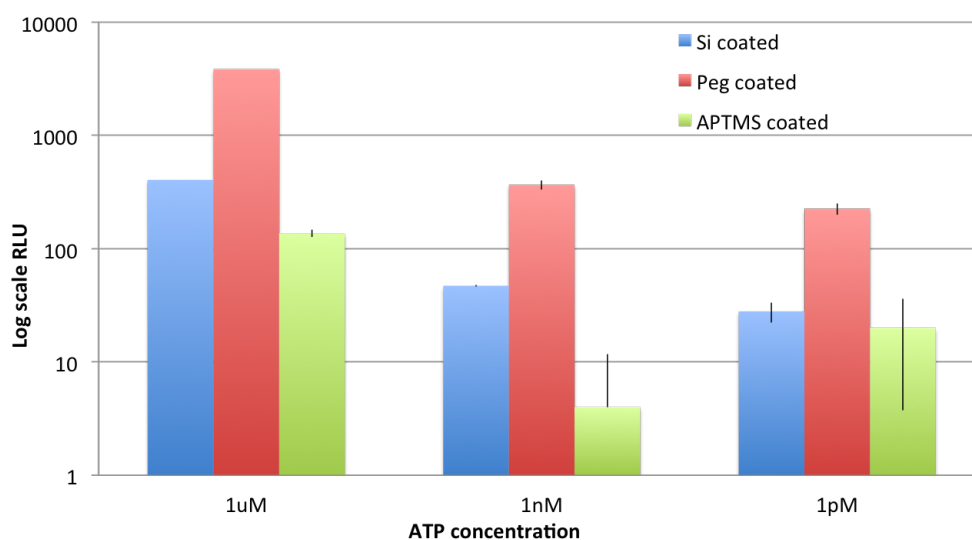


Figure 5.3: Luciferase luminescence at different ATP concentration with different surface coating. Si: Just Silicic Acid. APTMS: Silicic acid and APTMS. PEG: Silicic acid and PEG-2000

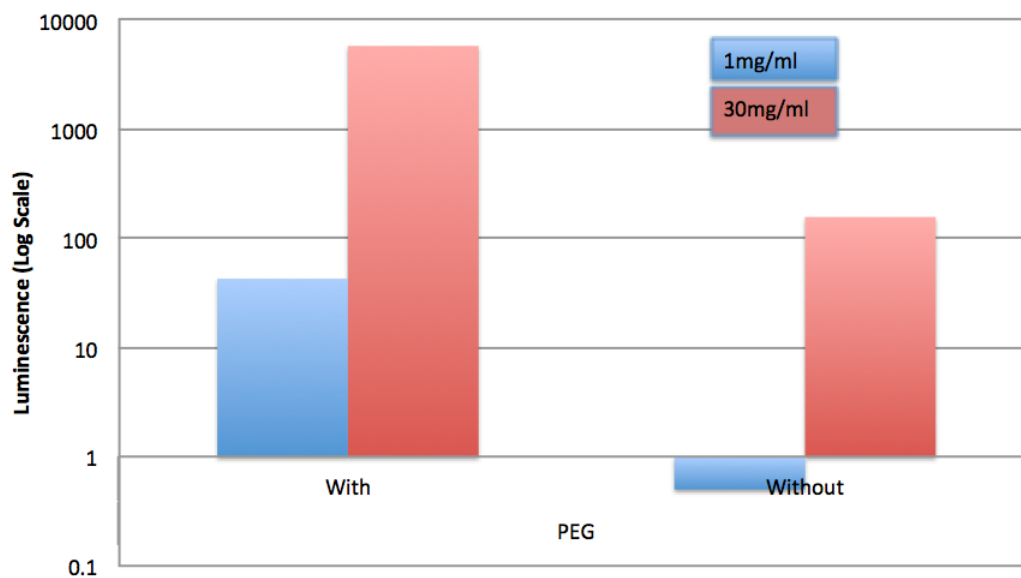


Figure 5.4: Luminescence of SHELS coated with and without PEG and loaded with different enzyme concentration, 1mg/ml and 30mg/ml at 1nM of ATP and 0.1mg/ml of D-luciferin

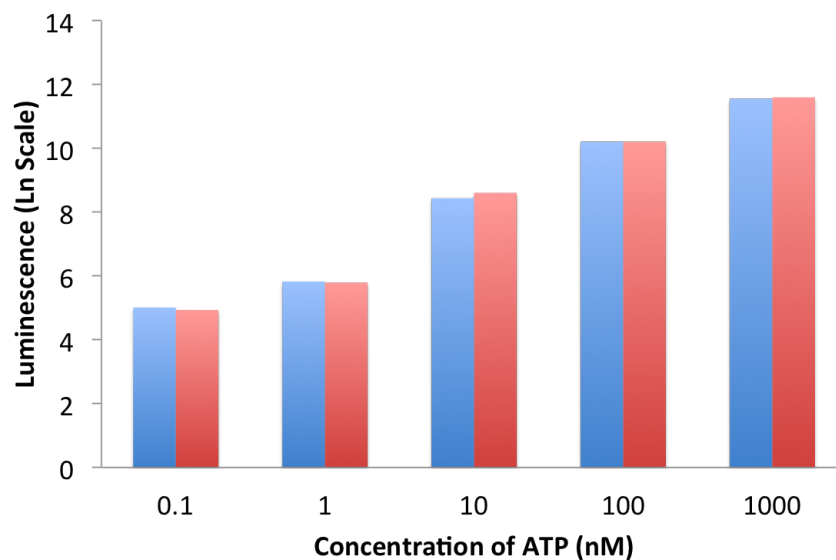


Figure 5.5: Comparison of enzyme kinetic study between the luciferase and LuciSHELS performed at different concentrations of ATP at 0.1mg/ml of D-Luciferin

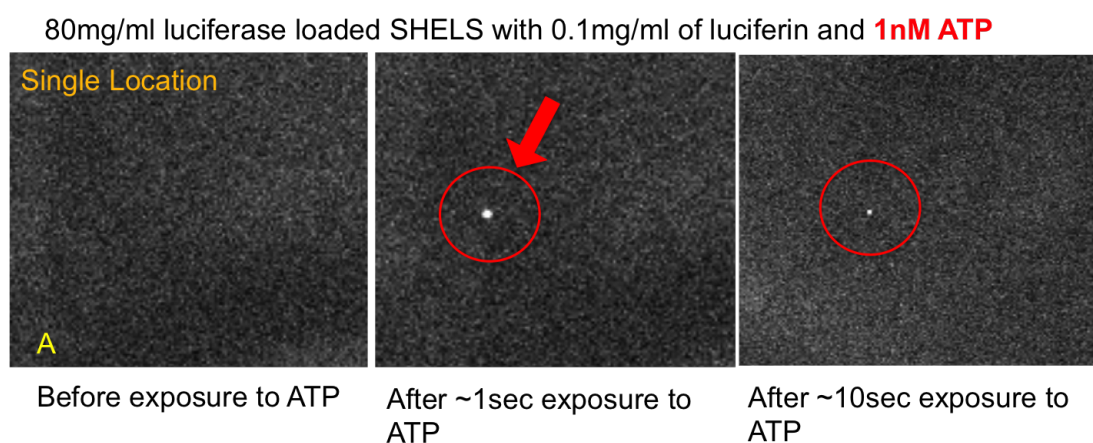


Figure 5.6: Luminescence measured at a single location after 1 second and 10 seconds after the addition of 1nM ATP

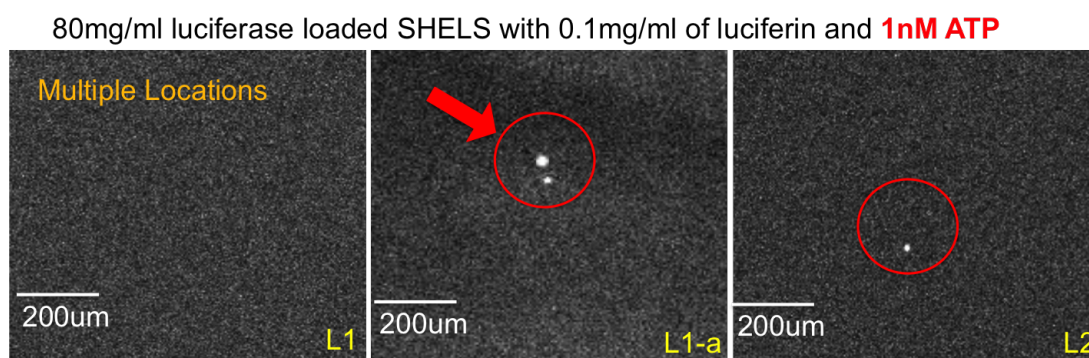


Figure 5.7: Luminescence measured at a multiple location at 10 seconds after the addition of 1nM ATP, L1: Location before the addition of ATP. L1-a: Area closer to ATP addition. L2: Location Further away laterally to L1-a.

Chapter 6

Conclusion and Final Notes

The application of SiLi are multi-faceted. The ability of the particle to encapsulate enzyme irrespective of the size and charge with minimal to none loss in activity and stability proves to be a promising platform in delivering bio active molecules in the body. Not only the biomolecules (here enzymes) retain similar activity to the free enzymes, it also provides protection to the bio molecules against specific and non specific neutralization from the immune system.

The fabrication procedure is general and should be applicable to many other materials. As shown previous in figures 2.9 and 4.6, SiLi can be made of different materials and for variety of different applications. With the addition of the inorganic layer (like silica and CaP) on the liposomes not only protects it from the immune system but it also opens up opportunities to functionalize the surface with specific targeting agents like EGFR, VegF, bungarotoxin which improves the therapeutic and diagnostic efficacy *in vivo*.

Not only can the nanoparticles be targeted upon the addition on several targeting moieties, the activity of the enzyme loaded can be also be manipulated upon the application of the ultrasound. The lipids in the liposomes are closely bound to prevent any interaction of the enzymes with the outside environment, however upon the exposure of ultrasound, the lipids tend to manipulate and perforate thereby exposing the enzyme to the substrate. Since the application of ultrasound doesn't affect the silica coating, the enzyme can be activated without hampering its activity and additionally also providing protection against any specific and non

specific immune reactions.

For the application in medicine, there are still many aspects of the SiLi that needs to be studied. The use of HiFU needs to be tested and quantified on the enzymes activity and stability loaded in SiLi. The toxicity and quantification of the immune response on SiLi will need further study.

More studies need to be conducted to determine the surface functionalization of the SiLi to improve the circulation half life, thereby eliminating the need for chemical modification of the enzyme payload. The use of CaP as a secondary coating instead of silica is promising and needs to be explored. However with the addition of the secondary layer - Si, the CeLi do not maintain the structural integrity and hence collapse. So further studies are required to explore the possibilities of using different lipids like sphingolipids, DOPE, Soy PC or DSPC etc. The use of polymer like PLGA, PCL, Dextran, can also be employed to further strengthen the lipid structure without compromising its echogenic properties. However in these conditions, the enzymes in SiLi have controlled access to substrate which makes it an excellent choice for treating brain diseases, cancer and pregnancy related problems.

The use of SiLi is not only limited to protein carrier it can also be employed to carry small molecules which can be used for imaging as well as for therapeutics. One such usage would be to encapsulate analgesics in these particles which would be very useful for trigger release of analgesics after an open wound surgery.

Bibliography

- [1] Roger RC New. *Liposomes: a practical approach*. Vol. 58. Oxford University Press, USA, 1990.
- [2] Thomas Linke, Gundo Wilkening, Farsaneh Sadeghlar, Heidi Mozcall, Katussevani Bernardo, Edward Schuchman, and Konrad Sandhoff. “Interfacial Regulation of Acid Ceramidase Activity stimulation of ceramide degradation by lysosomal lipids and sphingolipid activator proteins”. In: *Journal of Biological Chemistry* 276.8 (2001), pp. 5760–5768.
- [3] Ajay Kumar, Shital Badde, Ravindra Kamble, and Varsha B Pokharkar. “Development and characterization of liposomal drug delivery system for nimesulide”. In: *Int J Pharm Pharm Sci* 2.4 (2010), pp. 87–9.
- [4] Todd PW McMullen and Ronald N McElhaney. “New aspects of the interaction of cholesterol with dipalmitoylphosphatidylcholine bilayers as revealed by high-sensitivity differential scanning calorimetry”. In: *Biochimica et Biophysica Acta (BBA)-Biomembranes* 1234.1 (1995), pp. 90–98.
- [5] Eizo Sada, Shigeo Katoh, Masaaki Terashima, and Ken-Ichi Tsukiyama. “Entrapment of an ion-dependent enzyme into reverse-phase evaporation vesicles”. In: *Biotechnology and bioengineering* 32.6 (1988), pp. 826–830.
- [6] AD Bangham. “Liposomes: the Babraham connection”. In: *Chemistry and physics of lipids* 64.1-3 (1993), pp. 275–285.
- [7] Reto A Schwendener. “Liposomes as vaccine delivery systems: a review of the recent advances”. In: *Therapeutic advances in vaccines* 2.6 (2014), pp. 159–182.
- [8] OM Atrooz. “Effects of alkylresorcinolic lipids obtained from acetonic extract of Jordanian wheat grains on liposome properties”. In: *Int J Biol Chem* 5.5 (2011), pp. 314–321.
- [9] Tamer Shehata, Ken-ichi Ogawara, Kazutaka Higaki, and Toshikiro Kimura. “Prolongation of residence time of liposome by surface-modification with

- mixture of hydrophilic polymers”. In: *International journal of pharmaceuticals* 359.1 (2008), pp. 272–279.
- [10] Demetrios Papahadjopoulos. *Liposomes their use in biology and medicine*. Vol. 308. New York Academy of Sciences New York, 1978.
- [11] Christian Herzog, Katharina Hartmann, Valérie Künzi, Oliver Kürsteiner, Robert Mischler, Hedvika Lazar, and Reinhard Glück. “Eleven years of Inflexal Vi£jï£jï£ja virosomal adjuvanted influenza vaccine”. In: *Vaccine* 27.33 (2009), pp. 4381–4387.
- [12] Maria Laura Immordino, Franco Dosio, and Luigi Cattel. “Stealth liposomes: review of the basic science, rationale, and clinical applications, existing and potential”. In: *International journal of nanomedicine* 1.3 (2006), p. 297.
- [13] Michael Glantz, Kurt A Jaeckle, Marc C Chamberlain, Surasak Phuphanich, Lawrence Recht, Lode J Swinnen, Bernard Maria, Susan LaFollette, G Berry Schumann, Bernard F Cole, and Stephen B Howell. “A randomized controlled trial comparing intrathecal sustained-release cytarabine (DepoCyt) to intrathecal methotrexate in patients with neoplastic meningitis from solid tumors”. In: *Clinical cancer research* 5.11 (1999), pp. 3394–3402.
- [14] David W Denning, Jeanette Y Lee, John S Hostetler, Peter Pappas, Carol A Kauffman, Daniel H Dewsnup, John N Galgiani, John R Graybill, Alan M Sugar, Antonino Catanzaro, Harry Gallis, John R Perfect, Bonite Dockery, William E Dismukes, and David A Stevens. “NIAID Mycoses Study Group multicenter trial of oral itraconazole therapy for invasive aspergillosis”. In: *The American journal of medicine* 97.2 (1994), pp. 135–144.
- [15] Ran Mo, Tianyue Jiang, Jin Di, Wanyi Tai, and Zhen Gu. “Emerging micro- and nanotechnology based synthetic approaches for insulin delivery”. In: *Chemical Society Reviews* 43.10 (2014), pp. 3595–3629.
- [16] Gillian M Barratt. “Therapeutic applications of colloidal drug carriers”. In: *Pharmaceutical Science & Technology Today* 3.5 (2000), pp. 163–171.
- [17] Birgit Romberg, Wim E Hennink, and Gert Storm. “Sheddable coatings for long-circulating nanoparticles”. In: *Pharmaceutical research* 25.1 (2008), pp. 55–71.
- [18] Guohui Wu, Alexander Mikhailovsky, Htet A Khant, Caroline Fu, Wah Chiu, and Joseph A Zasadzinski. “Remotely triggered liposome release by near-infrared light absorption via hollow gold nanoshells”. In: *Journal of the American Chemical Society* 130.26 (2008), pp. 8175–8177.

- [19] Hirofumi Takeuchi, Hiromitsu Yamamoto, and Yoshiaki Kawashima. “Mucoadhesive nanoparticulate systems for peptide drug delivery”. In: *Advanced drug delivery reviews* 47.1 (2001), pp. 39–54.
- [20] Howard Rosen and Thierry Abribat. “The rise and rise of drug delivery”. In: *Nature Reviews Drug Discovery* 4.5 (2005), pp. 381–385.
- [21] Sang-Min Lee, Haimei Chen, Christine M Dettmer, Thomas V O’Halloran, and SonBinh T Nguyen. “Polymer-caged liposomes: a pH-responsive delivery system with high stability”. In: *Journal of the American Chemical Society* 129.49 (2007), pp. 15096–15097.
- [22] Claire S Peyratout and Lars Daehne. “Tailor-made polyelectrolyte microcapsules: from multilayers to smart containers”. In: *Angewandte Chemie International Edition* 43.29 (2004), pp. 3762–3783.
- [23] Paul F Noble, Olivier J Cayre, Rossitza G Alargova, Orlin D Velez, and Veselin N Paunov. “Fabrication of "hairy" colloidosomes with shells of polymeric microrods”. In: *Journal of the American Chemical Society* 126.26 (2004), pp. 8092–8093.
- [24] Liangfang Zhang and Steve Granick. “How to stabilize phospholipid liposomes (using nanoparticles)”. In: *Nano letters* 6.4 (2006), pp. 694–698.
- [25] Narayan K Raman, Mark T Anderson, and C Jeffrey Brinker. “Template-based approaches to the preparation of amorphous, nanoporous silicas”. In: *Chemistry of Materials* 8.8 (1996), pp. 1682–1701.
- [26] Qianyao Sun, Engel G Vrieling, Rutger A van Santen, and Nico AJM Sommerdijk. “Bioinspired synthesis of mesoporous silicas”. In: *Current Opinion in Solid State and Materials Science* 8.2 (2004), pp. 111–120.
- [27] Marc R Knecht and David W Wright. “Amine-terminated dendrimers as biomimetic templates for silica nanosphere formation”. In: *Langmuir* 20.11 (2004), pp. 4728–4732.
- [28] Inanc Ortac, Dmitri Simberg, Ya-san Yeh, Jian Yang, Bradley Messmer, William C Trogler, Roger Y Tsien, and Sadik Esener. “Dual-porosity hollow nanoparticles for the immunoprotection and delivery of nonhuman enzymes”. In: *Nano letters* 14.6 (2014), pp. 3023–3032.
- [29] Angel Tan, Spomenka Simovic, Andrew K Davey, Thomas Rades, and Clive A Prestidge. “Silica-lipid hybrid (SLH) microcapsules: a novel oral delivery system for poorly soluble drugs”. In: *Journal of controlled release* 134.1 (2009), pp. 62–70.

- [30] Pierre-Yves Bolinger, Dimitrios Stamou, and Horst Vogel. “Integrated nano reactor systems: triggering the release and mixing of compounds inside single vesicles”. In: *Journal of the American Chemical Society* 126.28 (2004), pp. 8594–8595.
- [31] Ye Li and Wai Tak Yip. “Liposomes as Protective Capsules for Active Silica Sol- Gel Biocomposite Synthesis”. In: *Journal of the American Chemical Society* 127.37 (2005), pp. 12756–12757.
- [32] M Babincova, P Čičmanec, V Altanerova, Č Altaner, and P Babinec. “AC-magnetic field controlled drug release from magnetoliposomes: design of a method for site-specific chemotherapy”. In: *Bioelectrochemistry* 55.1 (2002), pp. 17–19.
- [33] Anja Mueller, Bruce Bondurant, and David F O’Brien. “Visible-light- stimulated destabilization of PEG-liposomes”. In: *Macromolecules* 33.13 (2000), pp. 4799–4804.
- [34] Daryl C Drummond, Monia Zignani, and Jean-Christophe Leroux. “Current status of pH-sensitive liposomes in drug delivery”. In: *Progress in Lipid Research* 39.5 (2000), pp. 409–460.
- [35] Alexandre Marin, Hao Sun, Ghaleb A Hussein, William G Pitt, Douglas A Christensen, and Natalya Y Rapoport. “Drug delivery in pluronic micelles: effect of high-frequency ultrasound on drug release from micelles and intracellular uptake”. In: *Journal of Controlled Release* 84.1 (2002), pp. 39–47.
- [36] N Rapoport, A Marin, and DA Christensen. “Ultrasound-activated micellar drug delivery”. In: *Drug Delivery Syst Sci* 2.2 (2002), pp. 37–46.
- [37] Shao-Ling Huang and Robert C MacDonald. “Acoustically active liposomes for drug encapsulation and ultrasound-triggered release”. In: *Biochimica et Biophysica Acta (BBA)-Biomembranes* 1665.1 (2004), pp. 134–141.
- [38] Jacques S Abramowicz. “Ultrasound contrast media and their use in obstetrics and gynecology”. In: *Ultrasound in medicine & biology* 23.9 (1997), pp. 1287–1298.
- [39] Zvi R Cohen, Jacob Zaubermann, Sagi Harnof, Yael Mardor, Dvora Nass, Eyal Zadicario, Arik Hananel, David Castel, Meir Faibel, and Zvi Ram. “Magnetic Resonance Imaging-guided Focused Ultrasound For Thermal Ablation in the Brain: A Feasibility Study In A Swine Model”. In: *Neurosurgery* 60.4 (2007), pp. 593–600.

- [40] Samir Mitragotri and Joseph Kost. “Low-frequency sonophoresis: a review”. In: *Advanced drug delivery reviews* 56.5 (2004), pp. 589–601.
- [41] Avi Schroeder, Joseph Kost, and Yechezkel Barenholz. “Ultrasound, liposomes, and drug delivery: principles for using ultrasound to control the release of drugs from liposomes”. In: *Chemistry and physics of lipids* 162.1 (2009), pp. 1–16.
- [42] M Duvshani-Eshet, L Baruch, E Kesselman, E Shimoni, and M Machluf. “Therapeutic ultrasound-mediated DNA to cell and nucleus: bioeffects revealed by confocal and atomic force microscopy”. In: *Gene therapy* 13.2 (2006), pp. 163–172.
- [43] Simona Mura, Julien Nicolas, and Patrick Couvreur. “Stimuli-responsive nanocarriers for drug delivery”. In: *Nature materials* 12.11 (2013), pp. 991–1003.
- [44] Yechezkel Chezy Barenholz. “Doxil \ddot{u} \ddot{u} \ddot{u} \ddot{u} \ddot{u} the first FDA-approved nano-drug: lessons learned”. In: *Journal of controlled release* 160.2 (2012), pp. 117–134.
- [45] Andreas Wicki, Dominik Witzigmann, Vimalkumar Balasubramanian, and Jörg Huwyler. “Nanomedicine in cancer therapy: challenges, opportunities, and clinical applications”. In: *Journal of Controlled Release* 200 (2015), pp. 138–157.
- [46] Tove J Evjen, Esben A Nilssen, Robert A Fowler, Sibylla Røgnvaldsson, Martin Brandl, and Sigrid L Fossheim. “Lipid membrane composition influences drug release from dioleoylphosphatidylethanolamine-based liposomes on exposure to ultrasound”. In: *International journal of pharmaceuticals* 406.1 (2011), pp. 114–116.
- [47] Tove J Evjen, Esben A Nilssen, Sibylla Røgnvaldsson, Martin Brandl, and Sigrid L Fossheim. “Distearoylphosphatidylethanolamine-based liposomes for ultrasound-mediated drug delivery”. In: *European Journal of Pharmaceutics and Biopharmaceutics* 75.3 (2010), pp. 327–333.
- [48] Chong Li, Yan Zhang, Tingting Su, Lianlian Feng, Yingying Long, and Zhangbao Chen. “Silica-coated flexible liposomes as a nanohybrid delivery system for enhanced oral bioavailability of curcumin”. In: *International Journal Nanomedicine* 7.7 (2012), pp. 5995–6002.
- [49] Francis Szoka and Demetrios Papahadjopoulos. “Procedure for preparation of liposomes with large internal aqueous space and high capture by reverse-

- phase evaporation”. In: *Proceedings of the National Academy of Sciences* 75.9 (1978), pp. 4194–4198.
- [50] L Bildstein, C Dubernet, and P Couvreur. “Prodrug-based intracellular delivery of anticancer agents”. In: *Advanced drug delivery reviews* 63.1 (2011), pp. 3–23.
- [51] Martijn Rooseboom, Jan NM Commandeur, and Nico PE Vermeulen. “Enzyme - catalyzed activation of anticancer prodrugs”. In: *Pharmacological reviews* 56.1 (2004), pp. 53–102.
- [52] Gregor Zlokarnik, Paul A Negulescu, Thomas E Knapp, Lora Mere, Neal Burren, Luxin Feng, Michael Whitney, Klaus Roemer, and Roger Y Tsien. “Quantitation of transcription and clonal selection of single living cells with β -lactamase as reporter”. In: *Science* 279.5347 (1998), pp. 84–88.
- [53] Christian Betzel, TP Singh, M Visanji, K Peters, S Fittkau, W Saenger, and KS Wilson. “Structure of the complex of proteinase K with a substrate analogue hexapeptide inhibitor at 2.2-Å resolution.” In: *Journal of Biological Chemistry* 268.21 (1993), pp. 15854–15858.
- [54] Kazuyuki Morihara and Hiroshige Tsuzuki. “Specificity of proteinase K from *Tritirachium album* Limber for synthetic peptides”. In: *Agricultural and Biological Chemistry* 39.7 (1975), pp. 1489–1492.
- [55] Helmuth Hilz, Ulrich Wieggers, and Peter Adamietz. “Stimulation of proteinase K action by denaturing agents: application to the isolation of nucleic acids and the degradation of “masked” proteins”. In: *European Journal of Biochemistry* 56.1 (1975), pp. 103–108.
- [56] Verónica Salgueiriño-Maceira, Miguel A Correa-Duarte, Marina Spasova, Luis M Liz-Marzán, and Michael Farle. “Composite silica spheres with magnetic and luminescent functionalities”. In: *Advanced Functional Materials* 16.4 (2006), pp. 509–514.
- [57] Marian Valko, Mario Izakovic, Milan Mazur, Christopher J Rhodes, and Joshua Telser. “Role of oxygen radicals in DNA damage and cancer incidence”. In: *Molecular and cellular biochemistry* 266.1-2 (2004), pp. 37–56.
- [58] Wulf Dröge. “Free radicals in the physiological control of cell function”. In: *Physiological reviews* 82.1 (2002), pp. 47–95.
- [59] Jun Fang, Takahiro Seki, and Hiroshi Maeda. “Therapeutic strategies by modulating oxygen stress in cancer and inflammation”. In: *Advanced drug delivery reviews* 61.4 (2009), pp. 290–302.

- [60] Hiroshi Maeda and Takaaki Akaike. "Oxygen free radicals as pathogenic molecules in viral diseases". In: *Proceedings of the Society for Experimental Biology and Medicine* 198.2 (1991), pp. 721–727.
- [61] Sung Nim Han, Mohsen Meydani, Dayong Wu, Bradley S Bender, Donald E Smith, José Viña, Guohua Cao, Ronald L Prior, and Simin Nikbin Meydani. "Effect of long-term dietary antioxidant supplementation on influenza virus infection". In: *The Journals of Gerontology Series A: Biological Sciences and Medical Sciences* 55.10 (2000), B496–B503.
- [62] Helen Wiseman and Barry Halliwell. "Damage to DNA by reactive oxygen and nitrogen species: role in inflammatory disease and progression to cancer." In: *Biochemical Journal* 313.Pt 1 (1996), p. 17.
- [63] Yukiko Hasegawa, Toru Takano, Akira Miyauchi, Fumio Matsuzuka, Hiroshi Yoshida, Kanji Kuma, and Nobuyuki Amino. "Decreased expression of glutathione peroxidase mRNA in thyroid anaplastic carcinoma". In: *Cancer letters* 182.1 (2002), pp. 69–74.
- [64] Larry W Oberley. "Mechanism of the tumor suppressive effect of MnSOD overexpression". In: *Biomedicine & Pharmacotherapy* 59.4 (2005), pp. 143–148.
- [65] László Góth, Péter Rass, and Anikó Páy. "Catalase enzyme mutations and their association with diseases". In: *Molecular Diagnosis* 8.3 (2004), pp. 141–149.
- [66] Kenzo Sato, Keizo Ito, Hiromi Kohara, Yumi Yamaguchi, Koichi Adachi, and Hideya Endo. "Negative regulation of catalase gene expression in hepatoma cells." In: *Molecular and cellular biology* 12.6 (1992), pp. 2525–2533.
- [67] Duck-Hee Kang. "Oxidative stress, DNA damage, and breast cancer". In: *AACN Advanced Critical Care* 13.4 (2002), pp. 540–549.
- [68] Don Dreher and Alain François Junod. "Role of oxygen free radicals in cancer development". In: *European Journal of cancer* 32.1 (1996), pp. 30–38.
- [69] Takaaki Akaike, Shigemoto Fujii, Atsushi Kato, Jun Yoshitake, Yoichi Miyamoto, Tomohiro Sawa, Shinichiro Okamoto, Moritaka Suga, Makoto A, Yoshiyuki Nagai, and Hiroshi Maeda. "Viral mutation accelerated by nitric oxide production during infection in vivo". In: *The FASEB Journal* 14.10 (2000), pp. 1447–1454.

- [70] Toshikazu Yoshikawa, Satoshi Kokura, Kenzo Tainaka, Yuji Naito, and Motoharu Kondo. “A novel cancer therapy based on oxygen radicals”. In: *Cancer research* 55.8 (1995), pp. 1617–1620.
- [71] Lauren D Stegman, Hong Zheng, Eric R Neal, Oded Ben-Yoseph, Loredano Pollegioni, Mirella S Pilone, and Brian D Ross. “Induction of cytotoxic oxidative stress by D-alanine in brain tumor cells expressing *Rhodotorula gracilis* D-amino acid oxidase: a cancer gene therapy strategy”. In: *Human gene therapy* 9.2 (1998), pp. 185–193.
- [72] Edward D Owuor and Ah-Ng Tony Kong. “Antioxidants and oxidants regulated signal transduction pathways”. In: *Biochemical pharmacology* 64.5 (2002), pp. 765–770.
- [73] HN Green and JW Westrop. “Hydrogen peroxide and tumour therapy”. In: *Nature* 181.4602 (1958), pp. 128–129.
- [74] Peeter Karihtala and Ulla Puistola. “Hypoxia and oxidative stress in the pathogenesis of gynecological cancers and in therapeutical options”. In: *Current Cancer Therapy Reviews* 7.1 (2011), pp. 37–55.
- [75] Monica Marra, Ignazio M Sordelli, Angela Lombardi, Monica Lamberti, Luciano Tarantino, Aldo Giudice, Alberto Stiuso, Rossella Sperlongano, Marina Accardo, Massimo Agresti, Michele Caraglia, and Pasquale Sperlongano. “Molecular targets and oxidative stress biomarkers in hepatocellular carcinoma: an overview”. In: *Journal of translational medicine* 9.1 (2011), p. 171.
- [76] Sandip B Bankar, Mahesh V Bule, Rekha S Singhal, and Laxmi Ananthanarayan. “Glucose oxidase: an overview”. In: *Biotechnology advances* 27.4 (2009), pp. 489–501.
- [77] DA Parks and DN Granger. “Xanthine oxidase: biochemistry, distribution and physiology.” In: *Acta physiologica Scandinavica. Supplementum* 548 (1986), p. 87.
- [78] Kunio Yagi. “Reaction Mechanism of D-Amino Acid Oxidase”. In: *Advances in Enzymology and Related Areas of Molecular Biology, Volume 34* (1971), pp. 41–78.
- [79] Tomohiro Sawa, Jun Wu, Takaaki Akaike, and Hiroshi Maeda. “Tumor-targeting chemotherapy by a xanthine oxidase-polymer conjugate that generates oxygen-free radicals in tumor tissue”. In: *Cancer research* 60.3 (2000), pp. 666–671.

- [80] Arun K Iyer, Greish Khaled, Jun Fang, and Hiroshi Maeda. “Exploiting the enhanced permeability and retention effect for tumor targeting”. In: *Drug discovery today* 11.17 (2006), pp. 812–818.
- [81] Konno Ryuichi and Yasumura Yosihiko. “D-Amino-acid oxidase and its physiological function”. In: *International journal of biochemistry* 24.4 (1992), pp. 519–524.
- [82] Jun Fang, Tomohiro Sawa, Takaaki Akaike, and Hiroshi Maeda. “Tumor-targeted delivery of polyethylene glycol-conjugated D-amino acid oxidase for antitumor therapy via enzymatic generation of hydrogen peroxide”. In: *Cancer research* 62.11 (2002), pp. 3138–3143.
- [83] DG Hatzinikolaou and BJ Macris. “Factors regulating production of glucose oxidase by *Aspergillus niger*”. In: *Enzyme and Microbial Technology* 17.6 (1995), pp. 530–534.
- [84] Michael Samoszuk, Daniel Ehrlich, and Eiman Ramzi. “Preclinical safety studies of glucose oxidase.” In: *Journal of Pharmacology and Experimental Therapeutics* 266.3 (1993), pp. 1643–1648.
- [85] Marc Stanislawski, Véronique Rousseau, Martine Goavec, and Hiro-o Ito. “Immunotoxins containing glucose oxidase and lactoperoxidase with tumoricidal properties: in vitro killing effectiveness in a mouse plasmacytoma cell model”. In: *Cancer research* 49.20 (1989), pp. 5497–5504.
- [86] Carl F Nathan and Zanvil A Cohn. “Antitumor effects of hydrogen peroxide in vivo”. In: *The Journal of experimental medicine* 154.5 (1981), p. 1539.
- [87] Peter J Whitehouse, Donald L Price, Robert G Struble, Arthur W Clark, Joseph T Coyle, and Mahlon R Delon. “Alzheimer’s disease and senile dementia: loss of neurons in the basal forebrain”. In: *Science* 215.4537 (1982), pp. 1237–1239.
- [88] Daniel S McGehee and Lorna W Role. “Physiological diversity of nicotinic acetylcholine receptors expressed by vertebrate neurons”. In: *Annual review of physiology* 57.1 (1995), pp. 521–546.
- [89] RL BIRKs and FC MacIntosh. “Acetylcholine metabolism of a sympathetic ganglion”. In: *Canadian journal of biochemistry and physiology* 39.4 (1961), pp. 787–827.
- [90] Barbara E Jones. “Activity, modulation and role of basal forebrain cholinergic neurons innervating the cerebral cortex”. In: *Progress in brain research* 145 (2004), pp. 157–169.

- [91] Feng Yi, Elizabeth Catudio-Garrett, Robert Gábrriel, Marta Wilhelm, Ferenc Erdelyi, Gabor Szabo, Karl Deisseroth, and Josh Lawrence. “Hippocampal "cholinergic interneurons" visualized with the choline acetyltransferase promoter: anatomical distribution, intrinsic membrane properties, neurochemical characteristics, and capacity for cholinergic modulation”. In: (2015).
- [92] Héctor Romo-Parra, Carmen Vivar, Jasmín Maqueda, Miguel A Morales, and Rafael Gutiérrez. “Activity-dependent induction of multitransmitter signaling onto pyramidal cells and interneurons of hippocampal area CA3”. In: *Journal of neurophysiology* 89.6 (2003), pp. 3155–3167.
- [93] Yann S Mineur, Adetokunbo Obayemi, Mattis B Wigstrand, Gianna M Fote, Cali A Calarco, Alice M Li, and Marina R Picciotto. “Cholinergic signaling in the hippocampus regulates social stress resilience and anxiety- and depression-like behavior”. In: *Proceedings of the National Academy of Sciences* 110.9 (2013), pp. 3573–3578.
- [94] Naiyan Chen, Hiroki Sugihara, and Mriganka Sur. “An acetylcholine - activated microcircuit drives temporal dynamics of cortical activity”. In: *Nature neuroscience* 18.6 (2015), pp. 892–902.
- [95] I Gritti, P Henny, F Galloni, L Mainville, M Mariotti, and BE Jones. “Stereological estimates of the basal forebrain cell population in the rat, including neurons containing choline acetyltransferase, glutamic acid decarboxylase or phosphate-activated glutaminase and colocalizing vesicular glutamate transporters”. In: *Neuroscience* 143.4 (2006), pp. 1051–1064.
- [96] Palmer Taylor and Joan Heller Brown. “Synthesis, storage and release of acetylcholine”. In: (1999).
- [97] Stanley M Parsons, Ben A Bahr, Lawrence M Gracz, Rose Kaufman, Wayne D Kornreich, Lena Nilsson, and Gary A Rogers. “Acetylcholine transport: fundamental properties and effects of pharmacologic agents”. In: *Annals of the New York Academy of Sciences* 493.1 (1987), pp. 220–233.
- [98] Stanley M Parsons, Chris Prior, and Ian G Marshall. “Acetylcholine transport, storage, and release”. In: *International review of neurobiology* 35 (1993), pp. 279–390.
- [99] Martin Sarter and Vinay Parikh. “Choline transporters, cholinergic transmission and cognition”. In: *Nature Reviews Neuroscience* 6.1 (2005), pp. 48–56.

- [100] SK Fisher and S Wonnacott. “Chapter 13-Acetylcholine”. In: *Basic Neurochemistry, 8th ed.*; Brady, ST, Siegel, GJ, Albers, RW, Price, DL, Eds (2012), pp. 258–282.
- [101] Ezio Giacobini. *Cholinesterases and Cholinesterase Inhibitors: Basic Pre-clinical and Clinical Aspects*. Taylor & Francis, 2000.
- [102] Avigdor Shafferman, Baruch Velan, Arie Ordentlich, Chanoch Kronman, Haim Grosfeld, Moshe Leitner, Yehuda Flashner, Sara Cohen, Dov Barak, and Naomi Ariel. “Substrate inhibition of acetylcholinesterase: residues affecting signal transduction from the surface to the catalytic center.” In: *The EMBO journal* 11.10 (1992), p. 3561.
- [103] TM Bartol, Bruce R Land, EE Salpeter, and MM Salpeter. “Monte Carlo simulation of miniature endplate current generation in the vertebrate neuromuscular junction”. In: *Biophysical Journal* 59.6 (1991), pp. 1290–1307.
- [104] Lili Anglister, Joel R Stiles, and Miriam M Salpeter. “Acetylcholinesterase density and turnover number at frog neuromuscular junctions, with modeling of their role in synaptic function”. In: *Neuron* 12.4 (1994), pp. 783–794.
- [105] B Collier and HS Katz. “The synthesis, turnover and release of surplus acetylcholine in a sympathetic ganglion”. In: *The Journal of physiology* 214.3 (1971), p. 537.
- [106] Sandra Fitzpatrick-McElligott and Gunther S Stent. “Appearance and localization of acetylcholinesterase in embryos of the leech *Helobdella triseri- alis*”. In: *Journal of Neuroscience* 1.8 (1981), pp. 901–907.
- [107] H Betz, JP Bourgeois, and JP Changeux. “Evolution of cholinergic proteins in developing slow and fast skeletal muscles in chick embryo.” In: *The Journal of physiology* 302 (1980), p. 197.
- [108] Georg W Kreutzberg. “Neuronal dynamics and axonal flow, IV. Blockage of intra-axonal enzyme transport by colchicine”. In: *Proceedings of the National Academy of Sciences* 62.3 (1969), pp. 722–728.
- [109] Inbal Mor, Dan Grisaru, Lior Titelbaum, Tamah Evron, Carmelit Richler, Jacob Wahrman, Meira Sternfeld, Leah Yogev, Noam Meiri, Shlomo Seidman, and Hermona Soreq. “Modified testicular expression of stress-associated "readthrough" acetylcholinesterase predicts male infertility”. In: *The FASEB Journal* 15.11 (2001), pp. 2039–2041.

- [110] Varda R Deutsch, Marjorie Pick, Chava Perry, Dan Grisaru, Yoram Hemo, Dita Golan-Hadari, Alastair Grant, Amiram Eldor, and Hermona Soreq. “The stress-associated acetylcholinesterase variant AChE-R is expressed in human CD34+ hematopoietic progenitors and its C-terminal peptide ARP promotes their proliferation”. In: *Experimental hematology* 30.10 (2002), pp. 1153–1161.
- [111] Paul G Layer. “Cholinesterases preceding major tracts in vertebrate neurogenesis”. In: *Bioessays* 12.9 (1990), pp. 415–420.
- [112] Margaret E Appleyard. “Secreted acetylcholinesterase: non-classical aspects of a classical enzyme”. In: *Trends in neurosciences* 15.12 (1992), pp. 485–490.
- [113] Miroslav Pohanka. “Inhibitors of acetylcholinesterase and butyrylcholinesterase meet immunity”. In: *International journal of molecular sciences* 15.6 (2014), pp. 9809–9825.
- [114] Jee Hoon Roh, Yafei Huang, Adam W Bero, Tom Kasten, Floy R Stewart, Randall J Bateman, and David M Holtzman. “Disruption of the sleep-wake cycle and diurnal fluctuation of β -amyloid in mice with Alzheimer’s disease pathology”. In: *Science translational medicine* 4.150 (2012), 150ra122–150ra122.
- [115] Michel Goedert and Maria Grazia Spillantini. “A century of Alzheimer’s disease”. In: *science* 314.5800 (2006), pp. 777–781.
- [116] Erik D Roberson and Lennart Mucke. “100 years and counting: prospects for defeating Alzheimer’s disease”. In: *Science* 314.5800 (2006), pp. 781–784.
- [117] Christian Mirescu and Elizabeth Gould. “Stress and adult neurogenesis”. In: *Hippocampus* 16.3 (2006), pp. 233–238.
- [118] F Josef Van Der Staay and Arjan Blokland. “Behavioral differences between outbred Wistar, inbred Fischer 344, brown Norway, and hybrid Fischer 344 \times brown Norway rats”. In: *Physiology & behavior* 60.1 (1996), pp. 97–109.
- [119] Paul T Francis, Alan M Palmer, Michael Snape, and Gordon K Wilcock. “The cholinergic hypothesis of Alzheimer’s disease: a review of progress”. In: *Journal of Neurology, Neurosurgery & Psychiatry* 66.2 (1999), pp. 137–147.
- [120] Judith A Richter, Elaine K Perry, and Bernard E Tomlinson. “Acetylcholine and choline levels in post-mortem human brain tissue: preliminary obser-

- vations in Alzheimer's disease". In: *Life sciences* 26.20 (1980), pp. 1683–1689.
- [121] Nibaldo Inestrosa, Alejandra Alvarez, Cristian A Perez, Ricardo D Moreno, Matias Vicente, Claudia Linker, Olivia I Casanueva, Claudio Soto, and Jorge Garrido. "Acetylcholinesterase accelerates assembly of amyloid- β -peptides into Alzheimer's fibrils: possible role of the peripheral site of the enzyme". In: *Neuron* 16.4 (1996), pp. 881–891.
- [122] Yoo-Hun Suh and Frederic Checler. "Amyloid precursor protein, presenilins, and α -synuclein: molecular pathogenesis and pharmacological applications in Alzheimer's disease". In: *Pharmacological reviews* 54.3 (2002), pp. 469–525.
- [123] María-Ximena Silveyra, Geneviève Evin, María-Fernanda Montenegro, Cecilio J Vidal, Salvador Martínez, Janetta G Culvenor, and Javier Sáez-Valero. "Presenilin 1 interacts with acetylcholinesterase and alters its enzymatic activity and glycosylation". In: *Molecular and cellular biology* 28.9 (2008), pp. 2908–2919.
- [124] James M Conner, Kevin M Franks, Andrea K Titterness, Kyle Russell, David A Merrill, Brian R Christie, Terrence J Sejnowski, and Mark H Tuszynski. "NGF is essential for hippocampal plasticity and learning". In: *Journal of Neuroscience* 29.35 (2009), pp. 10883–10889.
- [125] Ad J Dekker, Dianna J Langdon, Fred H Gage, and Leon J Thal. "NGF increases cortical acetylcholine release in rats with lesions of the nucleus basalis." In: *Neuroreport* 2.10 (1991), pp. 577–580.
- [126] Siegfried Hoyer. "Causes and consequences of disturbances of cerebral glucose metabolism in sporadic Alzheimer disease: therapeutic implications". In: *Frontiers in Clinical Neuroscience*. Springer, 2004, pp. 135–152.
- [127] Hemant Kumar, Sandeep Vasant More, Sang-Don Han, Jin-Yong Choi, and Dong-Kug Choi. "Promising therapeutics with natural bioactive compounds for improving learning and memory - a review of randomized trials". In: *Molecules* 17.9 (2012), pp. 10503–10539.
- [128] Jose A Obeso, Maria C Rodriguez-Oroz, Christopher G Goetz, Concepcion Marin, Jeffrey H Kordower, Manuel Rodriguez, Etienne C Hirsch, Matthew Farrer, Anthony HV Schapira, and Glenda Halliday. "Missing pieces in the Parkinson's disease puzzle". In: *Nature medicine* 16.6 (2010), pp. 653–661.
- [129] Alan King Lun Liu, Raymond Chuen-Chung Chang, Ronald KB Pearce, and Steve M Gentleman. "Nucleus basalis of Meynert revisited: anatomy,

- history and differential involvement in Alzheimer's and Parkin's disease". In: *Acta neuropathologica* 129.4 (2015), pp. 527–540.
- [130] Richard L Doty. "Olfactory dysfunction in Parkinson disease". In: *Nature Reviews Neurology* 8.6 (2012), pp. 329–339.
- [131] Yasuo Hishikawa and Tetsuo Shimizu. "Physiology of REM sleep, cataplexy, and sleep paralysis." In: *Advances in neurology* 67 (1994), pp. 245–271.
- [132] Thomas M Hyde and Jeremy M Crook. "Cholinergic systems and schizophrenia: primary pathology or epiphenomena?" In: *Journal of chemical neuroanatomy* 22.1 (2001), pp. 53–63.
- [133] Mehmet Sofuoglu and Marc Mooney. "Cholinergic Functioning in Stimulant Addiction". In: *CNS drugs* 23.11 (2009), pp. 939–952.
- [134] José P Marques, Wietske Van Der Zwaag, Cristina Granziera, Gunnar Krueger, and Rolf Gruetter. "Cerebellar Cortical Layers: In Vivo Visualization with Structural High-Field-Strength MR Imaging 1". In: *Radiology* 254.3 (2010), pp. 942–948.
- [135] Joanna M Wardlaw, Colin Smith, and Martin Dichgans. "Mechanisms of sporadic cerebral small vessel disease: insights from neuroimaging". In: *The Lancet Neurology* 12.5 (2013), pp. 483–497.
- [136] Robert W Cox. "AFNI: software for analysis and visualization of functional magnetic resonance neuroimages". In: *Computers and Biomedical research* 29.3 (1996), pp. 162–173.
- [137] Seiji Ogawa, Tso-Ming Lee, Alan R Kay, and David W Tank. "Brain magnetic resonance imaging with contrast dependent on blood oxygenation". In: *Proceedings of the National Academy of Sciences* 87.24 (1990), pp. 9868–9872.
- [138] J Koivunen, N Scheinin, JR Virta, S Aalto, T Vahlberg, K Någren, S Helin, R Parkkola, M Viitanen, and JO Rinne. "Amyloid PET imaging in patients with mild cognitive impairment A 2-year follow-up study". In: *Neurology* 76.12 (2011), pp. 1085–1090.
- [139] William W Orrison Juniorr, Jeffrey Lewine, John Sanders, and Michael Hartshorne. *Functional brain imaging*. Elsevier Health Sciences, 2015.
- [140] Thomas R Insel, Story C Landis, and Francis S Collins. "The NIH brain initiative". In: *Science* 340.6133 (2013), pp. 687–688.

- [141] Anna Devor, Peter A Bandettini, David A Boas, James M Bower, Richard B Buxton, Lawrence B Cohen, Anders M Dale, Gaute T Einevoll, Peter T Fox, and Maria Angela Franceschini. “The challenge of connecting the dots in the BRAIN”. In: *Neuron* 80.2 (2013), pp. 270–274.
- [142] Matthew S Lebowitz and Woo-kyoung Ahn. “Effects of biological explanations for mental disorders on clinicians’ empathy”. In: *Proceedings of the National Academy of Sciences* 111.50 (2014), pp. 17786–17790.
- [143] Beáta Sperlágh and Sylvester E Vizi. “Neuronal synthesis, storage and release of ATP”. In: *Seminars in Neuroscience*. Vol. 8. 4. Elsevier. 1996, pp. 175–186.
- [144] Youssef Hatefi. “The mitochondrial electron transport and oxidative phosphorylation system”. In: *Annual review of biochemistry* 54.1 (1985), pp. 1015–1069.
- [145] Anna Falkowska, Izabela Gutowska, Marta Goschorska, Przemyslaw Nowacki, Dariusz Chlubek, and Irena Baranowska-Bosiacka. “Energy metabolism of the brain, including the cooperation between astrocytes and neurons, especially in the context of glycogen metabolism”. In: *International journal of molecular sciences* 16.11 (2015), pp. 25959–25981.
- [146] David Attwell and Simon B Laughlin. “An energy budget for signaling in the grey matter of the brain”. In: *Journal of Cerebral Blood Flow & Metabolism* 21.10 (2001), pp. 1133–1145.
- [147] Fahmeed Hyder, Anant B Patel, Albert Gjedde, Douglas L Rothman, Kevin L Behar, and Robert G Shulman. “Neuronal–glial glucose oxidation and glutamatergic–GABAergic function”. In: *Journal of Cerebral Blood Flow & Metabolism* 26.7 (2006), pp. 865–877.
- [148] Harvey T McMahon and David G Nicholls. “The bioenergetics of neurotransmitter release”. In: *Biochimica et Biophysica Acta (BBA)-Bioenergetics* 1059.3 (1991), pp. 243–264.
- [149] A Wieraszko, G Goldsmith, and TN Seyfried. “Stimulation-dependent release of adenosine triphosphate from hippocampal slices”. In: *Brain research* 485.2 (1989), pp. 244–250.
- [150] David G Satchell and G Burnstock. “Quantitative studies of the release of purine compounds following stimulation of non-adrenergic inhibitory nerves in the stomach”. In: *Biochemical pharmacology* 20.7 (1971), 1694IN91697–1696IN10.

- [151] Bertil B Fredholm and Louise Vernet. “Release of 3H-nucleosides from 3H-adenine labelled hypothalamic synaptosomes”. In: *Acta Physiologica* 106.2 (1979), pp. 97–107.
- [152] Alexander V Gourine, Enrique Llaudet, Nicholas Dale, and K Michael Spyer. “ATP is a mediator of chemosensory transduction in the central nervous system”. In: *Nature* 436.7047 (2005), pp. 108–111.
- [153] Nicholas Dale and Bruno G Frenguelli. “Release of adenosine and ATP during ischemia and epilepsy”. In: *Current neuropharmacology* 7.3 (2009), pp. 160–179.
- [154] Philippe Bodin and Geoffrey Burnstock. “Purinergetic signalling: ATP release”. In: *Neurochemical research* 26.8 (2001), pp. 959–969.
- [155] Richard M Roman, Yu Wang, Stephen D Lidofsky, Andrew P Feranchak, Noureddine Lomri, Bruce F Scharschmidt, and J Gregory Fitz. “Hepatocellular ATP-binding cassette protein expression enhances ATP release and autocrine regulation of cell volume”. In: *Journal of Biological Chemistry* 272.35 (1997), pp. 21970–21976.
- [156] IA Boyd and T Forrester. “The release of adenosine triphosphate from frog skeletal muscle in vitro”. In: *The Journal of physiology* 199.1 (1968), p. 115.
- [157] T Forrester. “An estimate of adenosine triphosphate release into the venous effluent from exercising human forearm muscle”. In: *The Journal of Physiology* 224.3 (1972), p. 611.
- [158] PI Parkinson. “Proceedings: The effect of graduated exercise on the concentration of adenine nucleotides in plasma.” In: *The Journal of physiology* 234.2 (1973).
- [159] MG Clemens and T Forrester. “Appearance of adenosine triphosphate in the coronary sinus effluent from isolated working rat heart in response to hypoxia.” In: *The Journal of Physiology* 312.1 (1981), pp. 143–158.
- [160] BM Paddle and G Burnstock. “Release of ATP from perfused heart during coronary vasodilatation”. In: *Journal of Vascular Research* 11.3 (1974), pp. 110–119.
- [161] JD Pearson and JL Gordon. “Vascular endothelial and smooth muscle cells in culture selectively release adenine nucleotides”. In: *Nature* 281.5730 (1979), pp. 384–386.

- [162] R Douglas Fields and Beth Stevens. “ATP:extracellular signaling molecule between neurons and glia”. In: *Trends in neurosciences* 23.12 (2000), pp. 625–633.
- [163] A Galindo, K Krnjević, and Susan Schwartz. “Micro-iontophoretic studies on neurones in the cuneate nucleus”. In: *The Journal of physiology* 192.2 (1967), p. 359.
- [164] Eugenio Maul and Marvin Sears. “ATP is released into the rabbit eye by antidromic stimulation of the trigeminal nerve.” In: *Investigative ophthalmology & visual science* 18.3 (1979), pp. 256–262.
- [165] Pamela Holton. “The liberation of adenosine triphosphate on antidromic stimulation of sensory nerves”. In: *The Journal of Physiology* 145.3 (1959), pp. 494–504.
- [166] I Von Kügelgen, C Allgaier, A Schobert, and K Starke. “Co-release of norepinephrine and ATP from cultured sympathetic neurons”. In: *Neuroscience* 61.2 (1994), pp. 199–202.
- [167] Li Mou Zheng, Arturo Zychlinsky, Chau-Ching Liu, David M Ojcius, and John Ding-E Young. “Extracellular ATP as a trigger for apoptosis or programmed cell death”. In: *J Cell Biol* 112.2 (1991), pp. 279–288.
- [168] Eric A Newman. “Glial cell inhibition of neurons by release of ATP”. In: *Journal of Neuroscience* 23.5 (2003), pp. 1659–1666.
- [169] Elena Bodas, Jordi Aleu, Gemma Pujol, Mireia Martín-Satué, Jordi Marsal, and Carles Solsona. “ATP crossing the cell plasma membrane generates an ionic current in *Xenopus* oocytes”. In: *Journal of Biological Chemistry* 275.27 (2000), pp. 20268–20273.
- [170] Collin Thomas, Asha Rajagopal, Brian Windsor, Robert Dudler, Alan Lloyd, and Stanley J Roux. “A role for ectophosphatase in xenobiotic resistance”. In: *The plant cell* 12.4 (2000), pp. 519–533.
- [171] Edward H Abraham, Paul Okunieff, Stefania Scala, Petra Vos, Michiel JS Oosterveld, Allan Y Chen, Brij Shrivastav, and Guido Guidotti. “Cystic fibrosis transmembrane conductance regulator and adenosine triphosphate”. In: *Science* 275.5304 (1997), pp. 1324–1326.
- [172] Herbert Zimmermann. “5'-Nucleotidase: molecular structure and functional aspects.” In: *Biochemical Journal* 285.Pt 2 (1992), p. 345.
- [173] Marlene Deluca and WD McElroy. “[1] Purification and properties of firefly luciferase”. In: *Methods in enzymology* 57 (1978), pp. 3–15.

- [174] Reza Beigi, Eiry Kobatake, Masuo Aizawa, and George R Dubyak. “Detection of local ATP release from activated platelets using cell surface-attached firefly luciferase”. In: *American Journal of Physiology-Cell Physiology* 276.1 (1999), pp. C267–C278.
- [175] Alain Trautmann. “Extracellular ATP in the immune system: more than just a "danger signal"”. In: *Sci Signal* 2.56 (2009), e6.
- [176] Fen Zhou, Shuhong Li, Cong Duan Vo, Jian-Jun Yuan, Shigan Chai, Qing Gao, Steven P Armes, Chaojing Lu, and Shiyuan Cheng. “Biomimetic deposition of silica templated by a cationic polyamine-containing microgel”. In: *Langmuir* 23.19 (2007), pp. 9737–9744.
- [177] Milton Cormier. *Chemiluminescence and bioluminescence*. Springer Science & Business Media, 2013.